

Nonlinear Analysis of Rectangular Double-Skin Concrete-Filled Steel Tubular Columns

Muhammad Rizwan

Bachelor of Science in Civil Engineering

Thesis submitted in fulfilment of the requirements for the degree of

Master of Applied Research

Victoria University, Australia

December 2022

ABSTRACT

Rectangular double-skin concrete-filled steel tubular (RDCFST) composite columns are increasingly utilized in the construction of buildings, bridges, transmission towers and offshore structures due to their high structural behavioral properties, including stiffness, ductility, energy absorption, and strength. The hollow internal steel tube used in a RDCFST column not only makes the column economical but also reduces its weight which is highly favorable for seismic design. However, the inner and outer rectangular tubes with a large depth to thickness ratio may undergo local buckling. This kind of composite columns is significantly different from conventional concrete-filled steel tubular (CFST) columns. Only very limited studies have been undertaken on the behavior of RDCFST columns. Therefore, this research develops an efficient and accurate numerical model for predicting the behavior of thin-walled RDCFST short columns under axial loads. The effects of localized buckling and high strength materials are incorporated in the numerical formulations for short RDCFST columns. The measurements from experiments documented elsewhere are used to verify the developed numerical model. Parametric investigations are carried out to quantify the effects of important parameters on the fundamental behavior of short RDCFST columns. Based on the parametric studies, a design formula is proposed for the strength calculations of short RDCFST columns including the post-local buckling strength of steel sections.

Thin-walled RDCFST slender columns composed of non-compact or slender steel sections loaded eccentrically may undergo local and global interaction buckling. There are no

computational modeling schemes that have been developed for the determination of the performance of slender RDCFST columns, accounting for interaction buckling. In this research, a computational modeling program of thin-walled RDCFST slender columns loaded eccentrically is developed, incorporating the interaction of local and global buckling failure modes. The modeling method also accounts for the effects of initial geometric imperfections, second order, and material nonlinearities. To compute the interaction buckling behavior of slender RDCFST columns, an incremental-iterative computational algorithm is designed, which implements Müller's method to solve the nonlinear equilibrium functions of slender RDCFST columns. The developed computer program is verified by experimentally obtained data documented elsewhere and utilized to analyze nonlinear RDCFST slender columns with important parameters to ascertain their structural behavior. It has been confirmed that the computer program predicts well the interaction responses of the local and global buckling of RDCFST slender columns.

This research makes significant contributions to the knowledge base by means of developing robust and efficient computational algorithms that can predict the responses of RDCFST short and slender columns and producing benchmark computational results on the performance of RDCFST columns incorporating interaction buckling, steel yielding and concrete crushing. The established mathematical and design models are efficient modeling and design tools, which can be used by structural engineers and researchers to accurately simulate the structural responses of RDCFST columns.

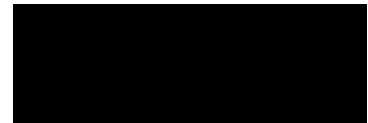
DECLARATION

I, Muhammad Rizwan, declare that the Master of Applied Research thesis entitled *Nonlinear Analysis of Rectangular Double-Skin Concrete-Filled Steel Tubular Columns* is no more than 50,000 words in length including quotes and exclusive of tables, figures, appendices, bibliography, references and footnotes. This thesis contains no material that has been submitted previously, in whole or in part, for the award of any other academic degree or diploma. Except where otherwise indicated, this thesis is my own work.

I have conducted my research in alignment with the Australian Code for the Responsible Conduct of Research and Victoria University's Higher Degree by Research Policy and Procedures.

Muhammad Rizwan

Dated: 05/12/2022



ACKNOWLEDGEMENTS

This thesis has become a reality with the help and support of several notable people, and I would like to offer my heartfelt gratitude to them.

Firstly, all glory to the almighty for granting me this research opportunity which has been a great privilege. I would like to express my sincerest gratitude to my supervisors Associate Professor Qing Quan Liang of Victoria University, Melbourne and Professor Muhammad N. S. Hadi of the University of Wollongong, NSW for their genuine support, guidance and continuous encouragement. Their expertise, vast knowledge and constant supervision enabled me to complete this endeavor to the best of my abilities. They went above and beyond their way time after time to open the opportunities for me for which I am forever grateful.

I would like to thank my parents who have always stood by me through thick n' thin with encouraging words and unconditional love. Thank you for all the sacrifices you made in giving me the opportunity to pursue my dreams. I am also very grateful to my father who financially supported me throughout the years, but also protected me, advised me and encouraged me during my time in Australia. Lastly, I would like to thank my brothers and sister for all the knowledge, advice and ideas they gave me before and during my post graduate studies. I am certain that I would not be who I am or where I am without the support of my family.

LIST OF PUBLICATIONS

The following papers have been published in international journals.

Journal Articles

1. Rizwan, M., Liang, Q. Q., & Hadi, M. N. S (2021). Fiber-based computational modeling of rectangular double-skin concrete-filled steel tubular short columns including local buckling. *Engineering Structures*, 248:113268.
2. Rizwan, M., Liang, Q. Q., & Hadi, M. N. S (2021). Numerical analysis of rectangular double-skin concrete-filled steel tubular slender columns incorporating interaction buckling. *Engineering Structures*, 245:112960.

PART A:

DETAILS OF INCLUDED PAPERS: THESIS BY PUBLICATION

Please list details of each Paper included in the thesis submission. Copies of published Papers and submitted and/or final draft Paper manuscripts should also be included in the thesis submission.

Chapter No.	Publication Title	Publication Status (e.g. published, accepted for publication, to be revised and resubmitted, currently under review, unsubmitted but proposed to be submitted)	Publication Title and Details (e.g. date published, impact factor etc.)
3	Fiber-based computational modeling of rectangular double-skin concrete-filled steel tubular short columns including local buckling	Published	<i>Engineering Structures</i> , 2021, 248:113268. SCImago Journal Rank = Q1, Impact Factor = 4.471.
4	Numerical analysis of rectangular double-skin concrete-filled steel tubular slender columns incorporating interaction buckling	Published	<i>Engineering Structures</i> , 2021, 245:112960. SCImago Journal Rank = Q1, Impact Factor = 4.471.

Declaration by [candidate name]:

Signature:

Date:

Muhammad Rizwan



05/12/2022

TABLE OF CONTENTS

	Page No.
Title	0
Abstract	i
Declaration	iv
Acknowledgements	v
List of Publications	vi
Details of Included Papers: Thesis by Publication	vi
Table of Contents	vii
Chapter 1 Introduction	1
1.1 Background.....	1
1.2 Research Significance.....	4
1.3 Aims of This Research.....	6
1.4 Thesis Layout.....	7

Chapter 2 Literature Review	9
2.1 Introduction.....	9
2.2 Local and Post Local Buckling of Steel Plates.....	10
2.3 Numerical Studies of CFST Columns.....	15
2.4 Double-Skin Concrete-Filled Steel Tubular (DCFST) Columns.....	21
2.4.1 Experimental Investigations of DCFST Columns.....	21
2.4.2 Numerical Investigations of DCFST Columns.....	26
2.5 Concrete-Filled Double Steel Tubular (CFDST) Columns.....	29
2.5.1 Experimental Studies of CFDST Columns	29
2.5.2 Numerical Studies of CFDST Columns	31
2.6 Concluding Remarks.....	32
Chapter 3 Modeling, Behavior and Design of RDCFST Short Columns	34
3.1 Introduction.....	34
3.2 Fiber-based computational modeling of rectangular double-skin concrete-filled steel tubular short columns including local buckling	38
3.3 Concluding Remarks.....	84

Chapter 4 Simulation and Behavior of RDCFST Slender Columns.....	85
4.1 Introduction.....	85
4.2 Numerical analysis of rectangular double-skin concrete-filled steel tubular slender columns incorporating interaction buckling	89
4.3 Range Analysis.....	140
4.4 Concluding Remarks.....	145
Chapter 5 Conclusions.....	147
5.1 Summary.....	147
5.2 Achievements.....	148
5.3 Further Research.....	149
References.....	151

Chapter 1

INTRODUCTION

1.1 BACKGROUND

Steel and concrete composite columns have been extensively employed in the construction of modern composite structures due to their high performance, such as higher ductility, better constructability, higher strength and energy absorption ability as compared to reinforced concrete columns. Concrete-filled steel tubular (CFST) columns perform excellently under seismic loads and are economical when compared to reinforced concrete columns. Using high strength materials such as high-strength concrete and steel tubes may decrease the cross-sectional area of composite columns or increase the strength of columns and it is effective for the construction of high-rise buildings or skyscrapers. However, the thin-walled steel tubes made of high-strength steel might undergo local buckling, which may affect the column performance. The sandwiched concrete prevents the steel tubes from inward buckling. As shown in the Fig. 1.1, the steel tubes are treated as the permanent formwork for the concrete so that the time and cost of construction might be significantly reduced. The use of high

strength concrete in the construction of columns increases the strengths of CFST columns but reduces their ductility and seismic resistance due to the brittleness of the material.

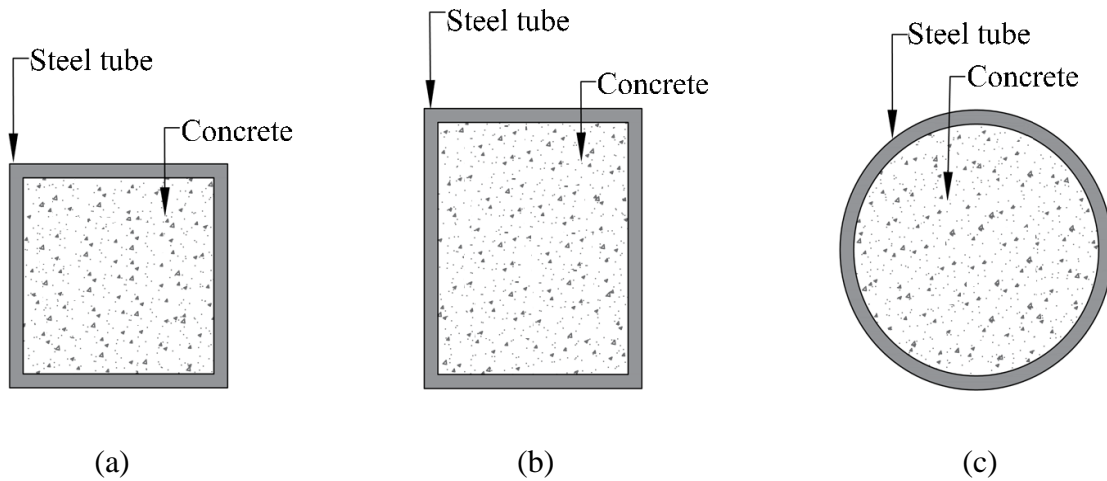


Fig. 1.1 Cross-sections of CFST columns: (a) square; (b) rectangular; (c) circular

In recent times, double-skin concrete-filled steel tubular (DCFST) columns as shown in Fig. 1.2. have been introduced, which were modified from conventional CFST columns. The selection of the materials, such as high strength steel or concrete, geometry of DCFST columns, and selection of cross section of columns for individual projects are totally dependent on the structural efficiency, architectural requirements, availability of the materials, cost of project and method of construction. The DCFST columns have better properties than conventional CFST columns. The inner tube of a circular DCFST column depicted in Fig. 1.2. (c) provides extra confinement to the filled concrete and participates in transferring the load to the sandwiched concrete. This phenomenon contributes to the fire resistance of the columns. The hollow inner steel tube in a DCFST column decreases the

weight of the composite column and can be used for facilitating general building services, such as drainage pipe, telephone, or electricity cables. Rectangular and square DCFST columns as illustrated in Fig. 1.2(a, b) offer ease connection to the steel beams that can be used in the areas where the seismic loads are large and bending stiffness is needed. The RDCFST columns are used in new tall composite buildings, bridges as well as transmission towers. The RDCFST columns are considered as highly efficient structural members in seismic areas because they possess high seismic resistance and better fire resistance when compared with conventional CFST and reinforced concrete columns. This is attributed to the sandwiched concrete and the presence of double skin steel tubes. So, it is important to study the behavior of RDCFST short and slender columns under axial and eccentric compression loads including local and global buckling to make sure they meet the requirements of safety, serviceability, and efficiency while designing for practice purpose.

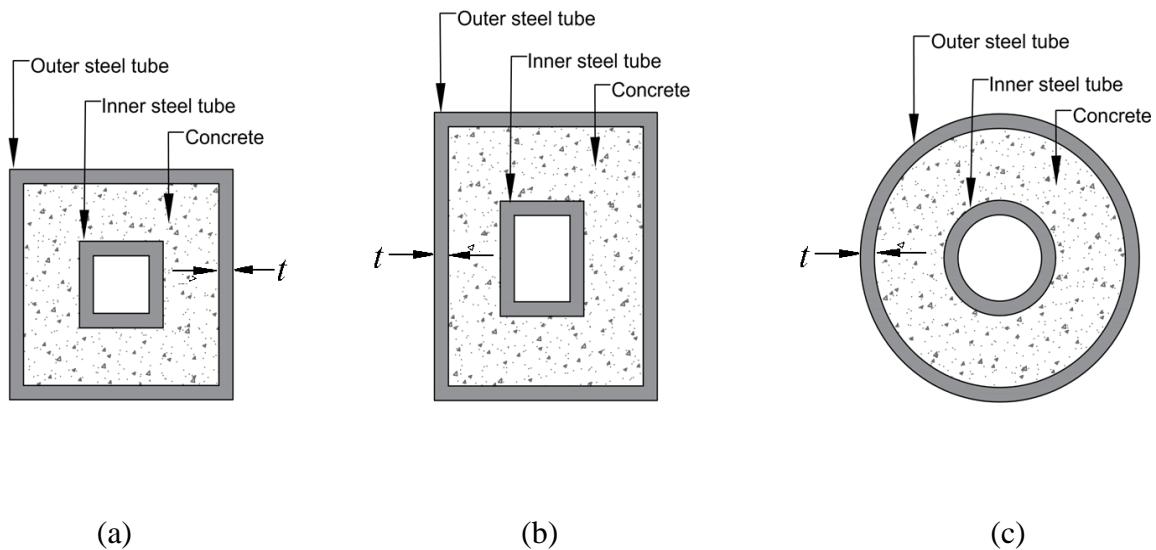


Fig. 1.2. Cross-sections of DCFST columns: (a) square (b) rectangular (c) circular

Additionally, the DCFST column void can also be filled to strengthen an existing DCFST column by pouring the concrete inside the inner steel tube. The void in DCFST column makes it flexible for designing structures. So, the DCFST columns can be used for multiple purposes and are flexible to increase strength later. Moreover, different strengths of materials such as high strength steel can be employed for the formation of external and internal steel tubes of DCFST columns and for the sandwiched concrete to accomplish economical designs. However, the ductility of composite columns might be compromised due to high strength concrete property which is being less ductile. Moreover, rectangular DCFST columns are vulnerable to local and global buckling which affects the columns performance. The walls of rectangular tubes in DCFST columns under axial load and uniaxial bending might be subjected to non-uniform stresses or in-plane bending stresses. The nonlinear analysis of RDCFST columns considering the interaction of local and post-local buckling is a complicated and challenging task in structural engineering.

The performance of RDCFST columns is influenced by the geometric and material properties, for instance the yield stress of steel, compressive strength of concrete, the depth to thickness ratio, width-to-thickness ratio, slenderness ratio and loading eccentric conditions. Even though the behavioral responses of every parameters of such types of columns can be experimentally examined, conducting experiment on every parameter is very expensive and time consuming. Therefore, the computer simulation program is the most cost and time saving alternative technique that can be utilized to determine the responses of DCFST columns.

1.2 RESEARCH SIGNIFICANCE

It has been found that very limited experimental studies as well as numerical investigations on the responses of RDCFST columns have been undertaken. The effects of local buckling and global buckling on the performance of RDCFST short and slender columns have not been incorporated in mathematical models. The purpose of this research is to develop efficient computational models, which can predict the structural performance of RDCFST short and slender columns considering interaction buckling. Therefore, this research makes significant contributions to the knowledge base of structural engineering. The contributions include a numerical based model for the simulation of the nonlinear behavior of RDCFST short columns under axial compression considering local buckling as well as a computational model for predicting the local and global interaction buckling responses of RDCFST slender columns under axial and eccentric loading. Moreover, parametric studies are undertaken, and design formula are proposed for RDCFST columns.

Due to the increasing use of RDCFST columns in the construction of new high-rise buildings and other composite structures, it is essential to investigate their behavior under axial compression and bending including buckling effects. This is to ensure that structures built upon these columns are safe and have no threat to public and society. Also, design engineers need computational models and design tools to design RDCFST columns. The contributions of this research are specifically significant to professionals by developing efficient computational simulation techniques and design tools that lead to safer and more cost-effective designs of composite structures. When RDCFST columns are made of high strength

materials, structural and economic benefits can be achieved. However, most of the design codes are limited to normal strength materials, due to the lack of numerical studies. This research project studies the effects of high strength materials on the behavior of RDCFST columns and proposes design recommendations that are suitable for inclusion in design codes. Therefore, the contributions of this study are significant to the committees of design standards of various countries to develop design specifications for RDCFST columns made of high strength steel and concrete.

This research provides significant contributions to the knowledge base of RDCFST composite columns by developing numerical models for the simulation of RDCFST short and slender columns accounting for the various loading conditions such as axial compression, eccentric compression and uniaxial bending. Benchmark numerical results obtained by the computer models provide new insight into the structural behavior of RDCFST columns and can be used to validate numerical models by other researchers.

1.3 AIMS OF THIS RESEARCH

The major objective of this study is to develop efficient computational models for accurately determining the nonlinear elastic responses of thin-walled RDCFST short and slender columns considering the effects of local and post-local buckling of both the outer and inner steel tubes. The interaction of local and global buckling in RDCFST slender columns that are axially and eccentrically loaded is considered in the computer models.

The specific aims of the research project are:

- (1) To develop a numerical model for the nonlinear analysis of RDCFST short columns under axial load, including local buckling of outer and inner tubes.
- (2) To develop a numerical model for simulating the responses of axially and eccentrically loaded RDCFST slender columns accounting for local and global interaction buckling.
- (3) To conduct parametric studies on the responses of short and slender RDCFST columns by employing the developed computer programs.
- (4) To propose design model for RDCFST short columns.

1.4 THESIS LAYOUT

There are 5 chapters in this thesis. In Chapter 2, literature review is presented on composite columns under several loading conditions. Firstly, the research investigations on the buckling of steel plates considering local and post-local buckling are reviewed. Then, the numerical and experimental research works on the response of concrete-filled steel composite columns made of different section shapes exposed to axial loads and bending are studied.

In Chapter 3, the behavior of RDCFST short columns composed of rectangular cross-sections under axial load is explored. A computational modeling scheme is proposed for the analysis of RDCFST short columns under concentric load incorporating local buckling and is verified by existing experimental data. The developed numerical model is utilized to quantify the responses of RDCFST short columns axially loaded. A design model is proposed that can be

used to calculate the ultimate axial capacity of RDCFST columns, accounting for the post-local strength of rectangular thin-walled sections.

Chapter 4 presents a numerical modeling approach for the prediction of the interaction behavior of local and global buckling in RDCFST slender columns. The model of the behavior of RDCFST slender columns accounts for material nonlinearities and geometric imperfection as well as the interaction of local and global buckling. The computational solution-algorithms are described in detail, implementing Müller's method to satisfy the equilibrium condition during the loading history. The numerical modeling program is verified with the measurements from experiments documented elsewhere and employed to quantify the responses of RDCFST slender columns under concentric and eccentric compression. The load-deflection response curves are obtained by the computer model and discussed. The load distributions in concrete and steel tubes and their contributions to the ultimate load of RDCFST columns are investigated.

Chapter 5 concludes the computational study on the behavior of RDCFST short and slender columns under concentric and eccentric loads. The research achievements are highlighted. Recommendations on further research are given for RDCFST columns.

Chapter 2

LITERATURE REVIEW

2.1 INTRODUCTION

The structural behavior of composite columns under different loading conditions has been investigated by many researchers. Experimental and numerical studies conducted in the past have provided important insights into the understanding of the behavior of composite columns under different loading conditions. Several books have been published on composite columns made of steel and concrete, such as “*Elementary Behaviour of Composite Steel and Concrete Structural Members*” by Oehlers and Bradford (1999), “*Performance-based Optimization of Structures: Theory and Applications*” by Liang (2004), “*Plasticity for Structural Engineers*” by Chen and Han (2007), “*Analysis and Design of Steel and Composite Structures*” by Liang (2014), “*Nonlinear Analysis of Concrete-Filled Steel Tubular Columns*” by Patel et al. (2015a), and “*Concrete-Filled Stainless Steel Tubular Columns*” by Patel et al. (2018). This thesis focuses on the structural performance of RDCFST short and slender columns. In this chapter, a detailed review is presented on the

behavior of composite CFST columns and DCFST columns with different cross-sectional shapes under various loading conditions. The review begins with a discussion of articles on local and post-local buckling of steel tubes, followed by an examination of computational and experimental research on the behavior of CFST and DCFST columns.

2.2 LOCAL AND POST-LOCAL BUCKLING OF STEEL PLATES

The local and post-local buckling of steel plate elements has been extensively studied by researchers since the eighteenth century. Notable works include those by Bryan (1890); Stowell and Lundquist (1939); Lundquist et al. (1943); Hoff and Mautner (1945); Reissner (1948); Bijlaard (1949); Chilver (1953); Ades (1957); Gerard and Becker (1957); Basler et al. (1960); Melosh (1963); Hutchinson and Budiansky (1966); Pifko and Isakson (1969); McDermott (1969); Murray and Wilson (1969); Bulson (1969); Maquoi and Massonnet (1976); Roberts and Rockey (1979); Usami (1982); Usami and Fukumoto (1982,1984); Mahendran and Murray (1986); Chan (1990); Azhari and Bradford (1993); Bradford et al. (1995); Wright (1995); Uy and Bradford (1995,1996); More recent works include those Liang and Uy (1998, 2000); Liang et al. (2003, 2004, 2007); Knobloch and Fontana 2006; Heidarpour and Bradford (2007); Heidarpour and Bradford (2008); Bedair (2009); Cao et al. (2010); Patel et al. (2012); Yuan and Yang (2013); Patel et al. (2014); Hassanein et al. (2015). Bryan (1890) is credited with being the first researcher to study the local buckling of rectangular steel plates, and he specifically investigated the buckling behavior of rectangular and circular sections under in-plane uniform compressive force. Stowell and Lundquist (1939) conducted investigations on the local instability of different cross-sectional plates that

formed I, Z and rectangular channel sections under uniform compression. Lundquist et al. (1943) studied the moment distribution principles for the stability of composed long steel tubes structures under axial load and longitudinal compression. Hoff and Mautner (1945) investigated the buckling of fifty-one flat rectangular sandwiched type panels under edge compression. Theoretical and experimental research works on the elastic solidity of plates and shells were conducted by Bijlaard (1949).

There have been different equations used to calculate the deflection of different cross sections made up of steel plates, taking into account the instability of plates. However, such formulas can be difficult to establish for complicated cross sections. This is why Ritz (1909) proposed the Rayleigh-Ritz method, which has been extensively used by many researchers to determine the critical local buckling stress of steel plate elements from 1950 to 1970, for instance, Chilver (1953), Gerard and Becker (1957), Basler et al. (1960), Singer (1962) and Bulson (1969). The development of digital computers in the early 1970s brought modern finite element analysis techniques, which utilized the matrix method, for buckling analysis of steel tubes. Predecessors in the field, who used the matrix method, included Przemieniecki (1963, 1968), Melosh (1963), Archer (1965), Kapur and Hartz (1966), Wittrick and Curzon (1968), McDermott (1969), and Williams and Wittrick (1969, 1972). Usami (1982) investigated the local and post-local buckling of welded steel boxes under axial compression with different parameters. Furthermore, Usami and Fukumoto (1982,1984) established a theoretical technique to ascertain the post-localized buckling behavior of rectangular steel plates under combined compression and bending. Kromm (1939) studied the compatibility of Marguerre's expressions beyond the buckling limits under shear and compressive stresses.

As a result of theoretical findings, effective width equations were extended and suggested for calculating the plates' response in compression and bending.

Bradford and Hancock (1984) studied the interaction of local buckling and post buckling in I-beams. The finite strip method was used to analyze the strengths of geometrically imperfect steel plates. A computational method was proposed for the post-local buckling of I-beams that were simply supported to provide an alternative method to Winter's expression of effective widths. The interaction of local buckling and flexural-torsional buckling in beams with thin steel flanges was studied. Azizian and Dawe (1985) also utilized a general finite strip technique to analyze rectangular steel plates loaded laterally, considering geometric nonlinear analysis. In the development of finite strip, the energy method was utilized to accomplish the plate stiffness expression and post stiffness expression by employing the Newton-Raphson method.

The distortional buckling of fictitious monophonic-symmetric steel I-beams under stress gradients was investigated by the finite element (FE) model developed by Bradford (1985). A design equation for computing the distortional stress of steel I-beams under moment gradients was given. Moreover, Bradford et al. (1988) extended the FE analysis technique to examine the non-prismatic I-section beam-column's elastic flexural-torsional buckling. The beam-columns were simulated by 3D elements in the computational technique. The flexural-torsional buckling loads of the beam-columns were calculated from the stability matrices and stiffness matrices. Thus, the buckling of steel plates under different end conditions by using

finite strip method was studied by Bradford and Azhari (1995) and the authors derived geometric matrices for the inelastic local buckling of steel plates.

A study on the local buckling of thin plates was conducted experimentally and theoretically by Uy and Bradford (1995). They developed the finite strip theoretical method which was adopted to investigate the elastic and inelastic post local buckling responses of composite steel concrete columns. In a subsequent study, Uy and Bradford (1996) used the finite strip method to study the inelastic buckling of composite steel concrete elements. The developed method was employed to quantify the width to thickness ratios on steel plates in composite elements.

Liang and Uy (1998, 2000) used the finite element (FE) analysis system Strand6 to study the post-local buckling of steel plates of CFST columns. A wide range of parameters were selected such as geometric imperfection as well as residual stresses to accurately verify the established model. Additionally, the initial local-buckling response of steel elements of a rectangular CFST column under uniform compression was predicted. The edges of the box column walls were considered to be clamped. The effective width mathematical equation was established to quantify the post-local buckling responses of steel plates under concentric loads.

A theoretical work based on the finite strip method for determining the local-buckling effects of CFST columns was reported by Uy (2000, 2001). The post-local buckling of steel boxes was expressed by employing the effective width model. It was reported that the local buckling

of CFST columns is not affected by decreasing the small B/t ratio. But there were significant local buckling effects recorded when B/t ratio is large.

Liang et al. (2003, 2004) studied the buckling behavior of double skin composite steel-concrete panels. They employed the FE computational software Strand7 to analyze the post-local buckling effects of steel members and the local buckling with stud connectors spaced regularly in double-skin steel-concrete composite panels subjected to shear stress and biaxial compression. The failure mode of steel skins between stud shear connectors in composite panels when subjected to combined stress was unilateral. The modeling of the critical local buckling of steel plate elements included the shear-slip effects of shear connectors. The post local buckling effects of plate elements under biaxial compression and shear stress had been investigated by using the geometric and material nonlinear analysis method. The expressions were derived, which satisfactorily calculate the local and post local buckling effects including geometric imperfection as well as different boundary conditions.

The behavior of local and post-localized buckling of steel plates in rectangular and square CFST columns under biaxial loads was researched by Liang et al. (2007). The FE analysis technique was adopted to create the FE model that was employed to quantify the local and post local buckling strengths. The geometrical imperfections, width to thickness ratios and residual stress were selected as the major investigated parameters. The mathematical expressions for the determination of the initial localized buckling stress of clamped steel plates as well as their effective width formulas were proposed in the study, which can be

implemented in computational models of nonlinear analysis to account for localized instability effects.

Kamil et al. (2019a) employed the fiber element technique to study the local and global buckling effects on the performance of rectangular CFST slender columns loaded axially under fire exposure. The columns ultimate axial strength was shown to decrease when fire exposure time increased. Local buckling reduced the CFST column's ultimate strength by 11% at ambient temperature when the B/t ratio was 100, whereas, at the fire exposed time of 20 minutes, it was reduced to 8%. Moreover, the fire exposure reduced the ultimate strength of CFST column significantly when the slenderness ratio increased. One-hour fire exposure time reduced the ultimate strength by 48% when the slenderness ratio was 60 as compared to slenderness ratio 22.

2.3 NUMERICAL STUDIES OF CFST COLUMNS

Xilin and Satoshi (1999) studied the behavior of rectangular CFST columns under axial compression numerically. The fiber element method was employed to investigate the failure mechanism, ductility and ultimate strength of the CFST columns as well as the effects of B/t ratio, concrete and steel strengths. The buckling response of CFST slender rectangular columns was studied by Vrcelj and Uy (2002). The valuated parameters were chosen to investigate the influences of slenderness ratio, steel yield strength, concrete strengths on the stiffness and strength of rectangular CFST slender columns. The constitutive effective width formula was employed to calculate the plate post buckling strengths in uniform edge

compression. The material model of the concrete which considered the strain softening and a linear non-linear constitutive law for the structural steel was implemented, but the tensile strength and shear deformation were not included. Moreover, the gradual post-local buckling of the steel boxes was also not taken into consideration. Mursi and Uy (2003) investigated local buckling effects on the strength of concrete filled steel boxed columns.

Hu et al. (2003) analyzed the nonlinear structural responses of CFST columns by using the FE package Abaqus. The equations were proposed for the lateral confining stresses that can be used in the modeling of circular CFST and square CFST columns with reinforced ties. The authors concluded from the FE results that the circular steel tubular section provides confinement to the sandwiched concrete, provided that its D/t ratio is smaller than 40. Moreover, the confinement effect on the ultimate strength of the square cross-sections is negligible when the B/t ratio is above 30. Therefore, it was reported that square cross-section confinement can be increased by spacing the reinforcing ties closely. The model proposed by Hu et al. (2003) for circular cross-sections was further investigated by Liang and Fragomeni (2009) who reported that the confinement model overestimates the responsive behavior of high-strength circular CFST columns, especially when the D/t ratio is less than 47.

Ellobody et al. (2006) investigated the nonlinear behavior of rectangular and square concrete filled steel columns loaded concentrically. The FE program Abaqus was employed, incorporated nonlinear material model of the confined concrete and the steel tubes. An extensive parametric analysis was conducted to investigate the influences of geometric

imperfections, concrete strengths, and steel strengths on the behavior of rectangular CFST and square CFST columns. The different concrete strengths were chosen from 30 MPa to 110 MPa and depth-to-thickness ratio ranged from 10 to 40. The investigation on the parameters showed a remarkable improvement in the ultimate capacity of the column when the steel tube strength and concrete strength increased. It was confirmed that the American specifications and Australian standards were shown to be conservative while the Eurocode predicts accurately the strength of the rectangular CFST column having the depth to thickness ratio of 40.

Liang et al. (2006) proposed a fiber element computational technique, which can analyze the structural nonlinear responses of rectangular and square CFST short columns under concentric loads. The effective width model proposed by Liang and Uy (2000) was employed in the fiber element technique to account for the post-local buckling effects of thin-walled steel sections. To account for post buckling, the in-plane fiber stresses of steel plates were gradually redistributed from the buckled area to edge strips. The sectional ductility indexes were calculated by the developed computational method. The verified model was utilized to evaluate the ductility and ultimate strength of concrete filled steel tubular columns. The concrete strength, steel yield stress, and B/t ratio of the steel section were also included in the parametric studies.

Liang (2009a, 2009b) formulated a performance-based analysis technique (PBA) based on fiber element method for rectangular CFST beam-columns including local buckling under axial load and biaxial bending. Strain hardening, residual stresses and geometric

imperfections were considered in the PBA method for the steel tubes. Moreover, a constitutive model for confined concrete was established as well. The stress-strain constitutive model was proposed for structural steels together with a coefficient of strength reduction for confined concrete in the post-yield regime. The mathematical modeling method was developed by using the expressions proposed by Liang et al. (2007) which considered the buckling effect of steel plates. Moreover, an effective computational technique was developed specially for modeling the local and post-local buckling of steel flanges and webs in CFST columns that were under axial loading or biaxial loads. The stresses of steel fibers were gradually updated based on the concept of effective widths. An iterative computational procedure was given that computed the load-axial strain curves in addition to moment-curvature curves of CFST columns. The efficient solution algorithms based on the secant method were written for obtaining satisfactory solutions. The verification of the computational model was made by using experimental data of CFST columns.

Liang and Fragomeni (2009) studied the behavior of circular CFST columns by using the fiber element simulation model developed. The computational technique was utilized to determine the confinement pressures provided by circular cross-section. In the parametric studies, it was shown that the thickness ratio of the inner tube to the outer tube ratio or the yield strength had insignificant effects, however, by using either high strength steel tubes or concrete significantly increased the ultimate resistance of CFST circular columns. Moreover, the nonlinear analysis of CFST circular short columns under eccentric loading was performed by Liang and Fragomeni (2010). The simulation model of fiber elements for short circular CFST columns under axial compression was proposed. A mathematical modeling procedure

was designed that iteratively computes the moment-curvature responses of eccentrically loaded CFST columns. The confinement effects of circular cross-section, yield strength of steel and B/t ratio's effects on the concrete have been ascertained in the modeling of circular CFST column. The equilibrium condition was satisfied during the loading history by iteratively adjusting the neutral axis depth. An efficient solution algorithm of the secant method was developed to solve the nonlinear equilibrium conditions. The proposed fiber modeling method was confirmed to be an accurate simulation tool of CFST circular columns. The predicted section ultimate loading capacity and bending resistance of CFST columns were verified with the experimental results reported elsewhere.

The overall buckling of slender CFST columns of circular section was studied by Liang (2011a, 2011b). He proposed a mathematical simulation technique that calculates the overall buckling responses of high-strength CFST circular slender columns loaded eccentrically. The fiber-based mathematical model accounts for the effects of significant features, including the concrete confinement and material nonlinearities as well as geometric imperfection. The computer simulation algorithms of the secant method have been developed that efficiently determine the true neutral axis depth and the moment-curvature of CFST columns subjected to eccentric loads. The comparison of predictions with experimental results reported elsewhere has confirmed the accuracy of the developed computer modeling approach.

Liang et al. (2012) proposed a multiscale computational model of pin-ended rectangular CFST slender columns under biaxial loads, considering the interaction of local and global buckling. The cross-section of a CFST column was divided into fiber elements. The

incremental-iterative modeling algorithms incorporating Müller's method were written to obtain satisfactory numerical solutions to the nonlinear equilibrium equations of a CFST column. Patel et al. (2015b) validated the mathematical modeling approach by Liang et al. (2012) by comparing computations with experimental measurements. The computer modeling scheme was used to determine the effects of steel and concrete contribution ratios as well as material strengths on the local-global interaction buckling characteristics of CFST slender columns loaded biaxially to failure.

The computational analysis technique utilizing fiber discretization was formulated by Patel et al. (2017a), which can be used to determine the load-deflection responses and strength envelopes of circular slender concrete-filled stainless-steel tubular (CFSST) columns. The confinement effects, second order, and material nonlinearities were the major considerations in the mathematical modeling technique. Müller's method was implemented to compute the solutions to the incremental highly nonlinear equilibrium equations of slender columns. Patel et al. (2017b) employed the fiber element technique to calculate the structural performance of rectangular CFSST slender columns loaded eccentrically to the local-global instability failure. The thin-walled steel plate responses of CFSST columns where local and post-local buckling occurred were studied by employing a set of equations given by Liang et al. (2007). Composite columns with important design variables were analyzed by the computer program to ascertain their strengths, deflections, and interaction diagrams.

Kamil et al. (2019b) researched the nonelastic behavior of the rectangular CFST short columns under axial compression at elevated temperatures. The fiber element model was

formulated, and its accuracy was confirmed by experimental results. The effects of local buckling and load distribution in the steel and concrete components were assessed in the investigation of CFST short columns. The computational model of round-ended CFST (RCFST) columns employing the fiber element technique has been presented by Patel et al. (2020). The local and post local buckling of the steel flanges and webs was considered in the simulation scheme. A new expression was proposed by analyzing the existing experimental results to quantify the confinement effect induced by the rectangular and circular shapes in RCFST columns on the sandwiched concrete. The structural behavior of RCFST columns and significant variables effects were determined by using the verified model.

2.4 DOUBLE-SKIN CONCRETE-FILLED STEEL TUBULAR (DCFST) COLUMNS

2.4.1 Experimental Investigations of DCFST Columns

Experimental investigations into the behavior of RDCFST columns under axial load and bending have been reported by several researchers. Tao and Han (2006) investigated the behavior of RDCFST short as shown in Fig. 2.1, and RDCFST slender beam-columns depicted in Fig. 2.2, with different eccentricity ratios varied from 0.0 to 60. A total of 30 specimens were made to study the behavior of the short and slender RDCFST columns as well as beams. The overall member length was selected as 3 times the column depth to avoid the columns from overall buckling. The hollow section ratio was kept the same for all type specimens and the thickness of the steel tubes was 3.2 mm. The cross-section dimensions of the inner tube were 45×75 mm and the outer tube had 75×150 mm. These columns were

fabricated by two rectangular cold-formed steel tubes which were concentrically deployed and then filled with concrete in between. The test results indicated that RDCFST members behaved the same as the conventional CFST specimens. The experiments showed that the failure mechanism of the outer tube was the outward buckling. However, all the tested RDCFST (RHS inner and RHS outer) specimens had high strength and high ductility due to the sandwiched concrete between the two tubes.

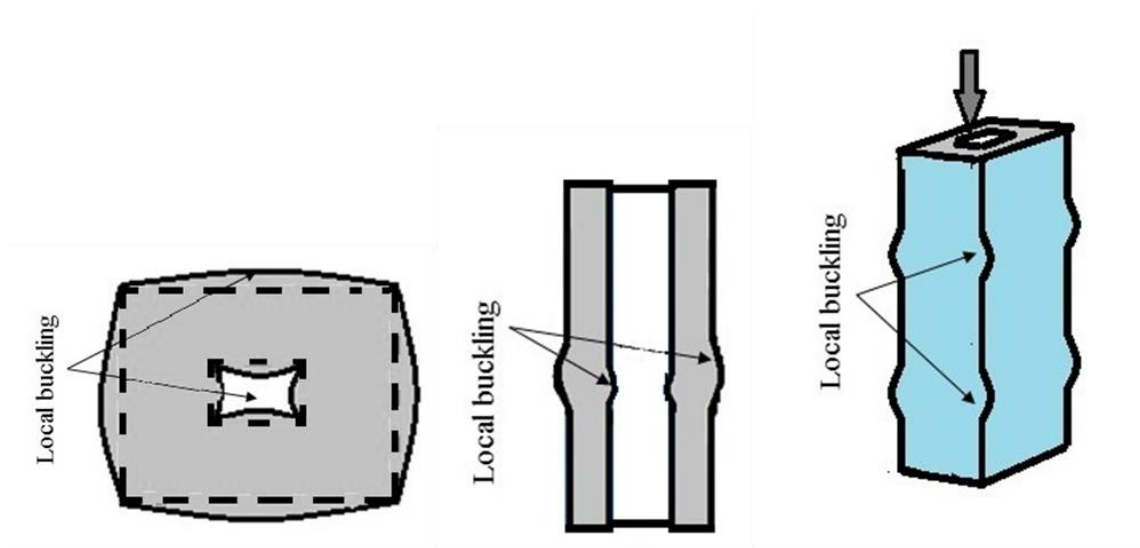


Fig. 2.1. Local buckling of DCFST short column

Zhao and Grzebieta (2002) investigated double-skin concrete filled square columns under axial load and pure bending to determine their ultimate strength and ductility. A theoretical model was given and validated by experimental data. The steel tubes were cold formed with the nominal yield strength of 450 MPa. Moreover, there were four cross-sectional types selected to investigate the influence of the width to thickness ratio ranging from 16.7 to 25 for external steel tube whereas, and the width to thickness ratio was 20 for the internal steel

tubes on structural responses. There was an increase in the ductility of the column under compression load and bending when the width to thickness ratio increased.

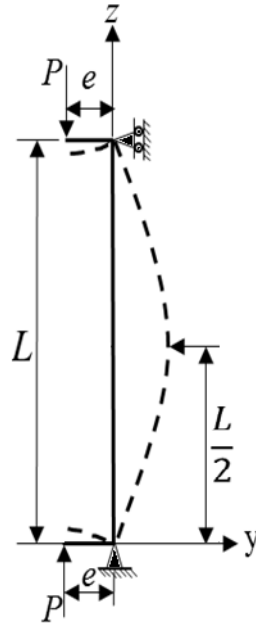


Fig. 2.2. Global buckling of RDCFST slender column

Furthermore, there were experimental and numerical studies on double skin concrete filled columns with various shapes. The short columns were tested under axial load by Yuan et al. (2013). The specimens were composed of an octagonal steel tube as an outer tube and a circular PVC pipe as an inner tube instead of an inner steel tube, a very high strength concrete packed in between the two layers. The parameters of this research focused on radius-to-thickness ratio, hollow section ratio, and most importantly the slenderness ratio. It was found that the use of high strength concrete improved the strength of DCFST columns. However, increasing the radius-to-thickness ratio or hollow section ratio reduced their strengths.

The local instability problem of DCFST short columns was investigated experimentally by Wei et al. (1995). The strength of 60 MPa of the polymer concrete was chosen to study the behavior of the stub columns. The steel tubes having different depth to thickness ratio and yield strength of 480 MPa were selected to design stub columns. The strength and ductility performance of the columns increased with increasing the lateral pressure exerted by the steel tubes. The steel tubes buckled outwardly, and the sandwiched concrete crushed inside the tubes, which resulted in the failure of the columns.

Elchalakani et al. (2002) experimentally studied the responses of short DCFST columns composed of a square outer tube and a circular inner steel tube. The external steel tube had width to thickness ratios varying from 19 to 55 whereas the depth to thickness ratios ranging from 20 to 26 were chosen for inner steel tubes. The concrete compression strength was figured out as 64 MPa for columns. All the 24 specimens failed without fracture. The member slenderness ratio significantly impacted the ductility and energy absorption resistance. Tao et al. (2004) investigated concentrically and eccentrically circular DCFST columns, incorporated important parameters, which included slenderness ratio, and depth to thickness ratio. The outer and inner steel tubes had yield strength ranging from 275 MPa to 294.5 MPa and 320.5 MPa to 396.1 MPa, respectively. The depth to thickness ratio recorded as the major factor that caused the local buckling of steel tubes. There was no local buckling reported when the depth to thickness ratio was small, whereas local buckling was detected at higher depth to thickness ratio. Moreover, the hollow section ratio influenced the ductility of DCFST columns significantly.

Han et al. (2011) conducted experimental research on the stainless-steel tubular DCFST columns with square, circular and round-ended rectangular cross-sections. The inclined loading was applied at different angles. The columns were made of high strength concrete. The local buckling occurred at the top end of the column, which looked like the elephant feet. Both the steel tubes buckled outward due to the presence of sandwiched concrete. The strength of DCFST columns was affected remarkably by the hollow section ratios. The use of higher tapered angle and hollow section ratio increased the strength of DCFST columns.

Farahi et al. (2016) investigated the compressive response of square double skin concrete filled columns with inner corrugated steel plates. The advantages of high strength infilled concrete and ductility were considered. The columns with corrugated steel tubes exhibited better strength under axial compression as compared with referenced specimen. The performance of DCFST columns was affected by the fabricated outer and inner corrugated plates insignificantly. However, the ductility and energy absorption capacity were seen to be improved drastically.

The performance of DCFST short columns with ferritic stainless steel as outer tube and carbon steel as inner tube under axial compression was investigated experimentally by Wang et al. (2017). The authors carried out experimental works on 14 RDCFST stub columns where the outer tube was made of ferritic stainless-steel section with width-to-thickness ratios varying from 26.1 to 42.1 and the inner tube was carbon steel section with width-to-thickness ratios ranging from 7.5 to 13.5. The columns were under constant axial compression and the length to depth ratio was chosen as 2.5 for DCFST columns. Above figures illustrated the

specimen's failure modes included the outward local buckling of the external steel tube, the inward local buckling of the internal steel tube and concrete crushing and the shear failure. Ding et al. (2020) studied the concrete filled double steel tubular square columns under axial compression experimentally and numerically. The effects of hollow section ratio on the mechanical properties of the composite columns were experimentally investigated and verified with the proposed model by using the FE element method.

2.4.2 Numerical Investigations of DCFST Columns

Huang et al. (2010) developed numerical models to study the nonlinear behavior of DCFST stub columns with square and circular outer sections and circular inner tube by using the finite element software ABAQUS. Longitudinal stress-strain relationship, the stress distribution of concrete, the bond strength between concrete and steel tubes, and the effects of hollow section ratio on the behavior of DCFST columns were determined by the numerical simulation model. Pagoulatou et al. (2014) also used finite element software to model the behavior of circular DCFST stub columns under concentric loading. The stress-strain relationship of concrete in CFST columns proposed by Han et al. (2011) was adopted in the numerical studies of DCFST short columns.

The elastic analysis of concentric deployed square steel tubular composite stub columns filled with concrete has been undertaken by Zhao et al. (2002). The concrete was modeled by considering the effects of concrete confinement induced by double steel tubes. The effect of local buckling on the collapse of the outer tube was ignored. However, the concrete model

including confinement and strength degradation was suggested to be used to simulate the collapse behavior, especially for outer thin-walled tubes. Hassanein et al. (2013) performed investigations on the behavior of circular concrete-filled short columns with duplex stainless steel and carbon steel tubes. The finite analysis software ABAQUS was used to predict the behavior of tested circular CFSCT short column under axial load. A new constitutive model for the core concrete confined by the inner and outer tubes was proposed and incorporated in the numerical analysis. Further investigation on the inelastic behavior of circular and square concrete-filled stub columns with external stainless-steel tubes under axial compression was reported by Wang et al. (2018). FE models were developed to investigate the nonlinear responses of composite columns. The load-deformation curves, ultimate strengths and failure modes were compared and verified through the FE software ABAQUS.

Huassnein and Khroob (2014) utilized the ABAQUS FE package to simulate the responses of axially loaded DCFST columns. Moreover, Hassanien et al. (2015, 2018) conducted computational research on the DCFST square columns with internal tube as square made of cold formed steel tubes. The FE models were adopted to investigate the response of short columns under axial load using experimentally obtained data from other researcher. The Ramberg-Osgood model was verified by using the Abaqus program which was proven to be accurate to simulate the responses of DCFST square columns. Parametric studies were also conducted to investigate the response in detail, for instance, width to thickness ratio, steel strengths, concrete compressive strengths, hollow section ratio, outer and inner tube thickness ratios and geometric imperfection. The FE analysis results indicated that the

column slenderness ratio and hollow section caused significant reductions in the performance of DCFST columns.

Liang (2017) developed the fiber element analysis technique for modeling the behavior of short DCFST columns loaded concentrically. The confinement provided by the external and internal steel tubes on the sandwiched concrete was incorporated in the fiber element model. Liang (2018) further numerically determined the behavior of DCFST slender columns by employing the fiber element model. The factors considered in the model included concrete confinement, structural strain hardening, geometric imperfections, and cross-sectional effects. Müller's method was implemented in the computational program to efficiently obtain converged solutions in the incremental-iterative simulation of slender columns. The contributions of the steel and concrete elements to the capacity of DCFST columns were assessed. The proposed computational model not only can monitor the loading history but also can accurately predict the responses of DCFST columns. Moreover, the geometric and material effects on the load-displacement relations and strength of the DCFST columns were studied. Hu and Su (2011) presented confinement models for filled concrete. The reduction factor of the concrete strength and the strain of concrete in the post-peak range were given. The responses of DCFST short columns under axial load were calculated and verified by the computational model.

Patel et al. (2019) developed a computational model of fiber analysis method for the determination of the responses of circular double-skin concrete-filled aluminum tubular (DCFAT) short column. The design recommendations were proposed for the circular

DCFAT stub column under concentric loading considering confinement effects offered by aluminum tubes on the sandwiched concrete. The proposed design formula was validated by existing experimental results. Patel et al. (2020) also established a fiber-based simulation technique for the simulation of circular double skin concrete-filled stainless-steel tubular (DCFSST) columns under axial compression.

2.5 CONCRETE-FILLED DOUBLE STEEL TUBULAR (CFDST) COLUMNS

2.5.1 Experimental studies of CFDST columns

Uenaka (2016) undertook experiments on CFDST stub columns with outer circular and inner square sections under axial compression. In the parametric study, the diameter-to-thickness and inner width-to-outer diameter ratios were selected as variables. From the results, it was observed that the local buckling of the double tubes and the shear failure of in-filled concrete caused the failure of the columns. These failure modes were affected by internal width to external diameter ratios. The columns axial load was affected by the above-described failure modes reported in the study.

Ahmed et al. (2019b) investigated the behavior of eccentrically loaded concrete filled double skin (CFDST) short square columns experimentally. The specimen's cross-section was selected as square cross-section for the external steel tube, whereas the circular shape chosen as internal steel tube. The yield strengths of steel tubes were chosen from 345 MPa to 412 MPa and concrete compressive strengths from 19.1 MPa to 20.6 MPa. The tensile strength

of steel tubes was recorded as 372 MPa to 471 MPa. Twenty columns were examined, sixteen specimens were under eccentric loading and four of the specimens reported were under concentric loads. The structural behavior of the specimens with various parameters was examined in detail to fully understand the contribution of loading conditions, geometric imperfections, depth to thickness ratios, confinement and materials strengths effects to the performance of the columns. The important parameters were cross-sectional measurements effects, external and internal steel tubes width to thickness ratios, loading conditions. Moreover, the stress-strain curves, extreme column resistance, load shortening, load lateral displacement curves and nature of failure were examined.

Furthermore, Ahmed et al. (2019c) investigated on the short circular CFDST columns with internal and external circular tubes. The total number of columns was nineteen in the experimental studies with different parameters under eccentric compressions. The length of the specimens was selected as three times of the diameter of the external steel tube to avoid overall buckling occurrence. The tubes were made of cold formed steel with yield strengths from 332 to 412 MPa and concrete compressive strengths from 19.1 MPa to 20.6 MPa. The tensile strength of the specimen's steel tube recorded varied from 372 MPa to 510 MPa. The specimens were tested till failure. The structural behavior of the circular columns and cross-sectional confinement effects were reported. The failure mode was observed as ordinary, the outer steel tube buckled outward whereas the internal steel tube did not buckle due to concrete and the sandwiched concrete did not crush inside the steel tubes because of confinement effects provided by the steel tubes.

2.5.2 Numerical Studies of CFDST Columns

Ahmed et al. (2018) examined the nonlinear behavior of concrete-filled double steel tubular (CFDST) rectangular short columns with local and post-local buckling effects by utilizing the fiber element analysis technique. The CFDST short columns consisted of an external rectangular steel tube and an internal circular steel tube filled with high or normal strength concrete were investigated. The local and post-local buckling of external steel tube and the confinement of the inner tube to the concrete were included in the fiber-based modeling scheme. The formulated model predicted well the experimental results.

The local and global-buckling of square CFDST slender beam-columns poured with high strength concrete has been investigated numerically by Ahmed et al. (2019a). The authors developed an efficient inverse quadratic technique to account for the interaction of the local and global buckling of square CFDST slender beam columns. The numerical solution scheme was employed to achieve the equilibrium conditions for CFDST square slender beam columns under eccentric loads. The accuracy of the fiber element based computational model was confirmed by experimental data documented elsewhere. The performance of circular CFDST short columns under eccentric loading with outer and inner circular cross-section have been investigated numerically by Ahmed et al. (2019c). A confinement model of lateral pressures was proposed for circular cross-sectional columns. Moreover, they also researched the eccentrically and concentrically loaded square CFDST short columns with an internal circular tube (2019b). The tested data was used to verify the developed fiber element analysis model.

Ahmed et al. (2020a, 2020b) further studied the performance of square and circular CFDST slender columns with preloads effects by using the fiber modeling technique. The progressive local buckling of the outer tube, imperfections, width to thickness ratios, and loading eccentricity were considered in the computational modeling of CFDST slender columns. An iterative numerical algorithm was developed to solve the nonlinear dynamic functions of the CFDST specimens with preloads effects. The tested data was used to verify the computational model and design model. A numerical study has been conducted on the rectangular CFDST short columns loaded eccentrically by Ahmed et al. (2020c). The fiber model simulates the progressive local buckling of the outer tube and the response of rectangular CFDST short columns. The proposed model was utilized to investigate the parametric effects on the performance of rectangular CFDST short columns. The computational model predicted well the response of experimentally investigated CFDST columns.

2.6 CONCLUDING REMARKS

This chapter has presented a literature review on the publications of research work associated with the current research project. The publications were discussed on the steel tube's local and post-local buckling, numerical studies on CFST columns, experimental and numerical research on DCFST and CFDST short and slender columns under axial compression, eccentric loading, uniaxial and biaxial bending, preload effects and under fire. The following research gaps have been identified:

1. The fiber element computational models of rectangular DCFST short columns under axial loading for the simulation of the load-strain response curves, considering the local buckling have not been formulated.
2. The nonlinear analysis of rectangular DCFST slender columns composed of internal and external rectangular steel tubes under concentric and eccentric loads with the interaction of local-global buckling has not been undertaken by using the computational fiber-based modeling method.

Chapter 3

MODELING, BEHAVIOR AND DESIGN OF RDCFST SHORT COLUMNS

3.1 INTRODUCTION

The external and internal steel tubes of a RDCFST short column under the increasing compressive stresses may suffer the outward local buckling, which leads to a decrease in the overall column's performance. This progressive local instability is so complex that has not been considered in any computational fiber-based modeling procedure for the inelastic behavior analysis of short RDCFST columns.

This chapter presents a fiber-based computational method for calculating the behavior of RDCFST short column loaded axially. The numerical simulation of RDCFST short columns incorporates the nonlinear inelastic behavior of steel and concrete in compression. The localized instability of external steel tube and internal steel tube is considered. The numerical modeling technique is verified by the test results documented elsewhere. The parametric

investigation is performed, and a simple design formula is proposed for calculating the ultimate strength of RDCFST short columns.

The following paper is included in this chapter:

Rizwan, M., Liang, Q. Q., & Hadi, M. N.S (2021). Fiber-based computational modeling of rectangular double-skin concrete-filled steel tubular short columns including local buckling. *Engineering Structures*, 248:113268.

<https://doi.org/10.1016/j.engstruct.2021.113268>



THE NEW WAY TO DO UNI

OFFICE FOR RESEARCH TRAINING, QUALITY AND INTEGRITY

DECLARATION OF CO-AUTHORSHIP AND CO-CONTRIBUTION: PAPERS INCORPORATED IN THESIS

This declaration is to be completed for each conjointly authored publication and placed at the beginning of the thesis chapter in which the publication appears.

1. PUBLICATION DETAILS (to be completed by the candidate)

Title of Paper/Journal/Book:	Rizwan, M., Liang, Q. Q., & Hadi, M. N. S (2021). Fiber-based computational modeling of rectangular double-skin concrete-filled steel tubular short columns including local buckling. <i>Engineering Structures</i> , 248:113268.		
Surname:	Rizwan	First name:	Muhammad
Institute:	Institute for Sustainable Industries and Liveat	Candidate's Contribution (%):	60
Status:			
Accepted and in press:	<input type="checkbox"/>	Date:	<input type="text"/>
Published:	<input checked="" type="checkbox"/>	Date:	27/09/2021

2. CANDIDATE DECLARATION

I declare that the publication above meets the requirements to be included in the thesis as outlined in the HDR Policy and related Procedures – policy.vu.edu.au.

<input type="text"/>	<input type="text" value="19/10/2021"/>
Signature	Date

3. CO-AUTHOR(S) DECLARATION

In the case of the above publication, the following authors contributed to the work as follows:

The undersigned certify that:

1. They meet criteria for authorship in that they have participated in the conception, execution or interpretation of at least that part of the publication in their field of expertise;
2. They take public responsibility for their part of the publication, except for the responsible author who accepts overall responsibility for the publication;

PO Box 14428, Melbourne,
Vic 8001, Australia
+61 3 9919 6100

Victoria University ABN 83776954731
CRICOS Provider No. 00124K (Melbourne),
02475D (Sydney), RTO 3113



THE NEW WAY TO DO UNI

3. There are no other authors of the publication according to these criteria;
4. Potential conflicts of interest have been disclosed to a) granting bodies, b) the editor or publisher of journals or other publications, and c) the head of the responsible academic unit; and
5. The original data will be held for at least five years from the date indicated below and is stored at the following location(s):

D:\RDCFST

Name(s) of Co-Author(s)	Contribution (%)	Nature of Contribution	Signature	Date
Muhammad Rizwan	60	Methodology, Software, Validation, Formal analysis, Investigation, Data curation, Writing-original draft, Visualization.	[Redacted Signature]	19/10/2021
Qing Quan Liang	30	Conceptualization, Methodology, Software, Validation, Writing-Review and Editing, Supervision, Project administration.		20/10/2021
Muhammad N. S. Hadi	10	Validation, Writing - Review and Editing, Supervision.		21.10.2021

Updated: September 2019

PO Box 14428, Melbourne,
Vic 8001, Australia
+61 3 9919 6100

Victoria University ABN 83776954731
CRICOS Provider No. 00124K (Melbourne),
02475D (Sydney), RTO 3113

Revised manuscript prepared for

Engineering Structures

September 2021

Fiber-based computational modeling of rectangular double-skin concrete-filled steel tubular short columns including local buckling

Muhammad Rizwan^a, Qing Quan Liang^a, Muhammad N. S. Hadi^b

^a College of Engineering and Science, Victoria University, PO Box 14428, Melbourne, VIC 8001, Australia

^b School of Civil, Mining and Environmental Engineering, University of Wollongong, Wollongong, NSW 2522, Australia

Corresponding author:

Associate Professor Qing Quan Liang
College of Engineering and Science
Victoria University
PO Box 14428
Melbourne, VIC 8001
Australia
E-mail: Qing.Liang@vu.edu.au
ORCID: <https://orcid.org/0000-0003-0333-2265>

Fiber-based computational modeling of rectangular double-skin concrete-filled steel tubular short columns including local buckling

Muhammad Rizwan^a, Qing Quan Liang^{a,1}, Muhammad N. S. Hadi^b

^a *College of Engineering and Science, Victoria University, PO Box 14428, Melbourne, VIC 8001, Australia*

^b *School of Civil, Mining and Environmental Engineering, University of Wollongong, Wollongong, NSW 2522, Australia*

ABSTRACT

Both the external and internal thin-walled steel sections of a rectangular double-skin concrete-filled steel tubular (RDCFST) short column loaded axially may be susceptible to progressive local buckling, which is rarely included in mathematical modeling programs employing the fiber discretization scheme for such composite members. This paper provides a description of a new computational simulation technology, which is developed for the nonlinear fiber analysis of short RDCFST columns axially loaded to failure. The progressive localized-buckling failure of thin-walled steel sections are included in the formulation of the computational simulation method. Experimental measurements and finite element analysis results obtained by ABAQUS software by other researchers are employed to evaluate the accuracy of the computer algorithms developed. Numerical studies are undertaken to ascertain the responses of RDCFST columns to the change of design parameters. Proposed

¹Corresponding author.

E-mail address: Qing.Liang@vu.edu.au (Q. Q. Liang)

ORCID: <https://orcid.org/0000-0003-0333-2265>

is a mathematical expression for the determination of the axial resistances of RDCFST columns considering the post-localized buckling strength of thin-walled steel sections. It is demonstrated that the proposed computational modeling and design technologies yield good predictions of the responses of RDCFST columns and can be used to undertake the nonlinear simulation of RDCFST columns with any class of steel sections.

Keywords: Composite columns; Computational modeling; Post-buckling; Nonlinear simulation.

1. Introduction

Rectangular double-skin concrete-filled steel tubular (RDCFST) columns as shown in Fig. 1 have been developed by modifying conventional concrete-filled steel tubular (CFST) columns [1,2]. The internal hollow tube in a double-skin concrete-filled steel tubular (DCFST) column decreases the weight of the composite column and can be used for facilitating the general building services, such as drainage pipes, telephone or electricity cables as discussed by Liang [3,4]. The DCFST columns are considered as highly efficient structural members in seismic areas because they possess higher seismic resistance, flexural stiffness-to-weight ratio, and fire resistance than conventional CFST columns with the same size [5,6] and have been used as high-rise bridge piers [7], and in transmission towers [8], tall composite buildings and structures subjected to ice loads [9,10]. Experiments showed that the failure of square DCFST (SDCFST) and RDCFST short columns was characterized by the localized buckling of both external and internal tubes [1,2]. Although significant

experiments and numerical research works using commercial finite element (FE) software have been undertaken on the performance of SDCFST short columns [1,2, 11-19], no fiber-based numerical simulation technique has been developed for RDCFST columns that explicitly accounts for the localized buckling of outer and inner tubes. In addition, the development of FE models and analysis of RDCFST columns by using commercial software are time-consuming when compared to the fiber element models [3,20]. Therefore, it is important to develop a computationally efficient modeling method utilizing fiber discretization for accurately determining the responses of RDCFST short columns including local and post-local buckling.

Experimental research on the behavior of short RDCFST and SDCFST columns has been reported by investigators. Zhao and Grzebieta [1] undertook experiments on the responses of square DCFST stub columns and beams, which were fabricated by C450 cold-formed steel boxes. The external steel sections of these columns had the width-to-thickness (B/t) ratios ranging from 16.7 to 25.0 while the inner tube had a B/t ratio of 20. It was observed that the external tube buckled locally outward while the internal tube buckled locally outward and inward. The internal tube generally buckled away from the filled concrete (inward localized buckling), except where the outer tube buckled, which resulted in the crushing of concrete nearby so that the outward localized buckling of the inner tube occurred. Tao and Han [2] experimentally investigated the responses of RDCFST short and slender beam-columns with hollow section ratios from 0.0 to 0.5, member slenderness ratios varying from 26 to 53 and loading eccentricities were 0, 30 and 60 mm. Their test results demonstrated that the localized outward buckling of the external steel tube of the tested RDCFST columns took place, and

the inner steel tube underwent inward local buckling while only the overall buckling failure took place in slender beam-columns. The concrete confinement in rectangular and square columns was not observed. Yang et al. [11] reported the experimental behavior of short SDCFST columns under partial axial compression. The investigated parameters covered the partial compression ratio, the thickness of end plates and the hollow ratio. The internal and external steel tubes were shown to buckle locally away from the filled concrete.

Liang et al. [12] conducted tests on 40 short SDCFST columns with longitudinal stiffeners which were loaded either axially or eccentrically. The columns loaded axially failed by the outward localized buckling of the outer tube, the inward localized buckling of the inner tube, the lateral buckling of the longitudinal stiffeners and the crushing of concrete in the vicinity of the buckled region. It was found that SDCFST columns with longitudinal stiffeners had a better ductility but a lower load-carrying capacity than the ones without stiffeners. Wang et al. [13] carried out experimental works on 14 SDCFST stub columns composed of ferritic stainless-steel outer tube, which had B/t ratios between 26.1 and 42.1 and the carbon inner tube having B/t ratios varying from 7.5 to 13.5. The tested column specimens failed by the concrete crushing, the localized buckling of the inner and outer skins, and shear. Tests on two full-scale SDCFST short columns with a large hollow ratio were carried out by Ding et al. [14] who reported that the inner and outer tubes buckled locally away from the sandwiched concrete.

Most of the numerical studies on circular DCFST columns where both tubes were circular and square DCFST columns composed of an internal circular tube were performed by means

of employing the commercial software ABAQUS. Huang et al. [21] carried out nonlinear finite element analyses of circular and square DCFST stub columns composed of circular inner tube by utilizing ABAQUS. The ABAQUS software was also used by Pagoulatou et al. [22] to simulate circular DCFST stub columns subjected to axial loading. They employed the stress-strain model for concrete in CFST columns proposed by Han [23] in the analysis of short DCFST columns. Hassanein et al. [24] undertook numerical analyses of the responses of DCFST short circular columns where the duplex stainless-steel section was employed as external tube and the internal tube was constructed by carbon steel. The ABAQUS package was employed with a confinement model proposed for the core concrete considering the restraints caused by the internal and external tubes. Further investigation into the inelastic behavior of square and circular DCFST short columns in which the outer tube was made of stainless-steel loaded concentrically was undertaken by Wang et al. [25] by means of utilizing the FE software ABAQUS. Liang [3,4] developed computer simulation programs employing fiber discretization for the modeling of nonlinear circular DCFST short and slender columns considering concrete confinement effects. A constitutive model of lateral confining stresses proposed by Hu et al. [26] was identified and a strength degradation factor for concrete was suggested and implemented in the fiber-based computer scheme. The developed fiber models were demonstrated to be accurate and robust computer simulation tools for such composite columns. However, the localized buckling of the circular tubes has not been accounted for in the numerical models as it does not have a significant effect on the behavior of practical circular DCFST columns with compact steel sections.

Rectangular CFST and DCFST short columns whose steel sections are identified as slender or non-compact will undergo localized buckling when they are loaded axially. Uy [27] and Vrcelj and Uy [28] developed numerical models that determine the strength of CFST columns incorporating local instability. The localized instability problem of rectangular CFST columns loaded axially and biaxially was solved by Liang et al. [29]. The mathematical expressions proposed by Liang et al. [29] for local and post-local buckling were incorporated by Liang [30,31] and Patel et al. [32] into the computer programs for the inelastic nonlinear response simulation of CFST rectangular columns. The fiber modeling technique was proposed by Ahmed et al. [20,32], which can be used to determine the responses of inelastic square concrete-filled double steel tubular (CFDST) columns in which the inner tube is circular, including the localized buckling of the external tube.

Computational models have been presented by researchers for the analysis of short SDCFST and RDCFST columns. The analysis of SDCFST short columns was undertaken by Zhao et al. [16] by means of using plastic mechanism method. The plastic method incorporated the concrete confinement caused by both tubes and the degradation of concrete strength. It was discovered that the method of plastic mechanism could determine the collapse state of SDCFST composite columns. However, the gradual localized buckling of steel tubes was not included in the plastic mechanics method. Tao and Han [2] developed a theoretical model for the simulation of the axial load-strain responses of short RDCFST columns loaded concentrically. The material model for concrete in rectangular CFST columns was adopted to simulate the behavior of concrete in RDCFST columns. The theoretical model reasonably captured well the load-axial strain responses of short RDCFST columns but overestimated

their ultimate loads. This may be caused by the fact that the localized buckling of both internal and external tubes was not taken into account in the theoretical model. Farahi et al. [15] investigated the performance of short SDCFST columns with and without corrugated tubes by utilizing ABAQUS. The confinement effect of concrete with improved ductility was included in the concrete damage plasticity model. The calibrated FE model was employed to undertake parametric investigations on the responses of SDCFST columns. The inelastic modeling of SDCFST columns was carried by Hassanein et al. [17] by using ABAQUS. The Ramberg-Osgood model was adopted to calculate the material responses of cold-formed steel tubes while the concrete confinement was incorporated in the material constitutive laws for concrete. The model was shown to generally ascertain well the load-axial strain responses and localized buckling mode of SDCFST columns.

Liang et al. [12] presented a model of finite elements developed using ANSYS for the determination of the performance of short SDCFST columns with longitudinal stiffeners loaded either axially or eccentrically. The stress-strain relations of concrete given by Han et al. [23] for CFST columns were employed. The effects of welding and localized instability of steel tubes were not considered. Their model generally predicted well the pre-peak responses of stiffened SDCFST columns but was not able to simulate the descending branch of load-strain curves for such concrete-filled composite columns. The axial performance of short SDCFST columns with a large hollow ratio was simulated by Ding et al. [14] by means of using ABAQUS. The model was found to capture well the pre-peak behavior of SDCFST columns but slightly overestimated their capacities and residual strengths. Wang et al. [18] presented FE models established by employing ABAQUS for the simulation of SDCFST

columns fabricated by an external stainless-steel tube and an inner carbon steel tube. The effects of concrete confinement induced by double tubes and localized plate buckling were incorporated in the investigations. The axial responses of DCFST columns made of an outer stainless-steel tube was accurately simulated. Further numerical studies on the behavior of SDCFST columns filled with rubberized concrete were reported by Ayough et al. [19].

More recently, numerical and experimental investigations into the behavior of CFST and DCFST columns filled with high-strength or ultra-high-strength concrete have been undertaken by various researchers [30-42]. These investigations have provided important insight into the behavior and design of composite columns. The behavior of RDCFST columns is significantly different from that of circular DCFST columns where both tubes are circular. Circular DCFST columns are characterized by the significant confinement which improves the strength and ductility of the filled concrete [3,4]. In contrast, RDCFST columns are characterized by the localized buckling of steel tubes, which provide little confinement to the filled concrete and this confinement improves the ductility of the filled concrete but not its compressive strength [1,2]. As discussed above, most of the numerical models were developed by means of using commercial software such as ABAQUS and ANSYS for axially loaded SDCFST short columns, which are computationally not efficient when compared to fiber element models. In addition, the effects of localized buckling have not been included in the theoretical models by Tao and Han [2] and Zhao et al. [15] and in most of the FE models reported. Moreover, no efficient fiber models have been developed for RDCFST columns with local instability. This paper focuses on the development of an efficient and robust fiber-based computational model for predicting the responses of RDCFST short columns,

incorporating the localized buckling of both the outer and inner thin-walled steel tubes for the first time. The interaction buckling of the flanges and webs of a RDCFST columns is also considered in the model. The computer simulation model allows RDCFST short columns made of any class cross-sections to be analyzed and designed, which overcomes the limitation of existing numerical models and codified methods in which only compact steel sections can be used. The computer model verified by experimental data is employed to examine the significance of important design variables on the performance of RDCFST columns, including the D_i/D_o ratio, D_o/t_o ratio, D_i/t_i ratio, steel yield stress, concrete strength and load distribution. A simple design expression is formulated that can be used to compute the axial resistance of RDCFST columns considering the post-buckling strengths of steel tubes.

2. Theory of computational modeling method

2.1 General

The computational modeling method is developed by means of utilizing the fiber discretization technique and has been implemented in a computer program. The fiber scheme discretizes the cross-section of a RDCFST column into small elements as shown in Fig. 2. The fiber method does not employ contact elements to model the interface between steel and concrete and does not divide the column into elements along the length of the column so that it significantly saves the model development and computational time when compared to the

traditional finite element method [3,20]. The fiber method has been approved to be an accurate numerical simulation technology for modeling the inelastic behavior of composite columns [43-48]. Steel and concrete material properties can be assigned to steel and concrete elements, respectively. The section center is chosen as the coordinate system origin. The thickness of the steel section is divided into layers, which can be specified by the user. The width of the steel section is divided based on the layer size to general elements as square as possible. The sandwiched concrete is also divided square elements. The uniaxial stress-strain models given in Sections 2.2 and 2.3 are employed to calculate fiber stresses from given incremental axial strains. The assumptions made in the formulation of the fiber model are: (a) all fiber elements are subjected to the same axial strain under a given axial compression; (b) the localized buckling of both inner and outer tubes is considered; (c) the improved ductility of concrete due to steel encasement is included in the material laws for concrete; (d) failure occurs if the extreme compression fiber strain of concrete reaches the specified maximum strain; (e) the time-dependent behavior of concrete due to shrinkage and creep is ignored.

2.2 Constitutive relations of structural steels

The idealized material model of stress-and strain for steel in compression and tension illustrated in Fig. 3, which is presented by Liang [11], is adopted in the modeling approach. The rounded part of the model depicted in Fig. 3 is used for cold-formed steels having yield stress below 460 MPa. The tri-linear curve is employed to model the response of high-

strength steel material. The rounded part ($0.9\varepsilon_{sy} < \varepsilon_s \leq \varepsilon_{st}$) is represented by using the expression of Liang [43] as follows:

$$\frac{\sigma_s}{f_{sy}} = \left[\frac{\varepsilon_s - 0.9\varepsilon_{sy}}{\varepsilon_{st} - 0.9\varepsilon_{sy}} \right]^{45} \quad (1)$$

in which σ_s represents steel stress, ε_s denotes steel strain, f_{sy} stands for the steel yield stress, ε_{sy} corresponds to the steel yield strain, ε_{st} is assigned to 0.05 for cold formed and high-strength steels. The ultimate strain ε_{su} is chosen as 0.2 for mild structural steels and 0.1 for high-strength steels to consider the steel ductility.

2.4 Constitutive relations of sandwiched concrete

The confinement of concrete in a rectangular CFST column is limited to the corners of the column and does not increase the compressive strength of the filled concrete [49,50]. The mechanism of concrete confinement in RDCFST columns is similar to that of concrete in rectangular CFST columns [2] and its effect on the concrete strength is ignored in the present computational model. However, the concrete ductility improves due to the encasement of the steel boxes, which is explicitly included in the modeling method. Figure 4 schematically illustrates the stress-strain relations of concrete in RDCFST columns. The stress-strain

relationship for concrete is described by Parts OA, AB and BC. The material laws for the filled concrete reported by Mander et al. [51] are used to represent Part OA, written as

$$\sigma_c = \frac{f'_{cc} (\varepsilon_c / \varepsilon'_{cc})^g}{(\varepsilon_c / \varepsilon'_{cc})^g + g - 1} \quad (2)$$

$$g = \frac{E_c}{E_c - (f'_{cc} / \varepsilon'_{cc})} \quad (3)$$

in which σ_c stands for the concrete compressive stress in longitudinal direction, f'_{cc} represents the concrete strength in compression, ε_c denotes the concrete strain, ε'_{cc} is the strain that corresponds to f'_{cc} and E_c is concrete Young's modulus, which can be computed by the expression suggested by ACI Committee 363 [52]:

$$E_c = 6900 + 3320\sqrt{f'_{cc}} \quad (\text{MPa}) \quad (4)$$

The strain ε'_{cc} depends on the concrete strength and is calculated by the following equations given by Liang [43]:

$$\varepsilon'_{cc} = \begin{cases} 0.002 & \text{for } f'_{cc} \leq 28 \text{ (MPa)} \\ (f'_{cc} - 28) / 54000 + 0.002 & \text{for } 28 < f'_{cc} \leq 82 \text{ (MPa)} \\ 0.003 & \text{for } f'_{cc} > 82 \text{ (MPa)} \end{cases} \quad (5)$$

The Parts AB, BC, and CD of the concrete stress-strain response shown in Fig. 4 are described by the mathematical expressions provided by Liang [43] as

$$\sigma_c = \begin{cases} f_{cc}' & \text{for } \varepsilon_{cc}' < \varepsilon_c \leq 0.005 \\ 100f_{cc}'(0.015 - \varepsilon_c)(1 - \beta_c) + \beta_c f_{cc}' & \text{for } 0.005 < \varepsilon_c \leq 0.015 \\ f_{cc}'\beta_c & \text{for } \varepsilon_c > 0.015 \end{cases} \quad (6)$$

where β_c represents the section effect on the ductility and varies with the width-to-thickness ratio (B_s/t) of the column cross-section, where B_s is the larger of B_o and D_o . The coefficient β_c was proposed by Liang [43] by analyzing the test data reported by Tomil and Sakino [53] as

$$\beta_c = \begin{cases} 1.0 & \text{for } B_s/t \leq 24 \\ 1.5 - B_s/(48t) & \text{for } 24 < B_s/t \leq 48 \\ 0.5 & \text{for } B_s/t > 48 \end{cases} \quad (7)$$

The effective strength (f_{cc}') of concrete in compression is affected by the concrete quality, column size and loading methods. It is determined as $\gamma_c f_c'$, where f_c' denotes the concrete cylindrical compressive strength, and γ_c is the coefficient given by Liang [43] to consider the influence of the column size and is written as

$$\gamma_c = 1.85D_c^{-0.135} \quad (0.85 \leq \gamma_c \leq 1.0) \quad (8)$$

where D_c is selected as the greater value of $(D_o - 2t_o)$ and $(B_o - 2t_o)$ for a rectangular cross-section, D_o represents the depth of the cross-section, B_o denotes the width of the cross-section and t_o stands for the thickness of the outer steel tube.

2.4 Mathematical modeling of initial local buckling

The internal and external tubes in a RDCFST column that are axially loaded are vulnerable to local buckling. When the in-plane compressive stress applied to the steel tube wall reaches its critical buckling stress, the initial localized instability occurs. Liang et al. [29] derived expressions based on the finite elements analyses for computing the initial localized buckling stress of steel tubes in rectangular CFST columns considering residual stresses as well as geometric imperfection. The mathematical expression developed by Liang et al. [29] is implemented in the proposed computational modeling procedure to account for the effect of the initial localized instability. The initial localized buckling stress of the steel tube wall [29] is determined by

$$\sigma_{cr} = f_{sy} \left[1.198 \times 10^{-7} \left(\frac{b}{t} \right)^3 - 9.869 \times 10^{-5} \left(\frac{b}{t} \right)^2 + 0.005132 \left(\frac{b}{t} \right) + 0.5507 \right] \quad (9)$$

where σ_{cr} is the initial localized buckling stress of the imperfected steel tubular wall, b stands for the clear width of the wall and t is the tube thickness. Equation (9) can be applied to rectangular RDCFST columns with clear b/t ratios ranging from 30 to 100.

2.5 Mathematical modeling of progressive post-buckling

After the initial localized buckling, the post-buckling of steel tubes in a RDCFST column under increasing compressive load takes place progressively. The post-buckling strength of steel tube walls of a rectangular CFST column was ascertained by Liang et al. [29] who formulated effective width expressions for computing the post-buckling strength of steel plates under uniform and non-uniform in-plane stresses as shown in Fig. 5. These effective-width expression of Liang et al. [29] is used in the proposed numerical simulation method:

$$\frac{b_e}{b} = 1.921 \times 10^{-6} \left(\frac{b}{t} \right)^3 - 3.994 \times 10^{-4} \left(\frac{b}{t} \right)^2 + 0.02038 \left(\frac{b}{t} \right) + 0.5554 \quad (10)$$

in which b_e stands for the plate's effective width. Equation (10) can be used to compute the effective widths of cross-sections that have the ratios of b/t varying from 30 to 100 [29].

The effective width of a steel plate decreases with increasing the applied compressive stress. In contrast, its ineffective width increases with increasing the applied compressive load. The maximum ineffective width (b_{mne}) of the steel plate at the ultimate strength state is determined as $b_{mne} = b - b_e$. Liang [43] reported that the ineffective width b_{ne} of the thin plate after the onset of initial localized instability can be computed by using the linear interpolation based on the stress level (σ_s) acting on the plate as follows:

$$b_{ne} = \left(\frac{\sigma_s - \sigma_{cr}}{f_{sy} - \sigma_{cr}} \right) b_{mne} \quad (11)$$

The fiber-based computational method for simulating the progressive post-buckling of steel plates developed by Liang [43] based on the method of effective widths is adopted in the present computer simulation procedure. A typical fiber mesh with two layers through the tube thickness is depicted in Fig. 2. The fiber mesh of the cross-section is maintained in the nonlinear analysis of the column under consideration. In this scheme, steel fibers in the ineffective width (b_{ne}) of a steel tube wall under a given strain increment are given zero stress value as shown in Fig. 5 while the stresses of steel fibers in the effective width are maintained and this process is repeated until b_{mne} is attained. When the maximum ineffective width b_{mne} of the tube wall is reached, the fibers in the effective width of the steel tube wall are assigned to the yield stress. This implies that the progressive post-buckling of the steel tube under increasing axial compression is characterized by the in-plane stress redistribution within the steel tube wall. Further details on the simulation of the gradual localized buckling can be found in the work of Liang [43].

2.6 Ductility indicator

The ductility indicator, which represents the axial strain ductility of a RDCFST column, is determined by

$$PI_{SD} = \frac{\varepsilon_{u,col}}{\varepsilon_{y,col}} \quad (12)$$

where $\varepsilon_{u,col}$ represents the axial strain that corresponds to the applied axial load falling to 90% of the column ultimate load or the ultimate strain in the post-yield range of strain-hardening. The column yield strain $\varepsilon_{y,col}$ is determined as $\varepsilon_{0.75} / 0.75$. The strain $\varepsilon_{0.75}$ is computed using the strain corresponding to the applied axial load that attains 75% of the column ultimate load.

3. Verification of the fiber-based computational model

To verify the accuracy of the computational modeling and simulation algorithms, the predictions are compared against the test results provided by Tao and Han [2], Wang et al. [13], Ding et al. [14] and Farahi et al. [15]. The tested columns under consideration are documented in Table 1. The ratio of the strength of concrete cylinder (f'_c) to the concrete cube strength was taken as 0.84 in the computer simulation as suggested by Oehlers and Bradford [54]. The computed ultimate loads ($P_{u,num}$) and experimentally obtained values ($P_{u,exp}$) of DCFST columns are compared in Table 1. As demonstrated in Table 1, the computer simulation program yields good results. The average value of $P_{u,num} / P_{u,exp}$ ratios is 0.96, which is sufficient for engineering design purpose. However, the computed resistance of Specimens FR100×4-NS20×2.5-C40 is less than 90% of the experimental value. The cause for this is probably because the actual strength and quality of concrete in these specimens are

unknown. As depicted in Fig. 6, the simulated load-strain relations of RDCFST short columns are generally in good agreement with those determined from experiments. Moreover, the computer modeling technique simulates well the residual strengths of the tested DCFST columns. However, there is a discrepancy between numerical simulations and experimental measurements because the idealized material laws and material properties of steel and concrete materials were used in the simulations, which might not represent the actual responses of the steel and concrete materials used in the tested column specimens. The Specimen Reference Sample shown in Fig. 6(b) exhibited very brittle failure, which might be caused by the poor quality of concrete and the premature fracture of the steel tubes in the tested specimen. Consequently, the post-peak experimental responses of the column deviated considerably from the simulation.

The fiber-based computational model is further verified by comparing the computational results of Specimens D-SS-a, X-0.49 and X-0.64 with those obtained by using the nonlinear finite element analysis software ABAQUS by Ding et al. [14]. It can be observed from Fig. 6 that the axial load-strain responses predicted by the developed fiber-based model are in good agreement with those obtained by the sophisticated finite element software ABAQUS. Both computer programs produce almost the same initial axial stiffness and ultimate axial load for each column, and very close post-peak behavior. However, it should be noted that the fiber-based computational model is significantly more computationally efficient than the finite element model created by ABAQUS as pointed out by Liang [3] and Ahmed et al. [20].

4. Structural behavior of RDCFST columns

The influences of geometric and material design parameters on the structural responses of RDCFST short columns were investigated by using the computational algorithms proposed. A total of 24 RDCFST columns shown in Table 2 were analyzed by taking into account the experimentally identified failure mode of local buckling. It was assumed that the internal and external steel tubes had the same material properties. A value of 200 GPa was used for Young's modulus of steel material.

4.1. The influences of D_i/D_o ratio

The computational algorithms written were used to determine the effects of the D_i/D_o ratio on the structural responses of RDCFST columns. The D_i/D_o ratios were determined to be 0.4, 0.5, 0.6 and 0.7 by means of altering the depth of the inner tube only as given in Group 1 in Table 2. Figure 7 gives the simulated responses of RDCFST columns having different D_i/D_o ratios. The figure indicates that changing the D_i/D_o ratio from 0.4 to 0.5, 0.6 and 0.7 causes a reduction in strength by 4.9%, 9.5%, 11.2% and 17.5%, respectively. This is because of the reduction in the concrete area which shares a large part of the applied load. As presented in Fig. 8, the column's ductility improves with an increase in the D_i/D_o ratio.

4.2. The influences of D_o/t_o ratio

Two cases were investigated to evaluate the significance of D_o/t_o ratio on the responses of RDCFST columns. The first case was to vary the depth of the outer steel box while other parameters were not changed as shown in Group 2 in Table 2. Figure 9 presents the axial load-strain relations of RDCFST columns, which are a function of the D_o/t_o ratio. A marked increase in the column's initial stiffness and axial resistance is obtained by means of using a larger D_o/t_o ratio. Changing the D_o/t_o ratio from 50 to 60, 65 and 70 results in the increases of 16.7%, 32.9% and 46.7% in the column's capacity, respectively. It is illustrated in Fig. 9 that the ratio of D_o/t_o notably influences the post-peak performance of RDCFST columns. The relationship between the D_o/t_o ratio and the column ductility is shown in Fig. 10, which indicates that a decrease in the ductility index is caused by increasing the D_o/t_o ratio. When altering the ratio of D_o/t_o from 50 to 60, 65 and 70, the ductility indicator varies from 5.71 to 5.40, 5.30 and 5.20, respectively.

The second situation was to change the thickness of the external tube only as demonstrated in Group 3 in Table 2. This means that the width $B_o = 375$ mm and depth $D_o = 600$ mm of the external tube were unchanged but its thickness was varied to determine the D_o/t_o ratios of 50, 60, 65 and 70. Figure 11 shows that the larger the D_o/t_o ratio, the lower the initial stiffness. A reduction in the axial resistance of RDCFST short columns is expected when the D_o/t_o ratio increases. As shown in Fig. 12, the use of a larger D_o/t_o ratio causes a slight

reduction in the column ductility. The ductility indicators of the RDCFST columns having D_o/t_o ratios of 50, 60, 65 and 70 are 5.50, 5.40, 5.36 and 5.30, respectively.

4.3. The influences of D_i/t_i ratio

The D_i/t_i ratios of 25, 30, 35 and 40 of the columns in Group 4 shown in Table 2 were determined by altering the inner tube thickness from 10 mm to 6.25 mm. The load-axial strain responses of RDCFST columns that have different D_i/t_i ratios are given in Fig. 13. Increasing the D_i/t_i ratio slightly decreases the initial-stiffness of the columns. In addition, the use of a larger D_i/t_i ratio considerably reduces the capacity of RDCFST columns. The relationship between the D_i/t_i ratio and the ductility is shown in Fig. 14. The column's ductility indicator reduces slightly from 6.15 to 5.91.

4.4. The influences of steel yield stress

The responses of RDCFST short columns in Group 5 given in Table 2 have been determined by the developed computer program to assess the significance of steel yield stress on their performance of ductility and strength. The predicted nonlinear responses of RDCFST columns to various steel yield stresses are presented in Fig. 15. The steel yield stress does not affect the column's initial stiffness. However, the use of steel tubes with higher yield stress improves the axial resistance of the RDCFST column. The column's capacity could be

improved by 8.33%, 16.6% and 33.3% respectively by means of changing the yield stress from 250 to 300, 350 and 450 MPa. Figure 16 shows the ductility indicators of these RDCFST columns designed by using steel tubes that have different yield stresses. The ductility indices of DCFST columns that have the yield stresses of 250, 300, 350 and 450 MPa have been determined as 6.03, 5.81, 5.44 and 4.9, respectively. It can be concluded that the steel yield stress does not have a significant influence on the column ductility.

4.5 The influences of concrete strength

The RDCFST short columns in Group 6 were designed with different concrete compressive strengths varying from 40 MPa to 100 MPa. The predicted relationships between the applied load and strain for RDCFST short columns with concrete strength as a design variable are given in Fig. 17. It is discovered that the axial capacity of RDCFST columns is remarkably improved by filling higher strength concrete into double-skin tubes. The axial load-carrying capacity of the composite column of double skins would have an increase of 13.8%, 24.1% and 63.7%, respectively if the concrete strength of 40 MPa is replaced by 50, 70 and 100 MPa. This implies that higher strength concrete can be used to improve the axial capacity of short RDCFST columns.

Figure 18 presents the relationship between the ductility indicator and concrete design strength. The use of higher concrete strength in RDCFST columns results in lower ductility. The ductility index of the RDCFST column filled with 40 MPa concrete is 6.15, which is reduced to 3.80 when 100 MP high-strength concrete is employed. This is attributed to the brittle property of high strength concrete.

4.6. Load distributions

The load distribution in Specimen C19 shown in Table 2 was ascertained by means of conducting a nonlinear inelastic analysis on this column using the computer program. Figure 19 shows the computed load-strain responses of the filled concrete and steel sections in the composite column. The figure indicates that the filled-concrete, outer steel section and inner steel section share 56.1%, 37.2% and 16.9% of the ultimate axial load of the column, respectively. A large portion of the applied load is resisted by the filled concrete.

5. Proposed design model

The developed computational modeling and simulation program can be used directly in the design of RDCFST shot columns. However, a simple expression for design purpose is needed in practice. As discussed previously, the use of non-compact or slender steel section in RDCST columns leads to economical designs, but localized buckling, which should be explicitly included in design. A new design expression for determining the section axial capacity of RDCFST short columns including post-local buckling effects is proposed here as

$$P_u = A_{seo} f_{syo} + A_{sei} f_{syi} + A_c (\gamma_c f'_c) \quad (14)$$

where P_u represents the ultimate axial load of the column; A_{seo} and A_{sei} represent the effective areas of the outer and inner steel sections, respectively, and are calculated by using the effective width expressed by Eq. (10); f_{syo} and f_{syi} stand for yield stresses of the external and internal steel sections, respectively; A_c represents the concrete cross-sectional area.

To verify the proposed design expression, the computed strengths of RDCFST columns by employing Eq. (14) are compared with the test results in Table 3, where $P_{u,cal}$ is the axial capacity calculated by using Eq. (14). The agreement between the calculations and experimentally measured values is shown to be good. The mean of the computed to the experimental loads is 0.959. The statistical analysis indicates that the standard deviation of $P_{u,cal}/P_{u,exp}$ is 5% and the coefficient of variation is 5.3%. This suggests that the design expression proposed can be utilized in designing RDCFST short columns.

6. Conclusions

This paper has described a computer simulation and modeling method incorporating an efficient fiber discretization scheme for the modeling of RDCFST and SDCFST short columns loaded concentrically to the localized buckling failure. The computational modeling technique proposed can detect the onset of initial localized buckling and simulate the progressive post-buckling of both outer and inner thin-walled steel sections in the inelastic

nonlinear response analysis of RDCFST columns. The comparison of fiber-based calculations with experimental measurements as well as the nonlinear finite element analysis results produced by ABAQUS documented elsewhere has verified the accuracy of the computational technique. The computational results obtained in the parametric studies provide a new insight into the behavior of RDCFST short columns where the progressive localized instability of steel tubes takes place under increasing compression. A simple expression has been proposed and can be used to design RDCFST columns. The developed computational modeling and simulation technology provide structural designers with efficient tools that can be employed to predict the responses of high-strength RDCFST columns constructed by rectangular steel sections of any class.

References

- [1] Zhao XL, Grzebieta R. Strength and ductility of concrete filled double skin (SHS inner and SHS outer) tubes. *Thin-Walled structures* 2002; 40(2):199-213.
- [2] Tao Z, Han LH. Behaviour of concrete-filled double skin rectangular steel tubular beam–columns. *Journal of Constructional Steel Research* 2006; 62(7):631-646.
- [3] Liang QQ. Nonlinear analysis of circular double-skin concrete-filled steel tubular columns under axial compression. *Engineering Structures* 2017; 131:639-650.
- [4] Liang QQ. Numerical simulation of high strength circular double-skin concrete-filled steel tubular slender columns. *Engineering Structures* 2018; 168:205-217.

- [5] Elchalakani M, Zhao XL, Grzebieta RH. Tests on concrete filled doubleskin (CHS outer and SHS inner) composite short columns under axial compression. *Thin-Walled Structures* 2002;40(5):415–441.
- [6] Han L-H, Huang H, Zhao X-L. Analytical behavior of concrete-filled double skin steel tubular (CFDST) beam-columns under cyclic loading. *Thin-Walled Struct* 2009;47(6–7):668–680
- [7] Yagishita F, Kitoh H, Sugimoto M, Tanihira T, Sonoda K. Double skin composite tubular columns subjected to cyclic horizontal force and constant axial force. *Proceedings of the 6th ASCCS conference; 2000; 497–503.*
- [8] Li W, Han L-H, Ren Q-X, et al. Behavior and calculation of tapered CFDST columns under eccentric compression. *J Constr Steel Res* 2013;83:127–136.
- [9] Goode CD. Composite construction to resist external pressure. *Specialty Conference on Concrete Filled Steel Tubular Structures, 1988:46-52.*
- [10] Shakir-Khalil H. Composite columns of double-skinned shells. *Journal of Constructional Steel Research* 1991;19:133–152.
- [11] Yang YF, Han LH, Sun BH. Experimental behaviour of partially loaded concrete filled double-skin steel tube (CFDST) sections. *Journal of Constructional Steel Research* 2012; 71:63-73.
- [12] Liang W, Dong JF, Wang QY. Mechanical behaviour of concrete-filled double-skin steel tube (CFDST) with stiffeners under axial and eccentric loading. *Thin-Walled Structures* 2019; 138:215-230.

- [13] Wang F, Young B, Gardner L. Experimental investigation of concrete-filled double skin tubular stub columns with ferritic stainless-steel outer tubes. *ce/papers*. 2017;1(2-3):2070-2079.
- [14] Ding FX, Wang WJ, Lu DR, Liu XM. Study on the behavior of concrete-filled square double-skin steel tubular stub columns under axial loading. *Structures* 2020; 23:665-676.
- [15] Farahi M, Heidarpour A, Zhao XL, Al-Mahaidi R. Parametric study on the static compressive behaviour of concrete-filled double-skin sections consisting of corrugated plates. *Thin-Walled structures* 2016; 107:526-542.
- [16] Zhao XL, Han B, Grzebieta RH. Plastic mechanism analysis of concrete-filled double-skin (SHS inner and SHS outer) stub columns. *Thin-Walled Structures* 2002; 40(10):815-833.
- [17] Hassanein MF, Elchalakani M, Karrech A, Patel VI, Yang B. Behaviour of concrete-filled double-skin short columns under compression through finite element modelling: SHS outer and SHS inner tubes. *Structures* 2018; 14:358-375.
- [18] Wang FY, Young B, Leroy Gardner L. Compressive behaviour and design of CFDST cross-sections with stainless steel outer tubes. *Journal of Constructional Steel Research* 2020; 170:105942.
- [19] Ayough P, Ibrahim Z, Ramli Sulong NH, Hsiao PC, Elchalakani M. Numerical analysis of square concrete-filled double skin steel tubular columns with rubberized concrete. *Structures* 2021; 32:1026-1047.

- [20] Ahmed M, Liang QQ, Patel VI, Hadi MNS. Nonlinear analysis of rectangular concrete-filled double steel tubular short columns incorporating local buckling. *Engineering Structures* 2018; 175:13-26.
- [21] Huang H, Han LH, Tao Z, Zhao XL. Analytical behaviour of concrete-filled double skin steel tubular (CFDST) stub columns. *Journal of Constructional Steel Research* 2010; 66(4):542-555.
- [22] Pagoulatou M, Sheehan T, Dai XH, Lam D. Finite element analysis on the capacity of circular concrete-filled double-skin steel tubular (CFDST) stub columns. *Engineering Structures* 2014; 72:102-112.
- [23] Han LH, Li YJ, Liao FY. Concrete-filled double skin steel tubular (CFDST) columns subjected to long-term sustained loading. *Thin-walled structures* 2011; 49(12):1534-1543.
- [24] Hassanein MF, Kharoob OF, Liang QQ. Circular concrete-filled double skin tubular short columns with external stainless steel tubes under axial compression. *Thin-Walled Structures* 2013; 73:252-263.
- [25] Wang FC, Han LH, Li W. Analytical behavior of CFDST stub columns with external stainless steel tubes under axial compression. *Thin-Walled Structures* 2018; 127:756-768.
- [26] Hu HT, Su FC. Nonlinear analysis of short concrete-filled double skin tube columns subjected to axial compressive forces. *Marine Structures* 2011; 24: 319-337.
- [27] Uy B. Strength of concrete filled steel box columns incorporating local buckling. *Journal of Structural Engineering, ASCE* 2000; 126(3):341-352.

- [28] Vrcelj Z, Uy B. Strength of slender concrete-filled steel box columns incorporating local buckling. *Journal of Constructional Steel Research* 2002; 58(2):275-300.
- [29] Liang QQ, Uy B, Liew JYR. Local buckling of steel plates in concrete-filled thin-walled steel tubular beam-columns. *Journal of Constructional Steel Research* 2007; 63(3):396-405.
- [30] Mollazadeh MH, Wang YC. New insights into the mechanism of load introduction into concrete-filled steel tubular column through shear connection. *Eng Struct* 2014;75:139–51.
- [31] Schnabl S, Jelenić G, Planinc I. Analytical buckling of slender circular concrete filled steel tubular columns with compliant interfaces. *J Constr Steel Res* 2015;115:252–62.
- [32] Ibañez C, Romero ML, Espinos A, Portolés JM, Albero V. Ultra-high strength concrete on eccentrically loaded slender circular concrete-filled dual steel columns. *Structures* 2017;12:64–74.
- [33] Huang Y, Fu J, Wu D, Liu A, Gao W, Pi YL. Dynamic stability of slender concrete-filled steel tubular columns with general supports. *International Journal of Structural Stability and Dynamics* 2019; 19(04):1950045.
- [34] Li YL, Zhao XL, Singh Raman RK. Load-strain model for concrete-filled double-skin circular FRP tubes under axial compression. *Engineering Structures* 2019;181: 629-642.
- [35] Su MN, Cai YC, Chen XR, Young B. Behaviour of concrete-filled cold-formed high strength steel circular stub columns. *Thin-Walled Structures* 2020; 157: 107078.

- [36] Shan B, Xu C, Lai DD, Xiao Y, Li TY. Experimental research on compressive behavior of seawater and sea sand concrete-filled RPC tubes. *Engineering Structures* 2020; 222: 111117.
- [37] Tao Z, Katwal U, Uy B, Wang WD. Simplified nonlinear simulation of rectangular concrete-filled steel tubular columns. *Journal of Structural Engineering, ASCE* 2021; 147(6): 04021061.
- [38] Nguyen TT, Thai HT, Ngo T, Uy B, Li DX. Behaviour and design of high strength CFST columns with slender sections. *Journal of Constructional Steel Research* 2021;182: 106645.
- [39] Xiong MX, Liew JYR. Fire resistance of high-strength steel tubes infilled with ultra-high-strength concrete under compression. *Journal of Constructional Steel Research* 2021; 176:106410.
- [40] Ho JCM, Ou XL, Li CW, Song W, Wang Q, Lai MH. Uni-axial behaviour of expansive CFST and DSCFST stub columns. *Engineering Structures* 2021; 237:112193.
- [41] Li GC, Yang Y, Yang ZJ, Fang C, Ge HB, Liu YP. Mechanical behavior of high-strength concrete filled high-strength steel tubular stub columns stiffened with encased I-shaped CFRP profile under axial compression. *Composite Structures* 2021; 275:114504.
- [42] Zhao H, Wang R, Lam D, Hou CC, Zhang R. Behaviours of circular CFDST with stainless steel external tube: slender columns and beams. *Thin-Walled Structures* 2021;158: 107172.

- [43] Liang QQ. Performance-based analysis of concrete-filled steel tubular beam–columns, Part I: Theory and algorithms. *Journal of Constructional Steel Research* 2009; 65(2):363-372.
- [44] Liang QQ. Performance-based analysis of concrete-filled steel tubular beam–columns, Part II: Verification and applications. *Journal of Constructional Steel Research* 2009; 65(2):351-362.
- [45] Patel VI, Liang QQ, Hadi MNS. High strength thin-walled rectangular concrete-filled steel tubular slender beam-columns, Part I: Modeling. *Journal of Constructional Steel Research* 2012; 70:377-384.
- [46] Ahmed M, Liang QQ, Patel VI, Hadi MNS. Local-global interaction buckling of square high strength concrete-filled double steel tubular slender beam-columns. *Thin-Walled Structures* 2019; 143:106244.
- [47] El-Tawil S, Sanz-Picón CF, Deierlein GG. Evaluation of ACI 318 and AISC (LRFD) strength provisions for composite beam–columns. *Journal of Constructional Steel Research* 1995;34(1):103–126.
- [48] El-Tawil S, Deierlein GG. Strength and ductility of concrete encased composite columns. *Journal of Structural Engineering, ASCE* 1999;125(9):1009–1019.
- [49] Furlong RW. Strength of steel-encased concrete beam-columns. *Journal of the Structural Division, ASCE* 1967; 93(5):113-124.
- [50] Knowles RB, Park R. (1969). Strength of concrete-filled steel tubular columns. *Journal of the Structural Division, ASCE*, 1969; 95(12): 2565-2587.
- [51] Mander JB, Priestley MJ, Park R. Theoretical stress-strain model for confined concrete. *Journal of structural engineering, ASCE* 1988; 114(8):1804-1826.

- [52] ACI Committee 363. State of the Art Report on High-Strength Concrete. ACI Publication 363R-92, 1992, Detroit, MI, American Concrete Institute.
- [53] Tomil M, Sakino K. Elasto-plastic behavior of concrete filled square steel tubular beam-columns. Transactions of the Architectural Institute of Japan 1979; 280:111-122.
- [54] Oehlers DJ, Bradford MA. Elementary behaviour of composite steel and concrete structural members. Oxford U.K.: Butterworth-Heinemann, 1999.

Figures and Tables

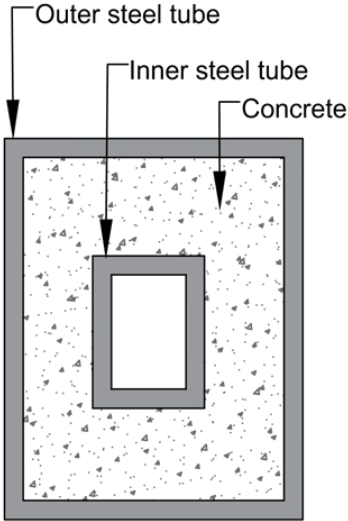


Fig. 1. Cross-section of RDCFST column

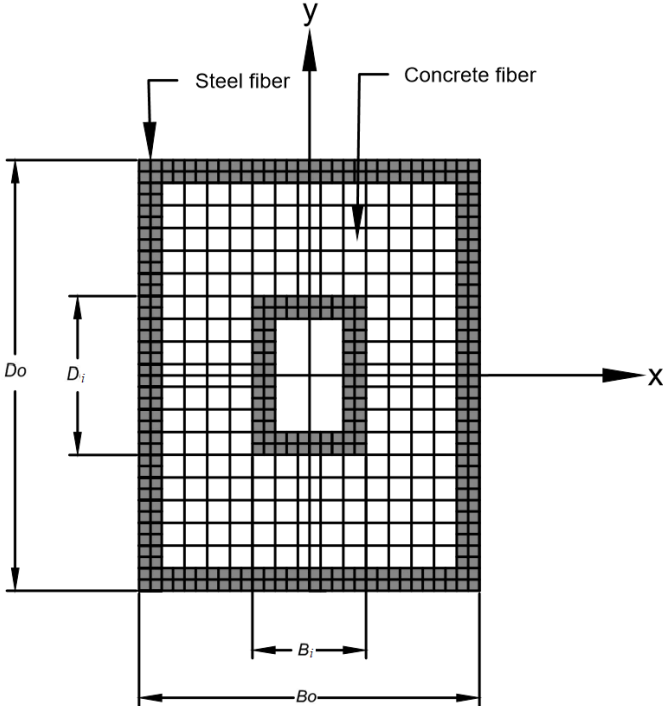


Fig. 2. Typical fiber element discretization of cross-section

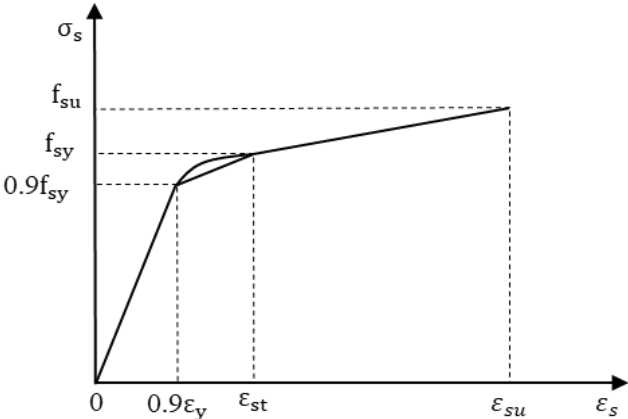


Fig. 3. Stress-strain curve for structural steel

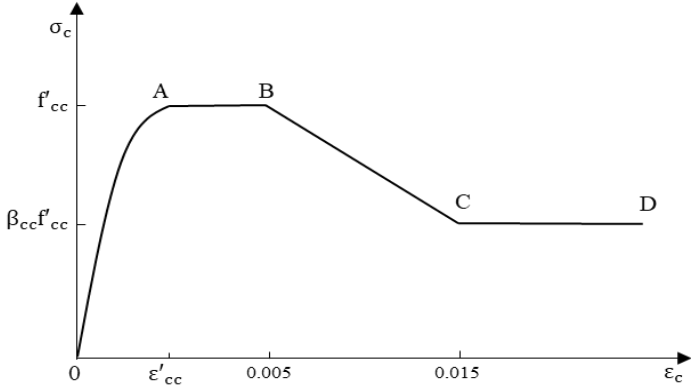


Fig.4 Stress-strain curve for sandwiched concrete in RDCFST columns.

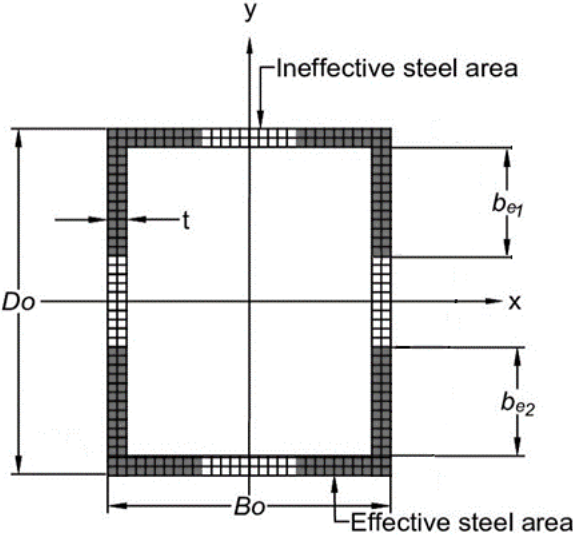


Fig. 5. Effective areas of outer steel tube cross-section

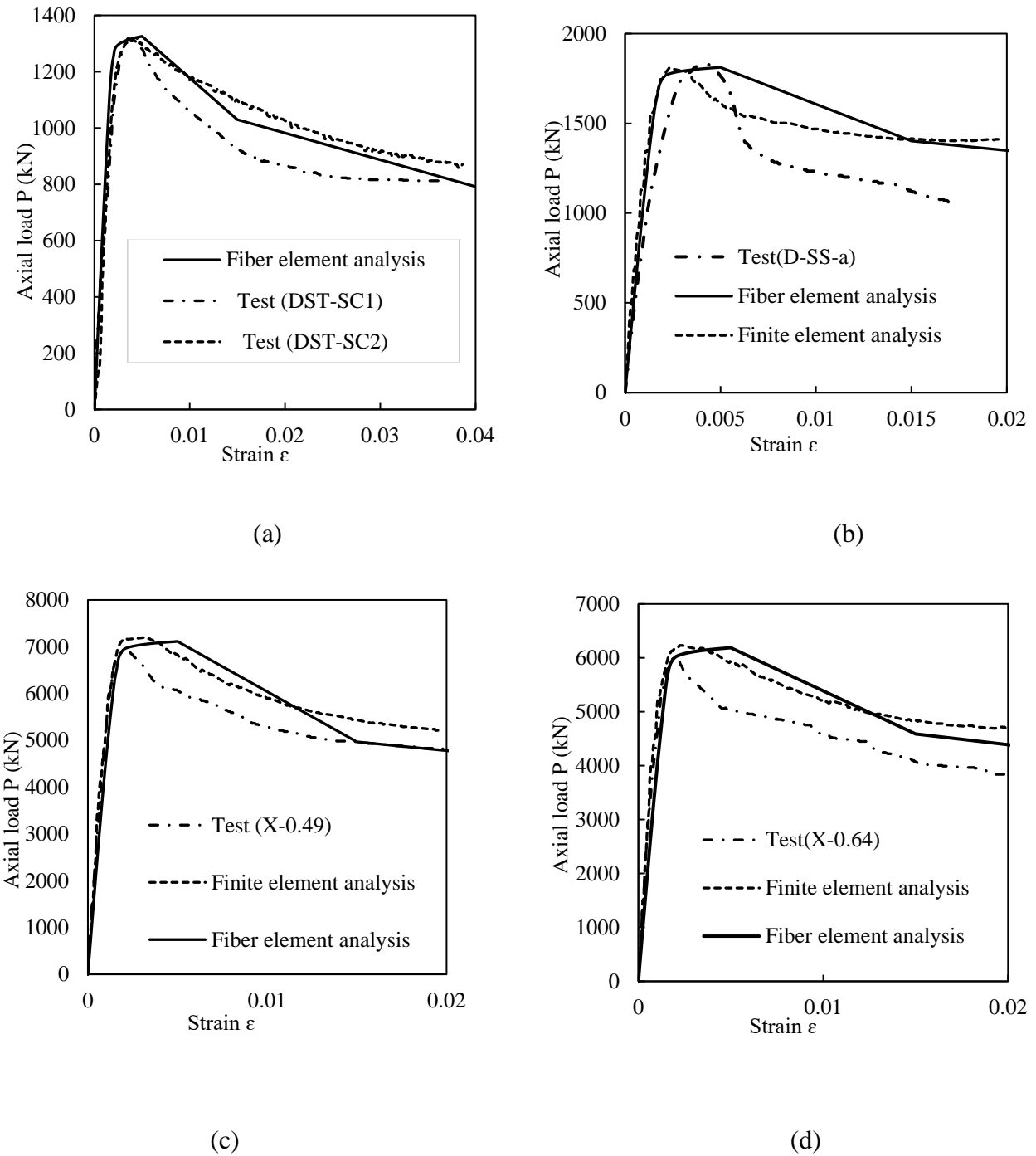


Fig. 6. Comparison of predicted and experimental axial load-strain curves of RDCFST and SDCFST short columns tested by (a) Tao and Han [2]; (b), (c) and (d) Ding et al. [14].

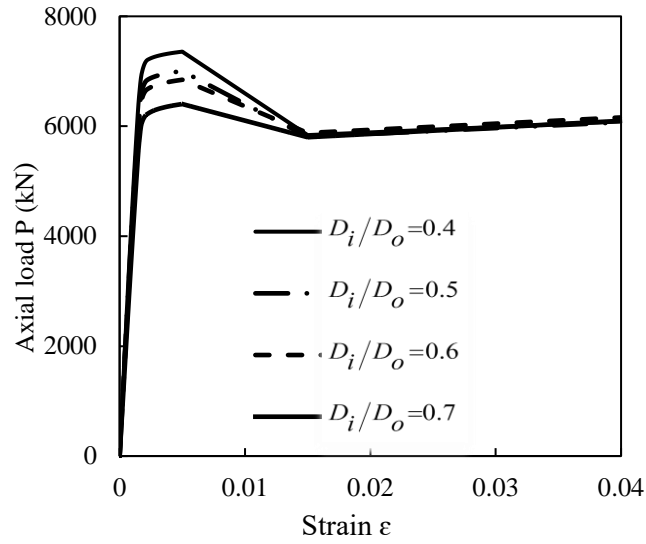


Fig. 7. Axial load-strain curves for RDCFST short columns with various D_i/D_o ratios.

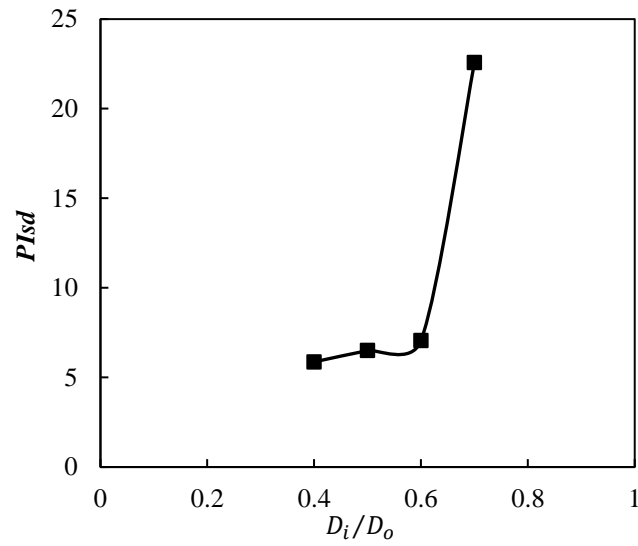


Fig. 8. The strain-ductility indices of RDCFST short columns with different D_i/D_o ratios

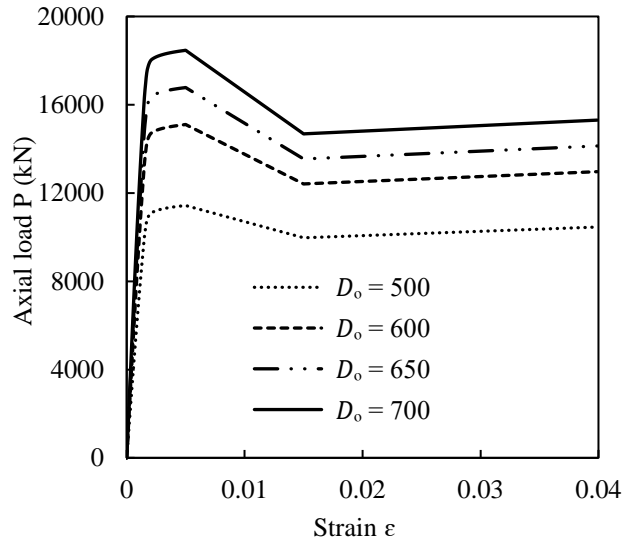


Fig. 9. The axial load-strain curves for RDCFST short columns with different D_o/t_o ratios ($D_o=500, 600, 650, 700$ mm $t_o=10$ mm)

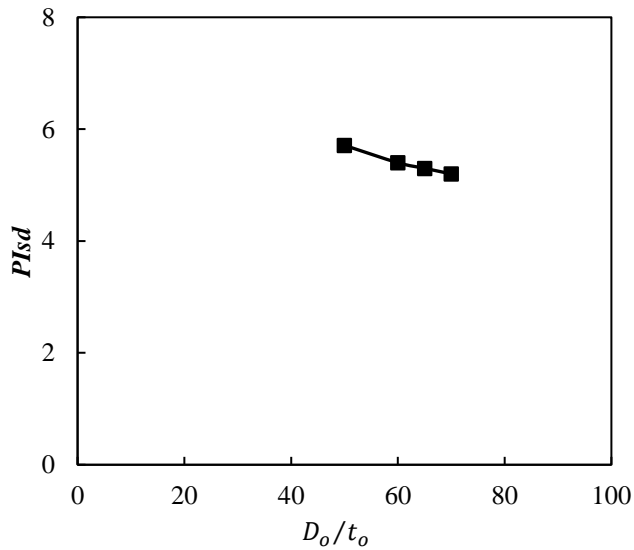


Fig. 10. The strain-ductility indices of RDCFST short columns with different D_o/t_o ratios ($D_o=500, 600, 650, 700$ mm $t_o=10$ mm)

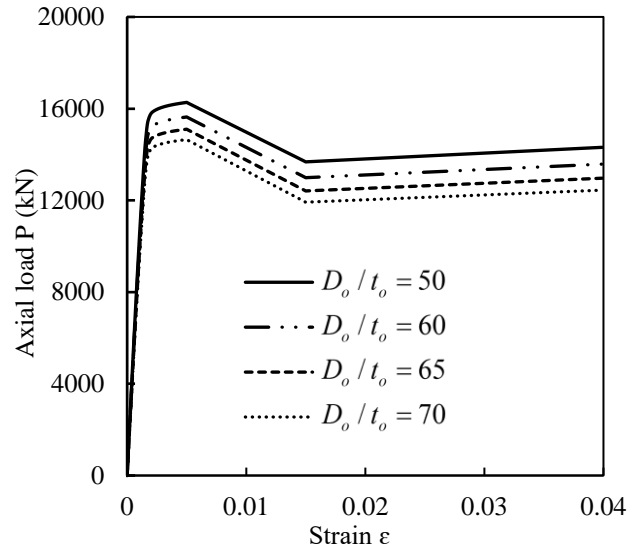


Fig. 11. The axial load-strain curves for RDCFST columns with different D_o/t_o ratios ($D_o=600$ mm, $t_o=12, 10, 9.23, 8.57$ mm)

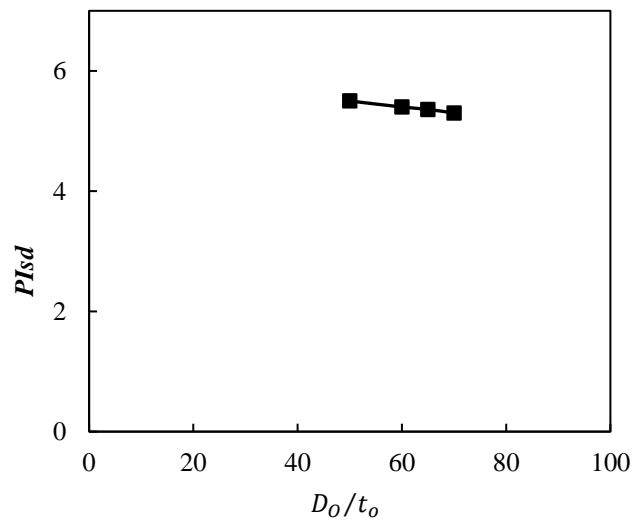


Fig. 12. The strain-ductility indices of RDCFST short columns with different (D_o/t_o) ratios ($D_o=600$ mm, $t_o=12, 10, 9.23, 8.57$ mm)

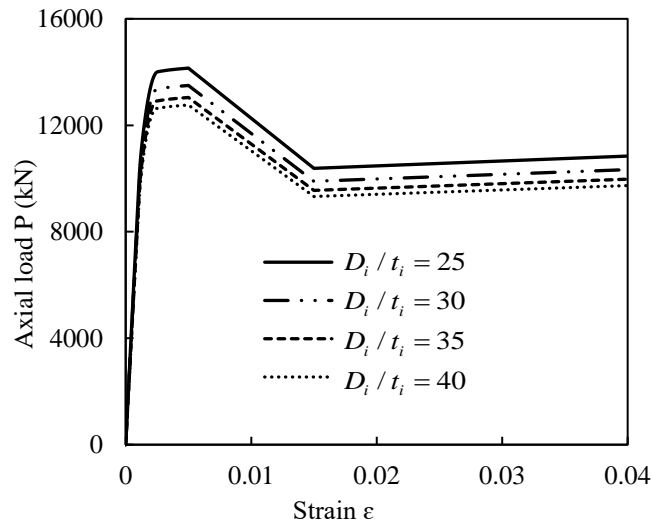


Fig. 13. The axial load-strain curves for RDCFST short columns with different D_i/t_i ratios

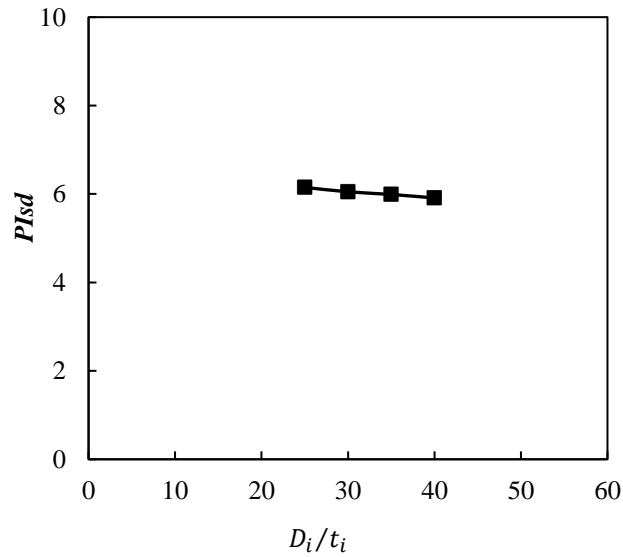


Fig. 14. The strain-ductility indices of RDCFST short columns with different D_i/t_i ratios

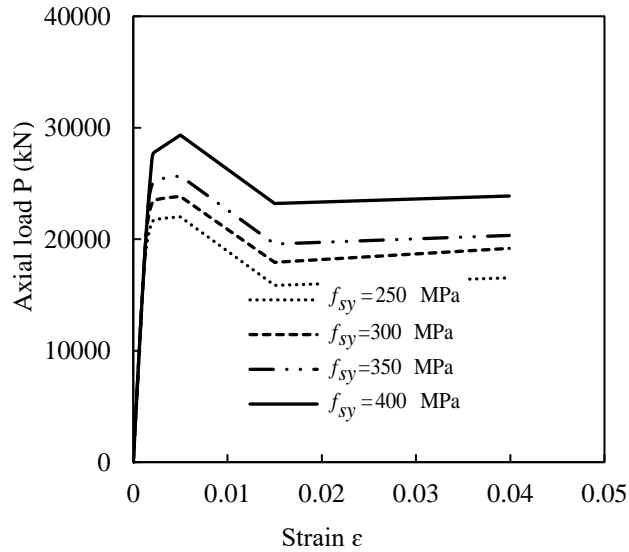


Fig. 15. Axial load-strain curves for RDCFST short columns with influences of steel yield strength

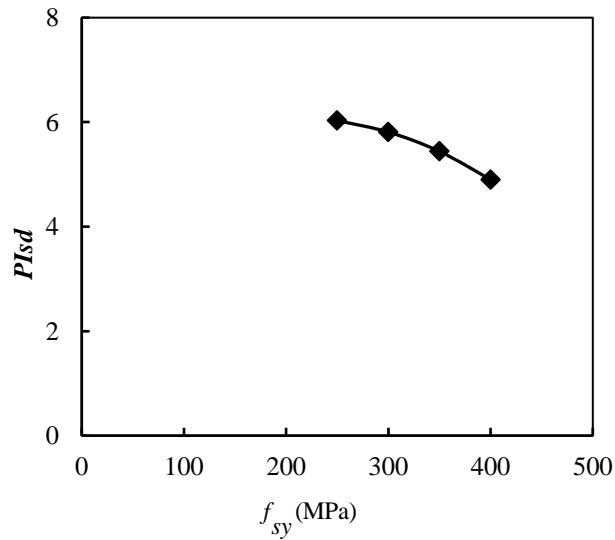


Fig. 16. Strain ductility indices of RDCFST short columns with influences of steel yield strength

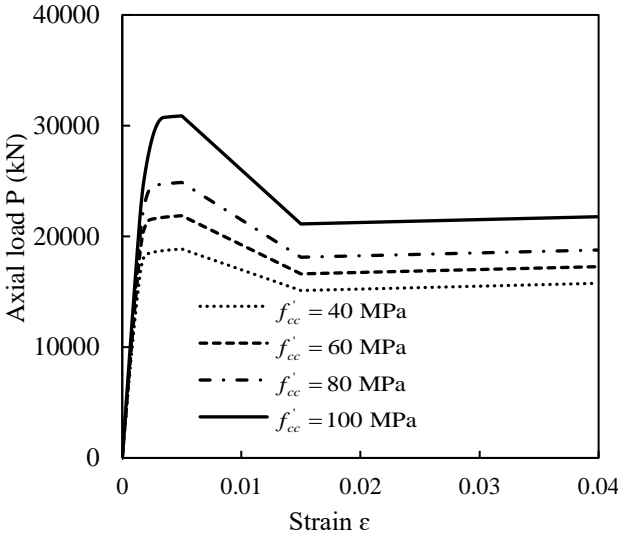


Fig. 17. Axial load-strain curves for RDCFST short columns with influences of concrete strength

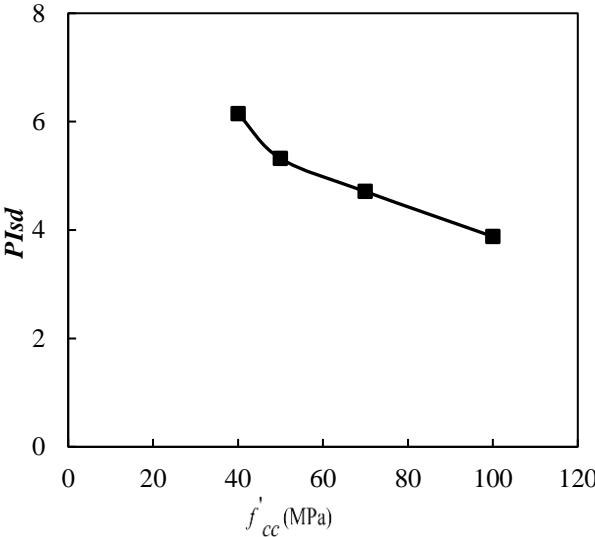


Fig. 18. Strain ductility indices of RDCFST short columns with influences of concrete strength.

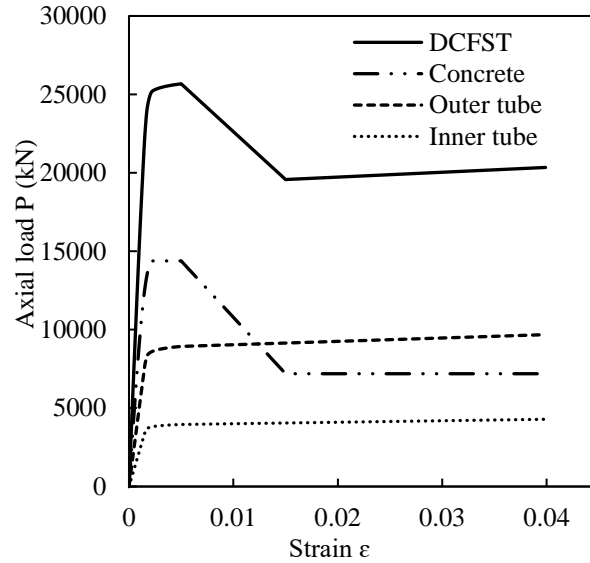


Fig. 19. Load distribution in concrete and steel tubes in a RDCFST column

Table 1 Ultimate axial strengths of RDCFST and SDCFST short columns.

Specimen	Outer tube			Inner tube			Concrete	Ultimate axial load			Ref
	$B_o \times D_o \times t_o$ <i>mm</i>	D_o / t_o	f_{sy0} <i>Mpa</i>	$B_i \times D_i \times t_i$ <i>mm</i>	D_i / t_i	f_{syi} <i>Mpa</i>	f'_{cc} <i>Mpa</i>	$P_{u,exp}$ <i>kN</i>	$P_{u,num}$ <i>kN</i>	$\frac{P_{u,num}}{P_{u,exp}}$	
DST-SC1	100×150×3.2	46.9	380	45×75×3.2	23.4	429	46	1320	1325.6	1.004	[2]
DST-SC2	100×150×3.2	46.9	380	45×75×3.2	23.4	429	46	1320	1325.6	1.004	
D-SS-a	160×160×3.62	44.2	374	53×53×2.7	19.6	304	50.5	1819	1811	0.995	[14]
X-0.49	500×500×3.0	166.7	353	350×350×3.0	116.7	353	39.8	6939	7112	1.02	
X-0.64	500×500×3.0	166.7	353	400×400×3.0	133.3	353	39.8	6090	6186	1.01	
FR120×3- NS20×2.5-C40	79.8×119.8×2.86	41.9	401	19.9×19.9×2.59	7.7	468	39.5	909.9	851.1	0.935	
FR120×3- NS20×2.5-C80	79.8×119.8×2.85	42.1	401	20.0×20.0 ×2.67	7.5	468	78.4	1161.3	1152.23	0.991	

FR120×3- NS20×2.5-C120	79.8×119.8×2.88	41.7	401	19.9×19.9×2.61	7.7	468	101.9	1469.3	1364.6	0.928	[13]
FR120×3- NS20×1.5-C40	79.8×119.8×2.87	41.7	401	20.3 ×20.3 ×1.52	13.3	357	39.5	855.9	790.2	0.923	
FR120×3- NS20×1.5-C40R	79.7×119.8×2.88	41.6	401	20.2 ×20.2 ×1.53	13.2	357	39.5	864.4	791.2	0.915	
FR120×3- NS20×1.5-C80	79.7×119.8×2.87	41.7	401	20.2 ×20.2 ×1.54	13.1	357	78.4	1154.9	1106	0.957	
FR120×3- NS20×1.5-C120	79.7×119.8×2.86	41.8	401	20.2 ×20.2 ×1.53	13.2	357	101.9	1408.5	1296	0.920	
FR100×4- NS20×2.5-C40	79.8×99.9×3.83	26.1	439	20.0 ×20.0 ×2.60	7.7	468	39.5	1030.4	922	0.894	
FR100×4- NS20×2.5-C80	79.8×100.0×3.79	26.4	439	20.0 ×20.0 ×2.65	7.5	468	78.4	1235.2	1167	0.944	

Table.2 Geometric and material properties of RDCFST short columns employed in parametric investigations.

Groupe	Columns	$B_o \times D_o \times t_o$ <i>mm</i>	D_o / t_o	f_{sy0} <i>Mpa</i>	$B_i \times D_i \times t_i$ <i>mm</i>	D_i / t_i	f_{syi} <i>Mpa</i>	f'_{cc} <i>Mpa</i>	f_{suo}, f_{sui} <i>Mpa</i>
1	C1	265×400×6.7	60	350	106×160×6	26.7	350	40	430
	C2	265×400×6.7	60	350	132×200×6	33.3	350	40	430
	C3	265×400×6.7	60	350	160×240×6	40	350	40	430
	C4	265×400×6.7	60	350	175×280×6	46.7	350	40	430
2	C5	310×500×10	50	350	150×240×10	24	350	40	430
	C6	375×600×10	60	350	150×240×10	24	350	40	430
	C7	405×650×10	65	350	150×240×10	24	350	40	430
	C8	435×700×10	70	350	150×240×10	24	350	40	430
3	C9	375×600×12	50	350	150×240×10	24	350	40	320
	C10	375×600×10	60	350	150×240×10	24	350	40	320
	C11	375×600×9.23	65	350	150×240×10	24	350	40	320

4	C12	375×600×8.57	70	350	150×240×10	24	350	40	320
	C13	340×550×10	55	250	150×250×10	25	250	60	320
	C14	340×550×10	55	250	150×250×8.33	30	250	60	320
	C15	340×550×10	55	250	150×250×7.14	35	250	60	320
	C16	340×550×10	55	250	150×250×6.25	40	250	60	320
5	C17	491×800×10	70	250	225×360×10	36	250	50	320
	C18	491×800×10	70	300	225×360×10	36	300	50	430
	C19	491×800×10	70	350	225×360×10	36	350	50	430
	C20	491×800×10	70	450	225×360×10	36	450	50	520
6	C21	435×700×10	70	350	175×280×10	28	350	40	430
	C22	435×700×10	70	350	175×280×10	28	350	50	430
	C23	435×700×10	70	350	175×280×10	28	350	70	430
	C24	435×700×10	70	350	175×280×10	28	350	100	430

Table 3 Comparison of calculated and experimental ultimate axial-loads of RDCFST and SDCFST short columns.

Specimen	γ_c	f'_{cc} Mpa	f_{syi} Mpa	f_{syo} Mpa	$P_{u,cal}$ kN	$P_{u,exp}$ kN	$\frac{P_{u,cal}}{P_{u,exp}}$
DST-SC1	0.94	46	429	380	1325.6	1320	1.004
DST-SC2	0.94	46	429	380	1325.6	1320	1.004
FR120×3-NS20×2.5-C40	0.97	39.5	468	401	851.1	909.9	0.935
FR120×3-NS20×2.5-C80	0.97	78.4	468	401	1152.23	1161.3	0.991
FR120×3-NS20×2.5-C120	0.97	101.9	468	401	1364.6	1469.3	0.928
FR120×3-NS20×1.5-C40	0.97	39.5	357	401	790.2	855.9	0.923
FR120×3-NS20×1.5-C40R	0.97	39.5	357	401	791.2	864.4	0.915
FR120×3-NS20×1.5-C80	0.97	78.4	357	401	1106	1154.9	0.957
FR120×3-NS20×1.5-C120	0.97	101.9	357	401	1296	1408.5	0.920
FR100×4-NS20×2.5-C40	1	39.5	468	439	922	1030.4	0.894
FR100×4-NS20×2.5-C80	1	78.4	468	439	1167	1235.2	0.944
Mean							0.946
SD (Standard deviation)							0.056
COV (Coefficient of variation)							0.059

3.3 CONCLUDING REMARKS

In this chapter, numerical investigations on the responses of RDCFST short columns that are concentrically loaded have been presented. A new computational modeling technology employing fiber discretization has been developed that calculates the structural performance of short RDCFST columns incorporating the gradual localized buckling of both the internal and external thin-walled sections. The developed computer simulation program can simulate the progressive localized buckling from the onset of the critical localized instability to the post-localized buckling failure. The accuracy of the modeling program has been confirmed

by experimental results documented elsewhere. The computational model described can be used to predict the ductility and strength performance of RDCFST columns when designing such composite columns. The numerical results obtained in the parametric studies by using the computer program have provided better understanding of the structural behavior of RDCFST columns. The proposed design formula, which accounts for the post-localized buckling strength of both external and internal steel tubes, can be used in the strength design of RDCFST short composite columns.

Chapter 4

SIMULATION AND BEHAVIOR OF RDCFST SLENDER COLUMNS

4.1 INTRODUCTION

Experiments indicated that the failure of RDCFST slender columns that were subjected to axial compression or eccentric loading was caused by the localized buckling of the outer and inner steel sections as well as the overall buckling. The interaction of local-global buckling problem is so complicated that it has not been considered in any existing fiber-based computational technique for nonlinear simulations. This chapter describes the formulations of a new mathematical modeling approach for slender RDCFST columns and the structural behavior of slender RDCFST columns. The computational fiber-element technique accounts for the interaction of local and global instability, material nonlinearity and geometric imperfections in the determination of load-deflection responses of RDCFST columns. The proposed computational simulation technique is verified by comparison of with the existing test results. The numerical model has been employed to study the significance of important parameters on the responses of RDCFST slender columns under eccentric loading conditions.

The following paper is included in this chapter:

Rizwan, M., Liang, Q. Q., & Hadi, M. N.S. (2021). Numerical analysis of rectangular double-skin concrete-filled steel tubular slender columns incorporating interaction buckling. *Engineering Structures*, 245:112960.

<https://doi.org/10.1016/j.engstruct.2021.112960>



THE NEW WAY TO DO UNI

OFFICE FOR RESEARCH TRAINING, QUALITY AND INTEGRITY

DECLARATION OF CO-AUTHORSHIP AND CO-CONTRIBUTION: PAPERS INCORPORATED IN THESIS

This declaration is to be completed for each conjointly authored publication and placed at the beginning of the thesis chapter in which the publication appears.

1. PUBLICATION DETAILS (to be completed by the candidate)

Title of Paper/Journal/Book:	Rizwan, M., Liang, Q. Q., & Hadi, M. N. S (2021). Numerical analysis of rectangular double-skin concrete-filled steel tubular slender columns incorporating interaction buckling. Engineering Structures, 245:112960.		
Surname:	Rizwan	First name:	Muhammad
Institute:	Institute for Sustainable Industries and Liveat	Candidate's Contribution (%):	60
Status:			
Accepted and in press:	<input type="checkbox"/>	Date:	<input type="text"/>
Published:	<input checked="" type="checkbox"/>	Date:	14/08/2021

2. CANDIDATE DECLARATION

I declare that the publication above meets the requirements to be included in the thesis as outlined in the HDR Policy and related Procedures – policy.vu.edu.au.

<input type="text"/>	<input type="text" value="19/10/2021"/>
Signature	Date

3. CO-AUTHOR(S) DECLARATION

In the case of the above publication, the following authors contributed to the work as follows:

The undersigned certify that:

1. They meet criteria for authorship in that they have participated in the conception, execution or interpretation of at least that part of the publication in their field of expertise;
2. They take public responsibility for their part of the publication, except for the responsible author who accepts overall responsibility for the publication;

PO Box 14428, Melbourne,
Vic 8001, Australia
+61 3 9919 6100

Victoria University ABN 83776954731
CRICOS Provider No. 00124K (Melbourne),
02475D (Sydney), RTO 3113



**VICTORIA
UNIVERSITY**

THE NEW WAY TO DO UNI

3. There are no other authors of the publication according to these criteria;
4. Potential conflicts of interest have been disclosed to a) granting bodies, b) the editor or publisher of journals or other publications, and c) the head of the responsible academic unit; and
5. The original data will be held for at least five years from the date indicated below and is stored at the following location(s):

D:\RDCFST

Name(s) of Co-Author(s)	Contribution (%)	Nature of Contribution	Signature	Date
Muhammad Rizwan	60	Methodology, Software, Validation, Formal analysis, Investigation, Data curation, Writing-original draft, Visualization.		19/10/2021
Qing Quan Liang	30	Conceptualization, Methodology, Software, Validation, Writing-Review and Editing, Supervision, Project administration.		20/10/2021
Muhammad N. S. Hadi	10	Validation, Writing - Review and Editing, Supervision.		21.10.2021

Updated: September 2019

PO Box 14428, Melbourne,
Vic 8001, Australia
+61 3 9919 6100

Victoria University ABN 83776954731
CRICOS Provider No. 00124K (Melbourne),
02475D (Sydney), RTO 3113

Manuscript prepared for

Engineering Structures

April 2021

Numerical analysis of rectangular double-skin concrete-filled steel tubular slender columns incorporating interaction buckling

Muhammad Rizwan^a, Qing Quan Liang^{a,*}, Muhammad N. S. Hadi^b

^a College of Engineering and Science, Victoria University, PO Box 14428, Melbourne, VIC 8001, Australia

^b School of Civil, Mining and Environmental Engineering, University of Wollongong, Wollongong, NSW 2522, Australia

Corresponding author:

Dr. Qing Quan Liang
College of Engineering and Science
Victoria University
PO Box 14428
Melbourne VIC 8001
Australia
E-mail: Qing.Liang@vu.edu.au

Numerical analysis of rectangular double-skin concrete-filled steel tubular slender columns incorporating interaction buckling

Muhammad Rizwan^a, Qing Quan Liang^{a,2}, Muhammad N. S. Hadi^b

^a *College of Engineering and Science, Victoria University, PO Box 14428, Melbourne, VIC 8001, Australia*

^b *School of Civil, Mining and Environmental Engineering, University of Wollongong, Wollongong, NSW 2522, Australia*

ABSTRACT

Rectangular double-skin concrete-filled steel tubular (RDCFST) slender columns made of non-compact or slender steel sections under axial load and bending may undergo local-global interaction buckling, which is rarely considered in existing fiber-based nonlinear modeling procedures for RDCFST columns. In this paper, a new computational model is presented, which can simulate the load-deflection responses of uniaxially loaded thin-walled RDCFST slender columns that are discretized into fiber elements. The important features associated with thin-walled RDCFST slender columns are explicitly accounted for in the computational model, including the interaction between the local buckling of outer and inner steel tubes and the column global buckling, initial geometric imperfections, material nonlinearities and

²Corresponding author.

E-mail address: Qing.Liang@vu.edu.au (Q. Q. Liang)

second order effects. An incremental-iterative computational algorithm is developed to capture the nonlinear buckling displacements of RDCFST columns. The nonlinear equilibrium equation generated at each iteration is solved by means of implementing Müller's numerical scheme. The computational model, which is verified by experimental results, is utilized to investigate the interaction buckling responses of RDCFST columns loaded eccentrically, considering a wide range of design parameters. It is demonstrated that the developed computational modeling and simulation technique can detect the initial local buckling of double-skins and capture the influences of the interaction of localized and global instability on the performance of nonlinear RDCFST slender columns. The benchmark numerical results obtained from the parametric study provide a new insight into the interaction buckling behavior of RDCFST columns.

Keywords: Concrete-filled composite beam-columns; Double-skins; Interaction buckling; Local and post-local buckling; Nonlinear simulation.

2. Introduction

Rectangular double-skin concrete-filled steel tubular (RDCFST) slender columns as shown in Fig. 1 have the advantages of high bending stiffness-to-weight ratio and high ductility over rectangular concrete-filled steel tubular (CFST) columns with the same size and steel area [1-5]. The internal hollow steel tube in a RDCFST column can be utilized to house building services to avoid external exposure. The RDCFST slender columns (with member

slenderness ratio greater than 22) are often employed in tall composite buildings owing to their ease of connection to composite beams in comparison with circular DCFST columns. However, the confinement produced by circular tubes in circular DCFST columns increases the strength of the filled concrete thereby the resistances of the DCFST columns [6-10]. To maximize the economic benefits, thin steel tubes that are non-compact or slender sections are used to form RDCFST slender columns. However, this may cause the interaction buckling of steel tubes and composite column. Under the increasing eccentric loading, the interaction between the localized instability of both the external and internal tubes and the column global buckling takes place progressively. This interaction buckling problem in a RDCFST column is so complicated that it has not been considered in existing computer modeling approaches. The codified methods are given for determining the strength of CFST columns without considering the interaction buckling and cannot be used to predict the complete responses of RDCFST composite columns. Therefore, an efficient computational model is much needed that can capture the interaction buckling characteristics of RDCFST slender columns when subjected to eccentric loading.

Experimental studies on the performance of high-strength slender CFST columns of rectangular and square cross-sections have been conducted by investigators. Varma et al. [11] reported experimental results on square CFST slender columns under uniaxial bending. The width-to-thickness (b/t) ratios of the steel tubes were in the range from 32 to 48. The high strength concrete with 110 MPa was used in the columns. It has been shown that CFST square slender columns failed by the interaction of buckling and the crushing of concrete. The effects of axial load and b/t ratio on the column ductility curvature were remarkable. Vrcelj and Uy

[12,13] investigated the responses of concentrically loaded slender square columns experimentally and numerically. Moreover, the experimental behavior of square CFST slender columns under eccentric loads has been investigated by Mursi and Uy [14]. The steel tubes filled with 60 MPa concrete and b/t ratios of 36, 46.4 and 56.8 were selected. Furthermore, Mursi and Uy [15] carried out experiments on square CFST slender columns eccentrically loaded and made of 20 MPa concrete and 761 MPa steel tubes. It has been stated that square CFST slender columns failed due to an outward localized buckling and global buckling. The behavior of eccentrically loaded high strength rectangular CFST columns was experimentally explored by Liu [16]. The steel tubes had 550 MPa yield stress and the strengths of concrete were selected as 70.8 MPa and 82.1 MPa which were used to construct high strength columns. The failure modes of CFST columns were stated as an outward local buckling occurred in outer tube and crushing of sandwiched concrete coupled with overall buckling of slender column. Recently, Du et al. [17, 18] conducted tests on rectangular CFST slender columns under eccentric compression. The studied parameter was selected as b/t ratios varying from 21 to 42.6. The failure modes were identified, which included the plate localized buckling, the column global instability, encased concrete crushing inside the tubes, and the weld cracking.

The strength and ductility of double-skin concrete-filled steel tubular (DCFST) columns with inner hollow tube as represented in Fig. 1 were researched by Tao and Han [3], Tao et al. [19], Zhao et al. [20] as well as Han et al. [21,22]. Han et al. [21,22] discussed the structural responses of eccentrically loaded square DCFST slender columns and DCFST members loaded cyclically. The hollow section ratio, loading eccentricity and slenderness ratio were

selected as variables. Han et al. [21] also proposed a model for the determination of the responses of slender DCFST square columns uniaxially loaded. Furthermore, a recommendation of the simplified method was made for determining the load-carrying capacities of DCFST columns. Ahmed et al. [23] conducted experiments on square CFST slender columns consisting of an internal circular steel tube. It has been confirmed that the incorporation of an inner steel tube and concrete enhanced the ultimate strength of CFST columns.

There were limited experimental studies conducted on RDCFST slender columns subjected to axial compression and eccentric loading in the past [3-5,24]. Tao and Han. [3] conducted experiments on 24 RDCFST slender columns that had the loading eccentricity ratios varying from 0.0 to 60, inner-to-outer tube-depth ratio of 0.5 and the slenderness ratios varying from 26 to 53. The test results showed that the overall buckling was the failure mode of the slender RDCFST columns. It was reported that the flexural stiffness and ultimate load of RDCFST slender columns were reduced by means of increasing the L/r ratio or e/D ratio. Specimens with a larger L/r ratio showed a better ductility. Liang et al. [4] tested 15 specimens under axial compressive load and 25 specimens under eccentric compression load. For the construction of steel tubes and stiffeners, a cold-formed steel tube with 2 mm thick, 235 MPa yield strength, and 210 GPa elasticity modulus was chosen. Moreover, the three different lengths of the specimens (400 mm, 500 mm, and 600 mm) were selected for each section type. It was shown that when the eccentricity ratio increased, the load-carrying capacity of the specimen decreased. By comparison with corresponding axially loaded columns, the typical ultimate strength of specimens with an eccentricity ratio of 0.3 decreased by 10 to

23%, whereas the strengths of specimens with an eccentricity ratio of 0.7 reduced by 29 to 38%. Moreover, when the eccentricity ratio was greater than 0.7, the load-carrying capacity of specimens decreased expressively with an increase in the length of specimens. The characteristic failure of the specimen was observed as that the outer steel tube buckled outward while the inner tube buckled inward, and the sandwiched concrete crushed. Overall, the columns failed due to the interaction of local and global buckling.

Sulthana and Jayachandran [5] studied the response of slender concrete filled columns with double skin steel tubes made of hot rolled steel. In the experimental investigations led by the authors, the specimen had a L/r ratio of 20. The failure manner of the slender columns was stated as the overall buckling associated with cross section yielding. At the stage of post buckling, the yielding of cross section took place at the mid-height of the column, where a local buckling shaped at the compression part of outer steel tube was identified. The yielded part of the column was reported as a blown out. The failure mode was an overall buckling in slender DCFST columns. Fan et al. [24] performed experiments on double skin concrete filled square columns. The parameters chosen were the thickness, and cross-sectional dimensions of the inner and outer tubes. The column length and outer depth were kept unchanged for all the specimens. The thickness of steel tubes was selected to avoid localized buckling according to design specifications. The authors informed that the concrete slowed down the process of accumulating the local buckling in the steel tubes and there was no crack detected.

The inflexible analysis techniques were used to model the structural behavior of rectangular CFST columns that were slender [12,25-27]. Shanmugam et al. [25] presented a numerical modeling scheme that computes the responses of slender CFST columns including localized buckling failure. Mursi and Uy [14,15] developed a numerical scheme, which ascertains the strength of eccentrically loaded thin-walled CFST slender columns including localized instability. However, the effective width expressions of steel plates under uniform stresses adopted by the authors are not applicable to steel tubes subjected to non-uniform compression. Furthermore, their approach has not accounted for the gradual post buckling. Patel et al. [26] and Liang et al. [27] presented the development of mathematical models employing fiber discretization for the response prediction of slender rectangular CFST columns that were designed to sustain axial loads in addition to uniaxial or biaxial bending. The numerical simulation scheme has demonstrated to yield accurate predictions of structural responses. Du et al. [17,18] and Xiong et al. [28] employed the computational program finite-element (FE) ABAQUS to examine the rectangular CFST slender columns eccentrically loaded without consideration of local buckling.

The computational simulation models that calculate the nonlinear effects of square and rectangular CFST columns have been established and implemented by Liang [29,30], Liang et al. [31], Patel et al. [32,33], and Patel [34]. A performance-based analysis technique incorporating local-buckling and post local-buckling response of rectangular CFST columns was proposed by Liang [29,30] and Liang et al. [31]. The numerical analysis methods suggested by Liang [29] give more accurate outcomes on the performance of square and rectangular CFST columns. However, very limited computational research has been

undertaken on the performance of DCFST short and slender columns composed of rectangular steel sections. The strength and responses of DCFST and CFDST short and slender columns with different cross-sections types were examined numerically by Ahmed et al. [23], Elchalakani et al. [35], Liang [36] and Hassanein et al. [37]. The computational based formulation method using fiber approach was presented by Ahmed et al. [38] for rectangular high-strength CFDST short columns under concentric loading incorporating the confinement as well as localized instability of the external steel tube. Furthermore, Ahmed et al. [23] formulated a theoretical method of nonlinear simulation of CFDST and DCFST slender columns with square outer and circular inner sections. The impacts of the specimen slenderness ratio, eccentricity, local and post local buckling, and the outer tube thickness on the load-deflection responses were studied. However, the above-stated numerical models have not been formulated for RDCFST slender columns.

This paper represents a new computational model of the performance of eccentrically-loaded RDCFST slender columns filled with concrete of different strengths. To analyze the axial load-deflection responses of RDCFST slender columns, the numerical model is developed that includes buckling effects, and material and geometric nonlinearities. The accurate constitutive relationships of structural steels and infilled concrete are given. The numerical model is verified by the experimental results documented elsewhere. A parametric investigation is conducted to determine the influences of material strengths and geometric factors on the performance of load-deflection, columns strength, and load contributions of slender RDCFST columns.

2. Modeling and simulation of interaction buckling

2.1 Fiber element simulation of composite cross-sections

The numerical model has been formulated by the fiber element method to simulate the nonlinear buckling of RDCFST slender columns [29-34]. The cross-section of a RDCFST column is meshed into fibers as shown in Fig. 2. The original mesh established by Liang [29] has been used to discretize the sandwiched concrete and steel tubes. It has been assumed that the plane section remains plane after it deforms. This means that the strain profile along the cross-sectional depth illustrated in Fig. 2 is linear. The strain profile ensures that the compatibility condition of strains in the cross-section under the applied load can be attained [29]. It should be noted that this is an approximate solution to the strain distribution in the inelastic range of the steel and concrete. The local buckling of steel tubes is simulated by using the local buckling models proposed by Liang et al. [39] based the nonlinear finite element analysis results and the warping of steel elements is neglected. The stress-strain models of steel and concrete are employed to calculate the stresses in fibers from corresponding strains. The fiber strain can be calculated by using the curvature function (ϕ) and the depth of neutral axis (d_n). The internal moment (M) and axial force (P) are calculated by means of integrating the fiber stresses over the rectangular cross-section as stress resultants [29].

2.2 Mathematical modeling of progressive local buckling

The capacity of a slender RDCFST column is significantly reduced by localized and global instability [29-31], which has been considered in the current mathematical formulation of RDCFST columns to predict their nonlinear responses accurately. The tubular walls of a rectangular DCFST column subjected to axial compression and uniaxial bending are either under uniform or non-uniform stresses. Liang et al. [39] proposed a model that can calculate the critical stress of the localized buckling of steel tubes in CFST columns subjected to non-uniform stresses. Tests [2-5, 40] showed that the steel tubes of a RDCFST column buckled outward locally. Therefore, the model of Liang et al. [39] is employed to detect the initial localized buckling in the current numerical simulation of RDCFST columns.

Experiments reported by Zhao and Grzebieta [2] indicated that the internal tube generally buckled away from the filled concrete (inward localized buckling), except where the outer tube buckled, which resulted in the crushing of concrete nearby so that the outward localized buckling of the inner tube occurred. Tests undertaken by Tao and Han [3] showed that the steel tube walls of both external and internal tubes buckled locally away from the filled concrete. The effective width models proposed by Liang et al. [39] are for steel plates restrained by concrete that buckle locally away from the concrete. Therefore, the same effective width formulas developed by Liang et al. [39] are employed to model the post-localized buckling of both external and internal steel tubes. Figure 3 illustrates the effective widths b_{e1} and b_{e2} of the tubular wall in a RDCFST column loaded uniaxially, which can be expressed in mathematical form provided by Liang et al. [39] as

$$\frac{b_{e1}}{b} = \begin{cases} 0.2777 + 9.605 \times 10^{-7} (b/t)^3 - 1.972 \times 10^{-4} (b/t)^2 + 1.019 \times 10^{-2} (b/t) & \text{for } \alpha_s > 0.0 \\ 0.4186 - 4.685 \times 10^{-7} (b/t)^3 + 5.355 \times 10^{-5} (b/t)^2 - 2.047 \times 10^{-3} (b/t) & \text{for } \alpha_s = 0.0 \end{cases} \quad (1)$$

$$\frac{b_{e2}}{b} = (2 - \alpha_s) \frac{b_{e1}}{b} \quad (2)$$

where t stands for the tube thickness, b represents the clear width of the steel plate under consideration as illustrated in Fig. 3, α_s is $\alpha_s = \sigma_2/\sigma_1$, where σ_2 and σ_1 denote the minimum and maximum edge stresses on the plate, respectively. The maximum ineffective width ($b_{ne,max}$) of a steel tube wall is $(b - b_{e2} - b_{e1})$. The ineffective width (b_{ne}) due to the gradual post-buckling can be calculated by linear interpolation means based on the steel fiber stress level, which is written as

$$b_{ne} = b_{mne} \left(\frac{\sigma_s - \sigma_{cr}}{f_{sy} - \sigma_{cr}} \right) \quad (3)$$

where σ_{cr} represents the critical localized buckling stress of the steel plate, and f_{sy} stands for the steel yield strength. The mathematical expressions proposed by Liang [29] for the post-localized buckling strengths of steel tube walls are incorporated in the current computational analysis method to include post-localized instability into the overall buckling modeling of slender RDCFST columns.

The computational simulation method uses the fiber element technique to discretize the cross-section of rectangular CFST and RDCFST slender columns as presented by Liang [29,30], Liang et al. [31,39], Patel et al. [26,32,33], and Ahmed et al. [23,38]. A typical mesh of fiber discretization of a cross section is presented in Fig .2. The fibers of external and inner steel tubes can be assigned different material properties, while the concrete properties are given to the fibers of sandwiched concrete. The uniaxial materials constitutive laws are used to calculate stresses in fibers from the corresponding strains, which can be determined by the curvature (ϕ) and neutral axis depth (d_n) with reference to eccentric compression as shown in Fig. 2. The stress resultants are determined by

$$P = \sum_{j=1}^{nso} \sigma_{so,j} A_{so,j} + \sum_{k=1}^{nsi} \sigma_{si,k} A_{si,k} + \sum_{n=1}^{nc} \sigma_{c,n} A_{c,n} \quad (4)$$

$$M = \sum_{j=1}^{nso} \sigma_{so,j} A_{so,j} y_j + \sum_{k=1}^{nsi} \sigma_{si,k} A_{si,k} y_k + \sum_{n=1}^{nc} \sigma_{c,n} A_{c,n} y_n \quad (5)$$

where P stands for the axial force; M is the bending moment about the x -axis; subscripts j , k and n represent the fibers in the outer and inner tubes, and concrete, respectively; notations so , si and c indicate the outer tube, internal tube and concrete, respectively; σ , A and y are the stress, area and coordinate of the fiber, respectively; nso , nsi and nc are the total number of fiber elements in the outer and inner tubes, and sandwiched concrete, respectively.

2.3 Mathematical modeling of global buckling

A numerical modeling scheme has been designed to simulate the interaction of local and global instability of RDCFST slender columns under axial compression and uniaxial bending. The formulation based on the mathematical expressions described by Liang [43], Liang et al. [27] and Patel et al. [26] for CFST columns is used to quantify the structural responses of slender RDCFST columns. The fiber method does not use connection elements to model the interface between the concrete and steel tubes. Consider a pin ended RDCFST slender column having an equal loading eccentricity (e) and under single curvature bending as depicted in Fig. 4. The modeling method employs the part-sine function for determining the buckling displacements of the slender RDCFST column. As shown by Liang [43], at the column mid-length, the curvature (ϕ_m) is

$$\phi_m = u_m \left(\frac{\pi}{L} \right)^2 \quad (6)$$

in which u_m represents the lateral deflection that occurs at the mid-height of the column, and L is the pin-ended column effective length.

In the formulation, the column's imperfection (u_o) and the second order effect due to the interaction of lateral displacement (u_m) and the axial load and are accounted for. The column mid-height is subjected to the following applied moment:

$$M_e = P(e + u_o + u_m) \quad (7)$$

The value of $L/1000$ is assigned to the imperfection (u_o) at the column mid-height. The simulation of a nonlinear slender RDCFST column loaded eccentrically is undertaken by means of gradually increasing the lateral displacement (u_m) at the column mid-height and determining the corresponding internal moment (M) and axial force (M), taking into account the localized buckling influence [26,27]. The axial load applied at the column ends is taken as the internal force that satisfies the condition of moment at the column mid-height. The above process can be repeated to produce a complete load-deflection response curve.

The moment equilibrium at the column mid-height can be maintained if the residual moment at each iteration is less than a specified small value, such as $|r_p| < \varepsilon_k = 10^{-4}$, where r_p is

$$r_p = M_i - P(e + u_o + u_m) \quad (8)$$

Figure 5 illustrates the computational flowchart for the axial load-displacement curve of a slender RDCFST column.

To satisfy the equilibrium condition, the neutral axis depth (d_n) of the column cross-section is iteratively adjusted by the efficient numerical solution algorithms incorporating Müller's method [42] as suggested by Patel et al. [26], Liang et al. [27] and Liang [43]. Three values

of the neutral axis depths d_{n1} , d_{n2} and d_{n3} are initialized before the computation can be started. The new neutral axis depth (d_{n4}) is determined by the following mathematical expressions and the process is repeated until the correct neutral axis depth is obtained:

$$d_{n4} = d_{n3} - \frac{2C}{B \pm \sqrt{B^2 - 4AC}} \quad (9)$$

$$A = \frac{(r_{p1} - r_{p2})(d_{n2} - d_{n3}) - (r_{p2} - r_{p3})(d_{n1} - d_{n3})}{(d_{n1} - d_{n2})(d_{n1} - d_{n3})(d_{n2} - d_{n3})} \quad (10)$$

$$B = \frac{(r_{p1} - r_{p3})(d_{n1} - d_{n3})^2 - (r_{p2} - r_{p3})(d_{n2} - d_{n3})^2}{(d_{n1} - d_{n2})(d_{n1} - d_{n3})(d_{n2} - d_{n3})} \quad (11)$$

$$C = r_{p3} \quad (12)$$

The values of d_{n1} , d_{n2} and d_{n3} are swapped to determine the true value [26,27,43].

3. Material constitutive relationships

3.1 Concrete in RDCFST columns

The stress-strain curves for infilled concrete in compression and tension are shown in Fig. 6. The ascending branch OA defines the early peak performance whereas the branches AB, BC and CD denote the post-ultimate behavior of concrete in compression. The improved ductility of concrete due to the steel encasement is taken into account in the constitutive laws of

concrete. The equations of Mander et al. [44] are employed to completely define branch OA depicted in Fig. 6 as follows:

$$\sigma_c = \frac{f'_{cc} \left(\varepsilon_c / \varepsilon'_{cc} \right) g}{g + \left(\varepsilon_c / \varepsilon'_{cc} \right)^g - 1} \quad (13)$$

$$g = \frac{E_c}{E_c - \left(f'_{cc} / \varepsilon'_{cc} \right)} \quad (14)$$

$$E_c = 6900 + 3320 \sqrt{f'_{cc}} \quad (\text{MPa}) \quad (15)$$

in which σ_c represents the longitudinal stress of compressive concrete, and ε_c is the strain. Young's modulus (E_c) of normal and high strength concrete is estimated by utilizing the equation provided by ACI Committee 363 [45].

The expressions for branches AB, BC and CD of the stress-strain curve illustrated in Fig. 6 are given as

$$\sigma_c = \begin{cases} f'_{cc} & \text{for } \varepsilon'_{cc} < \varepsilon_c \leq 0.005 \\ \beta_c f'_{cc} + 100(0.015 - \varepsilon_c)(f'_{cc} - \beta_c f'_{cc}) & \text{for } 0.005 < \varepsilon_c \leq 0.015 \\ \beta_c f'_{cc} & \text{for } \varepsilon_c > 0.015 \end{cases} \quad (16)$$

in which β_c represents the section influence on the ductility of concrete and it is subjected to the width-to-thickness ratio B_s / t of section of the RDCFST column, where B_s is chosen as

the higher value of B_o and D_o for a rectangular cross-section. The factor β_c was given by Liang [29] based on the tests outcomes offered by Tomi and Sakino [46] as

$$\beta_c = \begin{cases} 1.0 & \text{for } B_s / t \leq 24 \\ 1.5 - B_s / (48t) & \text{for } 24 < B_s / t \leq 48 \\ 0.5 & \text{for } B_s / t > 48 \end{cases} \quad (17)$$

The effective compressive strength of concrete f'_{cc} is influenced by the column size, the concrete quality and loading rate in the test and is determined as $f'_{cc}\gamma_c$, where γ_c is the strength reduction factor given by Liang [29] to account for the column size influence and is represented as

$$\gamma_c = 1.85D_c^{-0.135} \quad (0.85 \leq \gamma_c \leq 1.0) \quad (18)$$

in which D_c is chosen as the larger value of $(D_o - 2t_o)$ and $(B_o - 2t_o)$ for a rectangular cross-section, D_o denotes the cross-section depth, B_o represents the cross-section width and t_o indicates the steel tube thickness.

The sandwiched concrete in a RDCFST slender column that is eccentrically loaded can be in tension. The adopted stress-strain relationship of tensioned concrete is presented in Fig. 6. It is illustrated that the stress is a linear function of the tensile strain up to the cracking of concrete. After reaching the peak stress, the stress is assumed to linearly decrease with an

increase in the strain to zero. The tensile strength of concrete is estimated by the formula expressed as $0.6\sqrt{f'_{cc}}$. The ultimate tensile strain is assumed to be 10 times the cracking strain.

3.2 Structural steels

The adopted stress-strain relationships for structural steels is depicted in Fig. 7. The mild structural steels have a linear stress-strain relationship up to the yield stress. It is assumed that high strength steels and cold-formed steels have linear stress-strain relationship up to $0.9f_{sy}$, where f_{sy} is the yield strength of steel. The stress-strain curve's rounded part is described by the following expression provided by Liang [29]

$$\sigma_s = \left(\frac{\varepsilon_s - 0.9\varepsilon_{sy}}{\varepsilon_{st} - 0.9\varepsilon_{sy}} \right)^{\frac{1}{45}} f_{sy} \quad (0.9\varepsilon_{sy} < \varepsilon_s \leq \varepsilon_{st}) \quad (19)$$

where σ_s stands for steel stress, ε_s represents steel strain, f_{sy} indicates the steel yield stress, ε_{sy} stands for the yield strain of steel, ε_{st} is the steel strain at strain hardening. In the stress-strain relationship, the hardening strain ε_{st} is taken as $10\varepsilon_{sy}$ for mild structural steels and 0.005 for cold formed and high-strength steels. It is well-known that cold-formed and high-strength steels have less ductility than mild structural steels. The ultimate strain (ε_{su}) is

chosen as 0.2 for mild structural steels while it is taken as 0.1 for high-strength and cold-formed steels to account for the ductility of steel materials.

4. Verification of mathematical modeling

The experimental results on rectangular and square DCFST slender columns presented by Tao and Han [3], Liang et al. [4], Sulthana and Jayachandran [5] and Fan et al. [24] were utilized to validate the numerical model described in this paper. The particulars of the tested rectangular and square DCFST slender columns are listed in Table 1. The ratios of depth-to-thickness of all columns were in the ranges of $20 \leq D_o/t_o \leq 100$ and $15 \leq D_i/t_i \leq 55$. The outer and inner steel tubes tested by Tao and Han [3] had the tensile strengths of 476 and 473 MPa, respectively. The geometric imperfections of all columns were not measured in the experiments. However, in the numerical analyses, u_o at the column mid height was specified as $L/1000$.

The calculated ultimate axial strengths ($P_{u,num}$) and experimental ultimate axial strengths ($P_{u,exp}$) of DCFST slender columns are shown in Table 1. It appears that the average value of $P_{u,num}/P_{u,exp}$ is 0.959 associated with a standard deviation of 0.08 and a coefficient of variation of 0.081, which are acceptable for engineering purposes. The 23 specimens examined covered an extensive range of geometric and material properties as well as eccentric loads. It has been proved that the numerical modeling approach established an accurate analysis technique for quantifying the strengths of RDCFST slender columns.

Figure 8 shows the numerical and tested axial loads of RDCFST slender specimens as function of deflection investigated by Tao and Han [3]. The diagram demonstrates that the calculated axial load-deflection curves of RDCFST columns correlate reasonably well with measured responses. In addition, the predicted specimen's initial stiffness and ultimate loads are in good agreement with experimental ones. Moreover, the post-peak response of RDCFST columns has generally been well captured by the proposed simulation technique. However, a minor discrepancy between the tested and computed axial load-deflection responses can be identified. The experimental post-peak behavior of DCFST columns was significantly affected by the quality of concrete in the tested columns such as compaction, the premature fracture of steel tube, and loading rate. The discrepancy between the simulations and experiments in the post-peak behavior is likely caused by the poor quality of concrete and the premature fracture of steel tubes in the tested columns as the idealized stress-strain curves and material properties determined by compression and tension tests were used in the numerical model.

4. Parametric study

The developed computational modeling and simulation technique has been used to perform parametric studies on the structural performance of slender RDCFST columns exposed to eccentric loads. The parameters investigated were the D_i/D_o ratio, D_o/t_o ratio, D_i/t_i ratio, L/r ratio, e/D_o ratio, yield strengths of steel and concrete strengths. The specimens were categorized into seven groups and their particulars are given in Table 2. The Young's

modulus of steel was 200 GPa. The initial geometric imperfection of $L/1000$ at the column mid-height was incorporated in all analyses of slender columns.

4.1 The D_i/D_o ratio

The nonlinear analyses on the Category 1 specimens given in Table 2 have been undertaken to ascertain the effects of the D_i/D_o ratio on their axial load-deflection responses. The change to the depth of the internal tube was made to produce the D_i/D_o ratios of 0.25, 0.4, 0.55 and 0.7. Figure 9 shows the simulated response curves of RDCFST columns where the D_i/D_o ratios are from 0.25 to 0.7. The higher the D_i/D_o ratio, the lower the initial column stiffness and the ultimate axial load. It is noticeable that changing the ratio of D_i/D_o from 0.25 to 0.4, 0.55 and 0.7 has resulted in the decreases of 6.4%, 13.6% and 24.7% in the column's resistance, respectively. As demonstrated in Fig. 9, the column's ductility is decreased by means of increasing the ratio of D_i/D_o .

4.2 The D_o/t_o ratio

The computational simulations of RDCFST slender columns given in Group 2 in Table 2 have been performed to evaluate the impacts of the ratio of D_o/t_o on structural performance. The change of the depth of the outer tube from 500 mm to 650 mm was made to achieve the D_o/t_o ratios of 50, 55, 60 and 65. The axial loads with corresponding mid-height deflections

obtained are given in Fig. 10. It can be confirmed that the use of a higher D_o/t_o in terms of a larger D_o obviously increases the initial column stiffness. It is noted that the increase in the ultimate axial loads of DCFST slender columns due to employing a higher D_o/t_o ratio is significant. The computational results demonstrate that when the D_o/t_o ratio is changed from 50 to, 55, 60 and 65, the increase in the axial capacity of the columns is 23.20%, 43.2% and 63.8%, respectively.

4.3 The D_i/t_i ratio

The significance of the D_i/t_i ratios on the nonlinear responses of RDCFST columns has been studied by using the computer program. The specimens depicted in Group 3 listed in Table 2 had the $e/D_o = 0.2$ and $L/r = 50$. The change to the inner tube thickness was made to determine the D_i/t_i ratios of 20, 30, 35 and 40. The determined responses of the columns with varied D_i/t_i ratios with reference to axial loads and deflections are shown in Fig. 11. The D_i/t_i ratio does not have a noticeable effect on the column initial stiffness. However, increasing the ratio of D_i/t_i reduces the strength of RDCFST slender columns. The column's resistance could be reduced by 5.0%, 7.9% and 10.6%, respectively when the D_i/t_i ratio is altered from 20 to 30, 35 and 40.

4.4 Column slenderness ratio

The computer algorithms developed have been utilized to conduct the response simulations of slender RDCFST columns listed in Group 4 given in Table 2 to investigate the effects of slenderness ratios. The column length was changed to produce the member slenderness ratios of 40, 60, 80 and 100 and the column had a loading eccentricity (e/D_o) ratio of 0.25. The axial load-deflection responses of RDCFST columns are shown in Fig. 12. The initial stiffness and ultimate load of the columns considerably decrease due to the increase in the length of column. It appears from Fig. 12 that an increase in the L/r ratio improves the column's ductility. When the L/r ratio is changed from 40 to 60, 80 and 90, the column's resistance decreases by 9.22%, 20.4% and 25.7%, respectively. The slenderness ratio shows the most prominent influence on the performance of RDCFST columns.

4.5 Loading eccentricity ratio

The numerical model has been used to investigate the behavior of RDCFST columns with the e/D_o ratios from 0.1 to 0.4 as shown in Table 2 Group 5. The member slenderness ratio was 45. The simulated relations of axial load-deflections and loading eccentricity ratio are given in Fig. 13. The strength and ductility of RDCFST columns are considerably affected by the loading eccentricity. An increase in the eccentricity ratio causes a decrease in the strength and stiffness performance of RDCFST columns. Varying the ratio of e/D_o from 0.1

to 0.2, 0.3 and 0.4 causes the reductions of 19.1%, 33.5% and 46.1% in the resistance of the columns, respectively.

4.6. Concrete compressive strength

In Table 2 Group 6, RDCFST columns were designed with concrete strengths varying from 40 to 100 MPa. The column L/r ratio was 40 and the e/D_o ratio was 0.3. The slender RDCFST column's deflections with reference to increasing the loads are depicted in Fig. 14. It is seen that the usage of high strength concrete improves the initial stiffness of columns slightly. Most importantly, an increase in the sandwiched concrete strength results in a remarkable improvement in the ultimate axial strengths of the columns. By replacing the 40 MPa concrete with 60, 80 and 90 MPa concrete, the ultimate axial strength of the column increases by 18.4%, 36.5% and 53.5%, respectively.

4.7 Steel yield strength

The effects of the yield strengths of steel tubes in Group 7 presented in Table 2 on the behavior of RDCFST slender columns were examined. The specimens filled with high strength concrete of 90 MPa had the L/r ratio of 35 and e/D_o ratio of 0.35. The relations between the column axial loads, deflections and steel yield strengths are given in Fig. 15. The effect of the steel yield stress is not observed on the column's initial flexural stiffness. However, the use of steel tubes with a higher yield stress leads to an increase in the column's

capacity. The load-carrying capacity of the columns can be increased by 9.6%, 18.8% and 34.7% by changing the steel yield stress from 250 to 300, 350 and 450 MPa, respectively.

4.8 Load distributions in steel tubes and concrete

The developed computational technique has been utilized to quantify the load distributions in the sandwiched concrete and inner and outer steel tubes in eccentrically-loaded RDCFST columns. The numerical simulations of RDCFST slender columns in Group 4 provided in Table 2 have been performed to determine the significance of member slenderness on the distribution of loads in RDCFST columns. The simulated axial load and deflection responses of concrete and steel components of RDCFST slender columns are shown in Fig. 16. The sandwiched concrete resists most of the axial load. Both the concrete and steel tubes are subjected to compressive resultant forces irrespective of the L/r ratios when the axial load reduce to 60% of the column ultimate loads. The contribution ratios of concrete and steel tubes are shown in Fig. 17. It would appear that increasing the L/r ratio reduces the contribution of the inner and external steel tubes to the column capacity but increases the concrete contribution. The contribution ratios of inner tube, external tube and concrete were calculated as 0.22, 0.411 and 0.77, respectively.

In Group 5, the responses of RDCFST columns that had the L/r ratio of 45 as given in Table 2 were simulated to ascertain the significance of e/D_o ratio on the distribution of loads in slender RDCFST columns. Schematically depicted in Fig. 18 is the load distributions in the

components of concrete and steel. Both the steel tubes and concrete are subjected to compressive resultant forces when the axial load reduces to 60% of the column ultimate loads. Figure 19 shows that the contribution ratios of internal steel tube, external steel tube and the sandwiched concrete increase by increasing the e/D_o ratio.

5. Conclusions

A numerical model has been developed in this research paper for the response simulation of nonlinear slender RDCFST columns that are eccentrically loaded. The mathematical modeling approach explicitly accounts for the experimentally observed failure modes of the interaction of local and global instability, steel yielding and concrete crushing. The computer program developed can detect the initial localized buckling of both outer and inner steel tubes and fully monitor the progressive post-localized buckling in the nonlinear simulation of RDCFST columns in addition to the global column buckling. Measurements from experiments documented elsewhere have been used to verify the accuracy of the proposed computational simulation program. Parametric studies have been undertaken by means of using the computer program written. It has been demonstrated that the modeling scheme developed is an accurate and efficient computational technology for determining the ductility and strength performance of RDCFST columns incorporating non-compact or slender steel sections, which is not well treated in other numerical models and design codes.

References

- [1] Elchalakani M, Zhao XL, Grzebieta RH. Tests on concrete filled doubleskin (CHS outer and SHS inner) composite short columns under axial compression. *Thin-Walled Structures* 2002;40(5):415–41.
- [2] Zhao XL, Grzebieta RH. Strength and ductility of concrete filled double skin (SHS inner and SHS outer) tubes. *Thin-Walled Structures* 2002;40(5):415–41.
- [3] Tao Z, Han LH. Behaviour of concrete-filled double skin rectangular steel tubular beam–columns. *Journal of Constructional Steel Research* 2006; 62(7):631-646.
- [4] Liang W, Dong J, Wang Q. Mechanical behaviour of concrete-filled double-skin steel tube (CFDST) with stiffeners under axial and eccentric loading. *Thin-Walled Structures* 2019; 138:215-230.
- [5] Sulthana UM, Jayachandran SA. Axial compression behaviour of long concrete filled double skinned steel tubular columns. *Structures* 2017; 9:157-164.
- [6] Wei S, Mau ST, Vipulanandan C, Mantrala SK. Performance of new sandwich tube under axial loading: Experiment. *J Struct Eng, ASCE* 1995; 121(12): 1806-1814.
- [7] Zhao XL, Grzebieta R, Elchalakan M. Tests of concrete-filled double skin CHS composite stub columns. *Steel Compos Struct* 2002; 2(2): 129-146.
- [8] Han LH, Huang H, Tao Z, Zhao XL. Concrete-filled double skin steel tubular (CFDST) beam–columns subjected to cyclic bending. *Eng Struct* 2006; 28(12):1698-1714.
- [9] Uenaka K, Kitoh H, Sonoda K. Concrete filled double skin circular stub columns under compression. *Thin-Walled Struct* 2010; 48: 19-24.

- [10] Hassanein MF, Kharoob OF, Liang QQ. Circular concrete-filled double skin tubular short columns with external stainless steel tubes under axial compression. *Thin-Walled Structures* 2013; 73:252-263.
- [11] Varma AH, Ricles JM, Sause R, Lu LW. Experimental behavior of high strength square concrete-filled steel tube beam-columns. *Journal of Structural Engineering, ASCE* 2002; 128(3):309-318.
- [12] Vrcelj Z, Uy B. Strength of slender concrete-filled steel box columns incorporating local buckling. *Journal of Constructional Steel Research* 2002; 58(2):275-300.
- [13] Vrcelj Z, Uy B. Behaviour and design of steel square hollow sections filled with high strength concrete. *Australian Journal of Structural Engineering* 2002; 3(3):153-170.
- [14] Mursi M, Uy B. Strength of concrete filled steel box columns incorporating interaction buckling. *Journal of Structural Engineering, ASCE* 2003; 129(5):626-639.
- [15] Mursi M, Uy B. Strength of slender concrete filled high strength steel box columns. *Journal of Constructional Steel Research* 2004; 60(12):1825-1848.
- [16] Liu D. Behaviour of eccentrically loaded high-strength rectangular concrete-filled steel tubular columns. *Journal of Constructional Steel Research* 2006; 62(8):839-846.
- [17] Du Y, Chen Z, Wang YB, Liew JYR. Ultimate resistance behavior of rectangular concrete-filled tubular beam-columns made of high-strength steel. *Journal of Constructional Steel Research* 2017; 133:418-433.
- [18] Du Y, Chen Z, Liew JYR, Xiong MX. Rectangular concrete-filled steel tubular beam-columns using high-strength steel: experiments and design. *Journal of constructional steel research* 2017; 131:1-8.

- [19] Tao Z, Han LH, Zhao XL. Behaviour of concrete-filled double skin (CHS inner and CHS outer) steel tubular stub columns and beam-columns. *Journal of Constructional Steel Research* 2004; 60(8):1129-1158.
- [20] Zhao XL, Tong LW, Wang XY. CFDST stub columns subjected to large deformation axial loading. *Engineering Structures* 2010; 32(3):692-703.
- [21] Han LH, Tao Z, Huang H, Zhao XL. Concrete-filled double skin (SHS outer and CHS inner) steel tubular beam-columns. *Thin-Walled Structures* 2004; 42(9):1329-1355.
- [22] Han LH, Huang H, Tao Z, Zhao XL. Concrete-filled double skin steel tubular (CFDST) beam-columns subjected to cyclic bending. *Engineering Structures* 2006; 28(12):1698-1714.
- [23] Ahmed M, Liang QQ, Patel VI, Hadi MNS. Local-global interaction buckling of square high strength concrete-filled double steel tubular slender beam-columns. *Thin-Walled Structures* 2019; 143:106244..
- [24] Fan J, Baig M, Nie J. Test and analysis on double-skin concrete filled tubular columns. *Tubular Structures XII: Proceedings of Tubular Structures XII, Shanghai, China, 8-10 October 2008*; 407.
- [25] Shanmugam NE, Lakshmi B, Uy B. An analytical model for thin-walled steel box columns with concrete in-fill. *Engineering Structures* 2002; 24(6):825-838.
- [26] Patel VI, Liang QQ, Hadi MNS. High strength thin-walled rectangular concrete-filled steel tubular slender beam-columns, Part I: Modeling. *Journal of Constructional Steel Research* 2012; 70:368-376

- [27] Liang QQ, Patel VI, Hadi MNS. Biaxially loaded high-strength concrete-filled steel tubular slender beam-columns, Part I: Multiscale simulation. *Journal of Constructional Steel Research* 2012; 75:64-71.
- [28] Xiong MX, Xiong DX, Liew JYR. Behaviour of steel tubular members infilled with ultra high strength concrete. *Journal of Constructional Steel Research* 2017; 138:168-183.
- [29] Liang QQ. Performance-based analysis of concrete-filled steel tubular beam-columns, Part I: Theory and algorithms. *Journal of Constructional Steel Research* 2009; 65(2):363-372.
- [30] Liang QQ. Performance-based analysis of concrete-filled steel tubular beam-columns, Part II: Verification and applications. *Journal of Constructional Steel Research* 2009; 65(2):351-362
- [31] Liang QQ, Uy B, Liew JYR. Nonlinear analysis of concrete-filled thin-walled steel box columns with local buckling effects. *Journal of Constructional Steel Research* 2006; 62(6):581-591.
- [32] Patel VI, Liang QQ, Hadi MNS. High strength thin-walled rectangular concrete-filled steel tubular slender beam-columns, Part II: Behavior. *Journal of Constructional Steel Research* 2012; 70:368-376.
- [33] Patel VI, Liang, QQ and Hadi, MNS. Numerical analysis of high-strength concrete-filled steel tubular slender beam-columns under cyclic loading. *Journal of Constructional Steel Research* 2014; 92:183-194.
- [34] Patel VI. Nonlinear Inelastic Analysis of Concrete-Filled Steel Tubular Slender Beam-Columns. PhD Thesis, College of Engineering and Science, Victoria University, 2013.

- [35] Elchalakani M, Zhao XL, Grzebieta R. Tests on concrete filled double-skin (CHS outer and SHS inner) composite short columns under axial compression. *Thin-Walled structures*. 2002; 40(5):415-441.
- [36] Liang QQ. Nonlinear analysis of circular double-skin concrete-filled steel tubular columns under axial compression. *Engineering Structures* 2017; 131:639-650.
- [37] Hassanein MF, Elchalakani M, Karrech A, Patel VI, Yang B. Behaviour of concrete-filled double-skin short columns under compression through finite element modelling: SHS outer and SHS inner tubes. *Structures* 2018; 14:358-375.
- [38] Ahmed M, Liang QQ, Patel VI, Hadi MNS. Experimental and numerical investigations of eccentrically loaded rectangular concrete-filled double steel tubular columns. *Journal of Constructional Steel Research* 2020; 167:105949.
- [39] Liang QQ, Uy B, Liew JYR. Local buckling of steel plates in concrete-filled thin-walled steel tubular beam-columns. *Journal of Constructional Steel Research* 2007; 63(3):396-405.
- [40] Jiaru QI, Zhang Y, Zhang W. Eccentric compressive behavior of high strength concrete filled double-tube short columns. *Journal of Tsinghua University (Science and Technology)* 2015; 55(1):1-7.
- [41] Ahmed M, Liang QQ, Patel VI, Hadi MNS. Nonlinear analysis of rectangular concrete-filled double steel tubular short columns incorporating local buckling. *Engineering Structures* 2018; 175:13-26.
- [42] Müller DE. A method for solving algebraic equations using an automatic computer. *Mathematical Tables and Other Aids to Computation* 1956; 10(56):208-215.

- [43] Liang QQ. Numerical simulation of high strength circular double-skin concrete-filled steel tubular slender columns. *Engineering Structures* 2018; 168:205-217.
- [44] Mander JB, Priestley MJ, Park R. Theoretical stress-strain model for confined concrete. *Journal of structural engineering, ASCE* 1988; 114(8):1804-1826.
- [45] ACI Committee 363. *State of the Art Report on High-Strength Concrete*. ACI Publication 363R-92, 1992, Detroit, MI, American Concrete Institute.
- [46] Tomil M, Sakino K. Elasto-plastic behavior of concrete filled square steel tubular beam-columns. *Transactions of the Architectural Institute of Japan* 1979; 280:111-122.

Figures and Tables

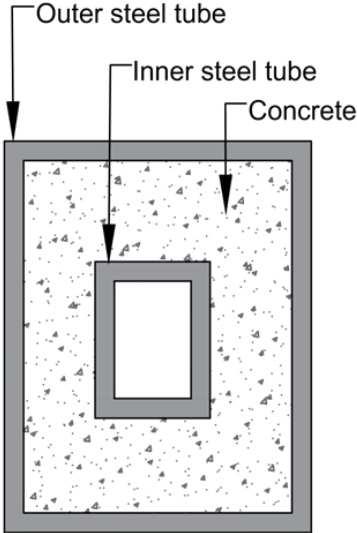


Fig. 1. Cross-section of RDCFST column.

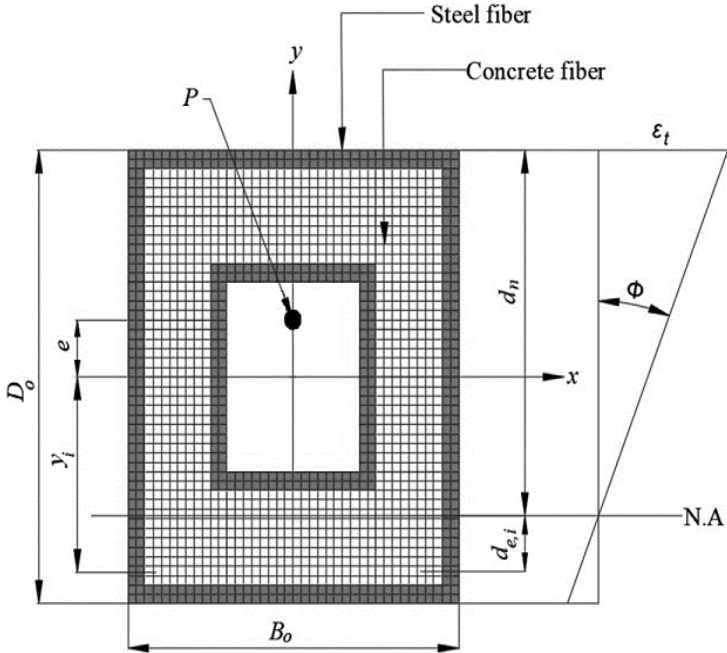


Fig.2. Discretization and strain profile.

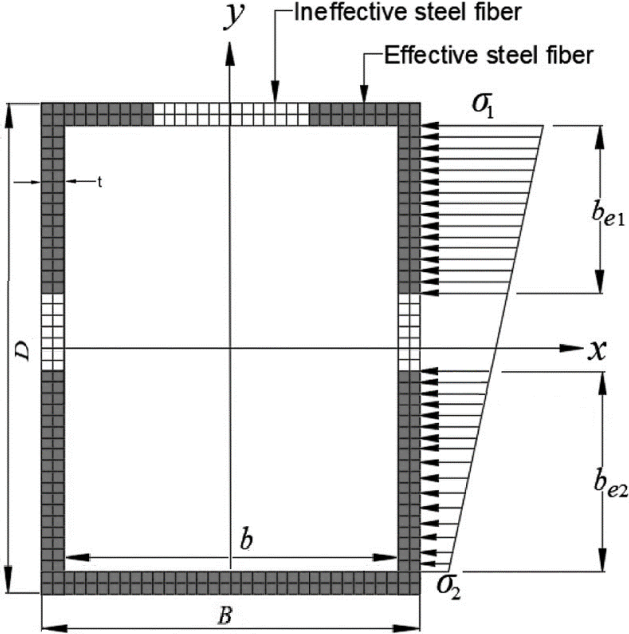


Fig. 3. Effective widths of section under uniaxial bending

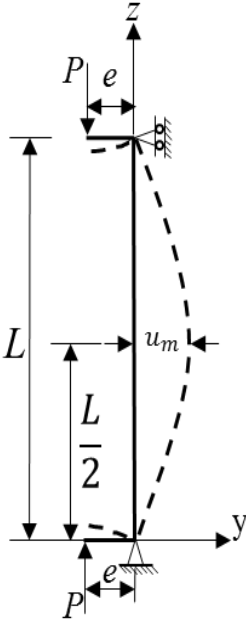


Fig. 4. Eccentrically loaded RDCFST slender column with pin-ended supports

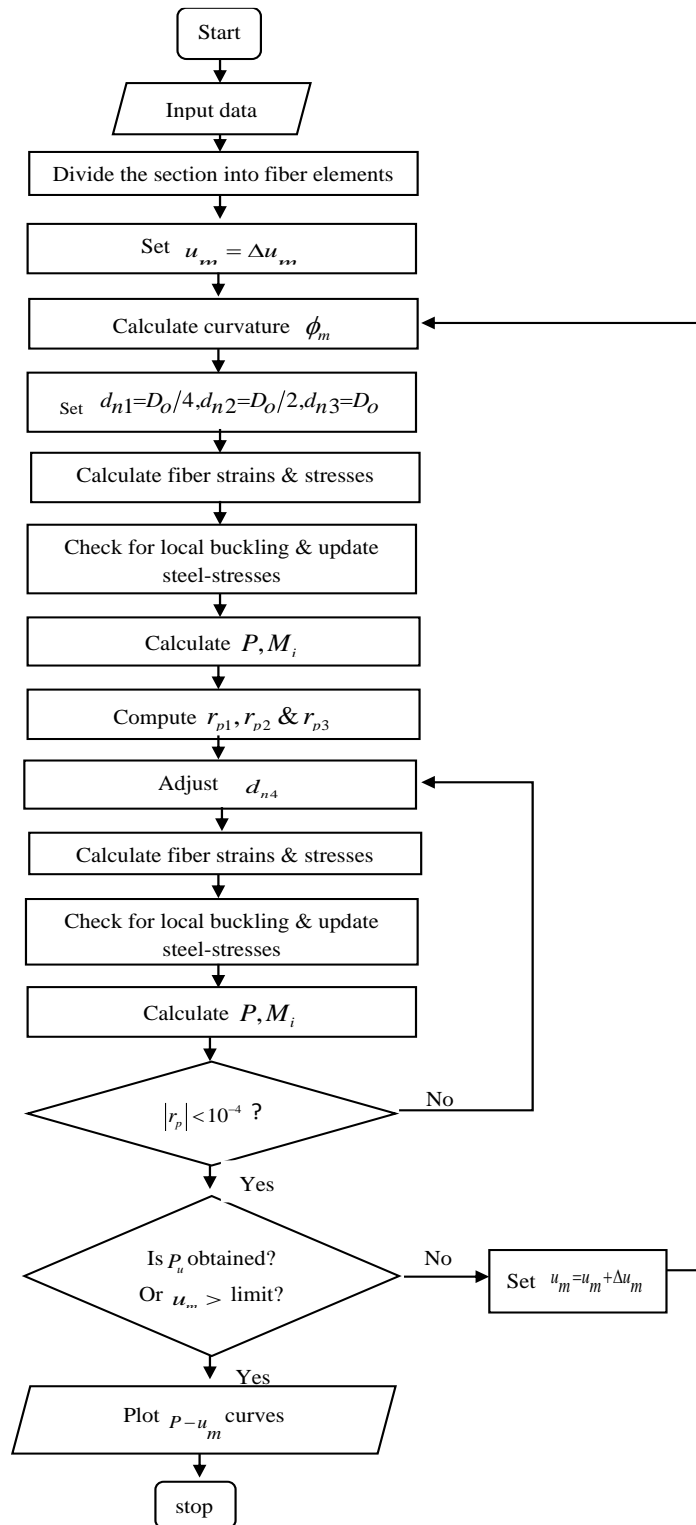


Fig. 5. Computer flowchart for computing the load-deflection responses.

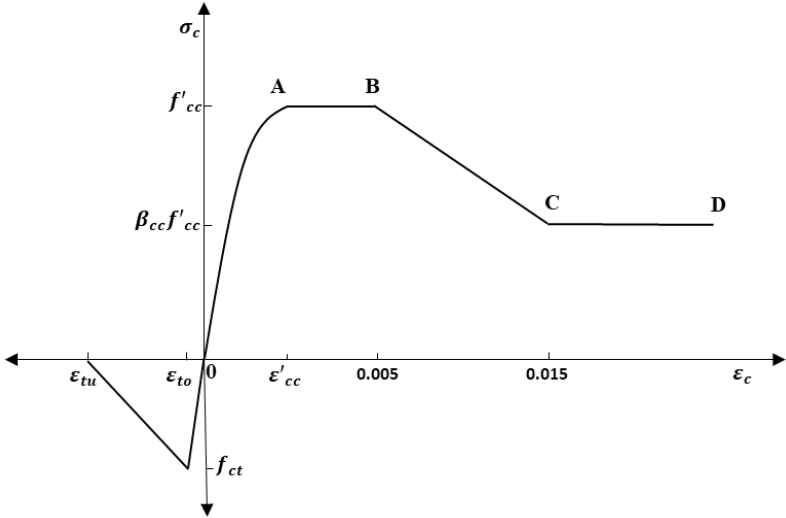


Fig. 6. Stress-strain curves for concrete in compression and tension

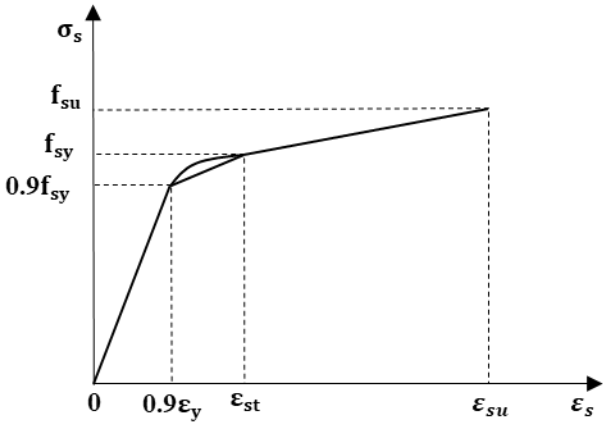
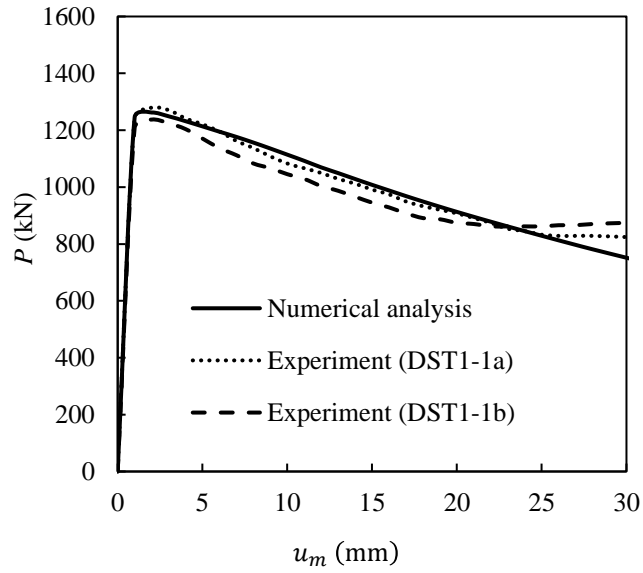
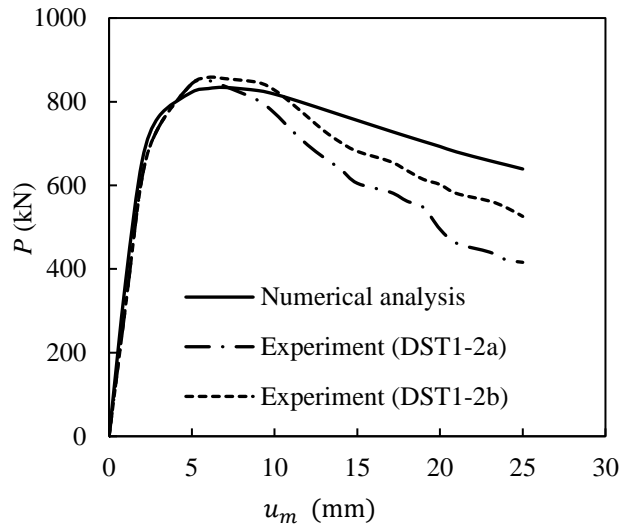


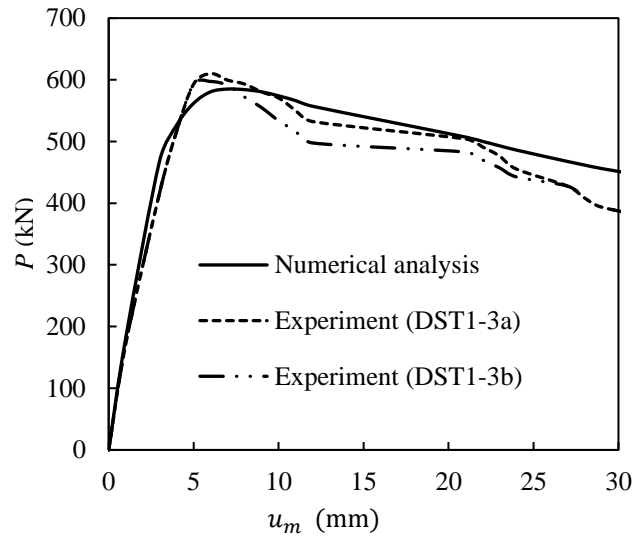
Fig. 7. Stress-strain relationships for steels



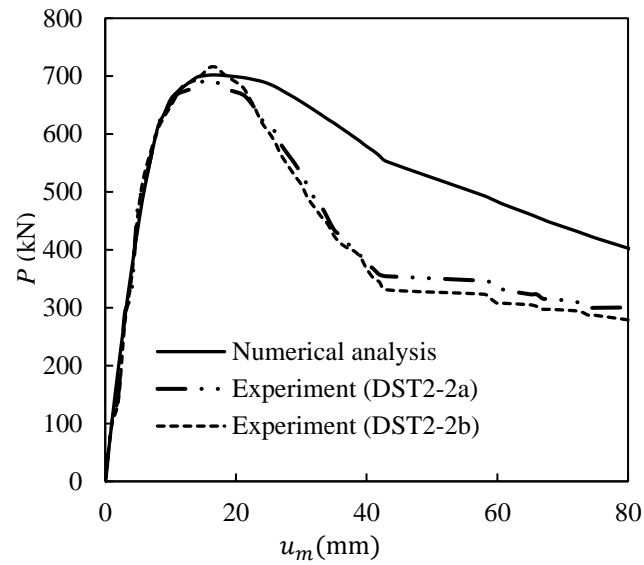
(a) $e = 0$ mm



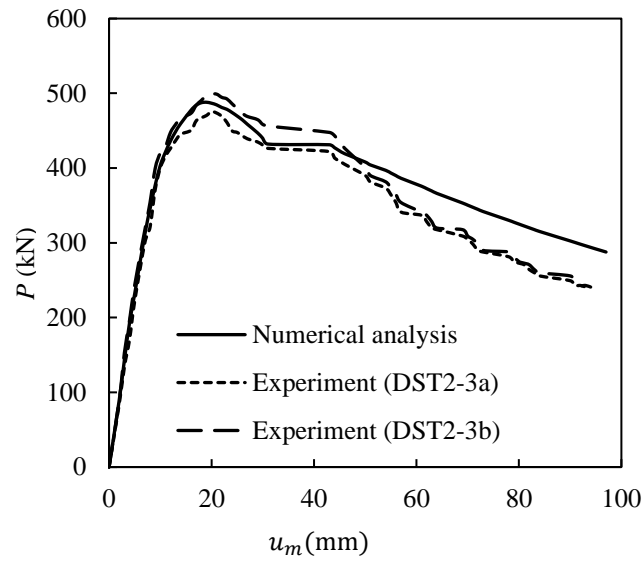
(b) $e = 30$ mm



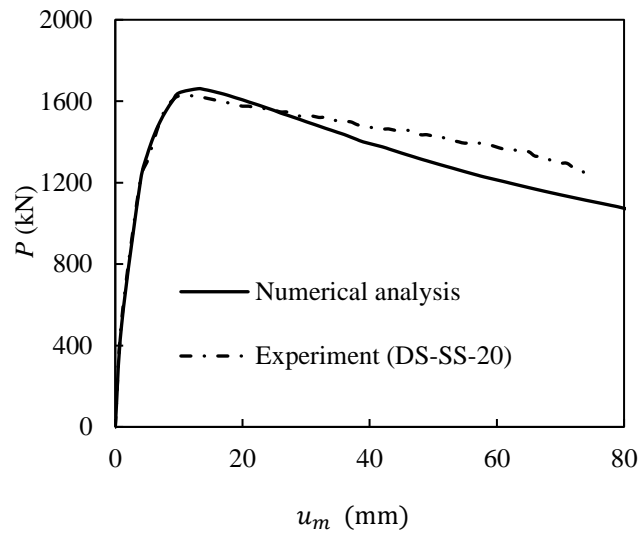
(c) $e = 60$ mm



(d) $e = 30$ mm



(e) $e = 60$ mm



(f) $e = 0$ mm

Fig. 8. Verification of computational model by experimental results

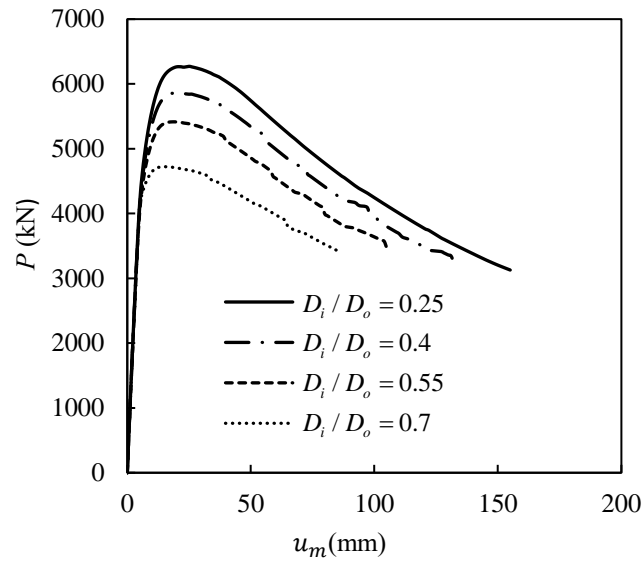


Fig. 9. Load-deflection responses with influences of D_i / D_o ratios

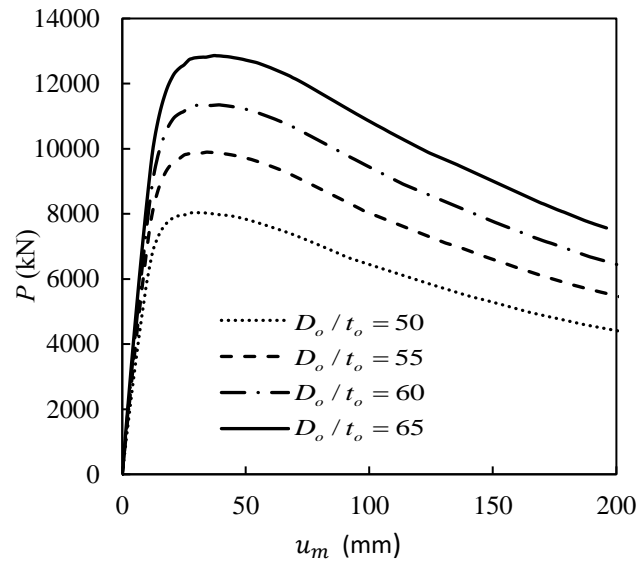


Fig. 10. Load-deflection responses with effects of D_o / t_o ratios.

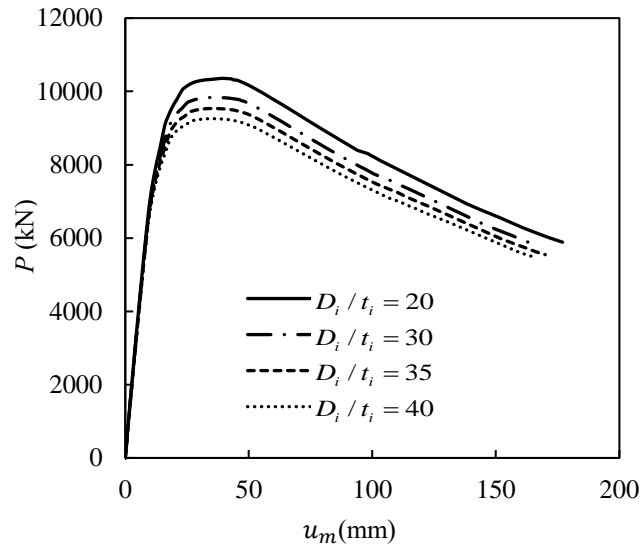


Fig. 11. Load-deflection responses with influences of D_i/t_i ratios.

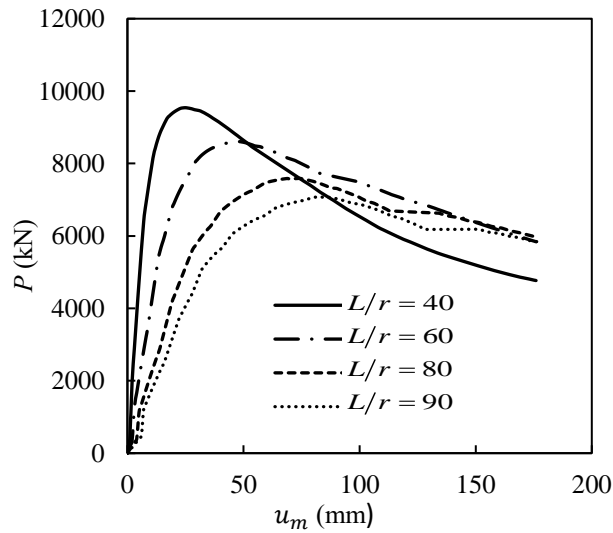


Fig. 12. Load-deflection responses with influences of L/r ratios.

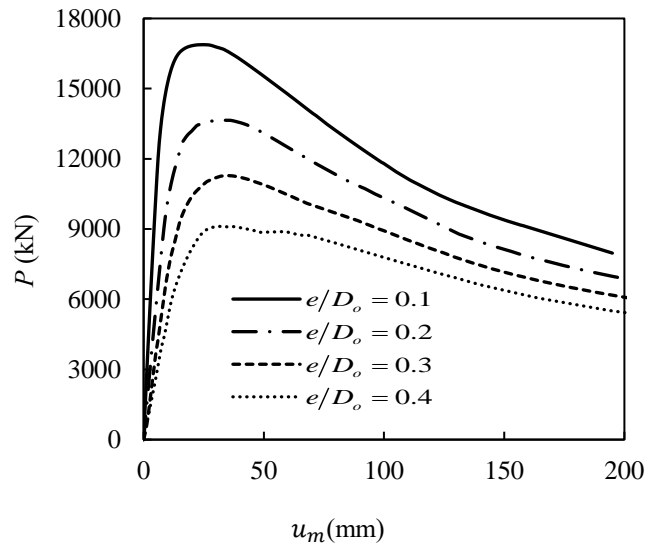


Fig. 13. Load-deflection responses with influences of e/D_o ratios.

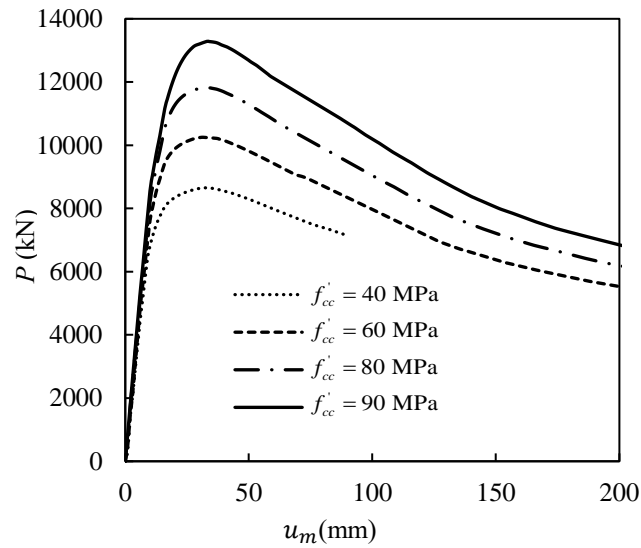


Fig. 14. Load-deflection responses with influences of concrete strengths.

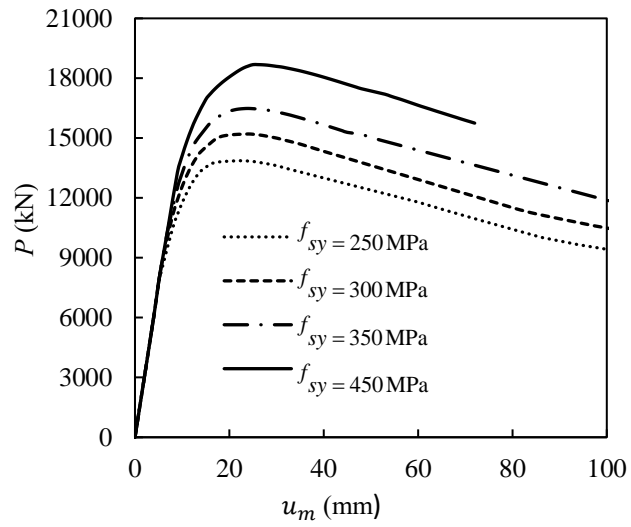
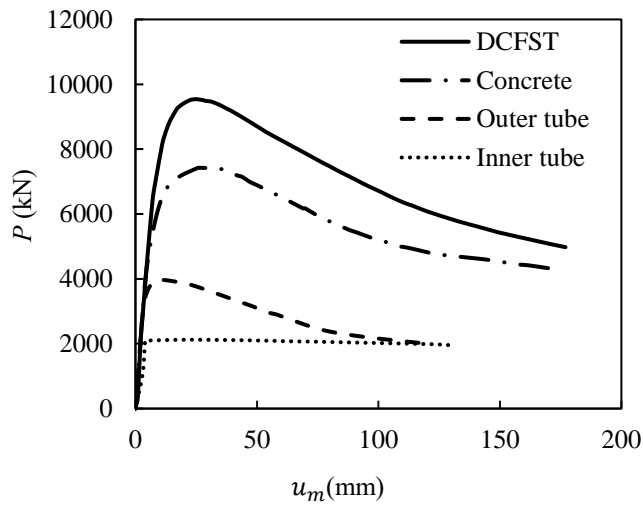
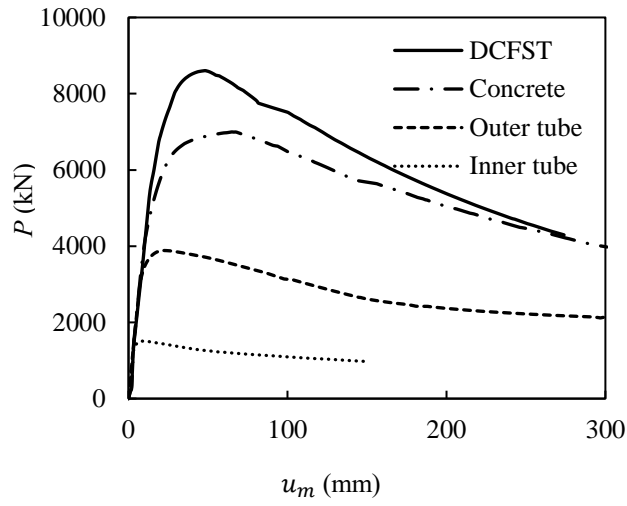


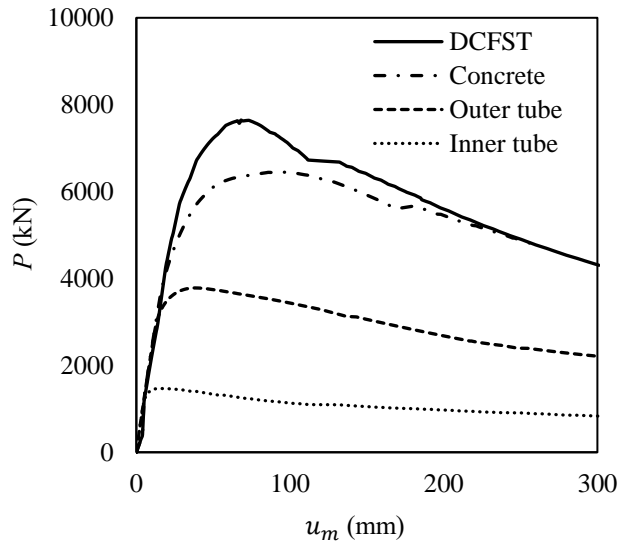
Fig. 15. Load-deflection responses with influences of steel yield stresses.



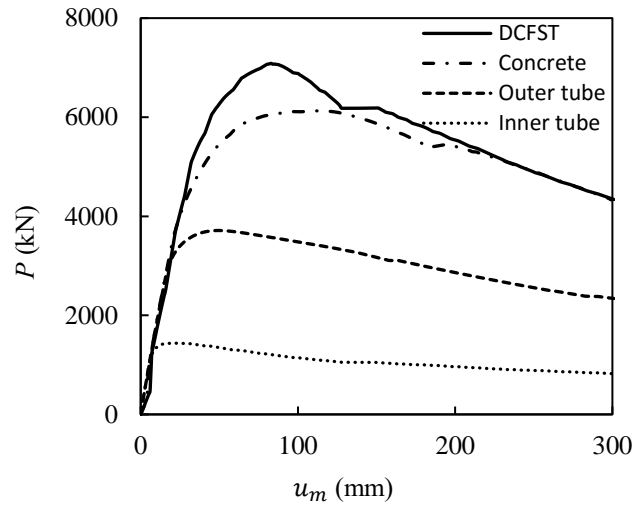
(a) $L/r = 40$



(b) $L/r = 60$



(c) $L/r = 80$



(d) $L/r = 90$

Fig. 16. Load distributions in rectangular DCFST columns with influences of L/r ratios

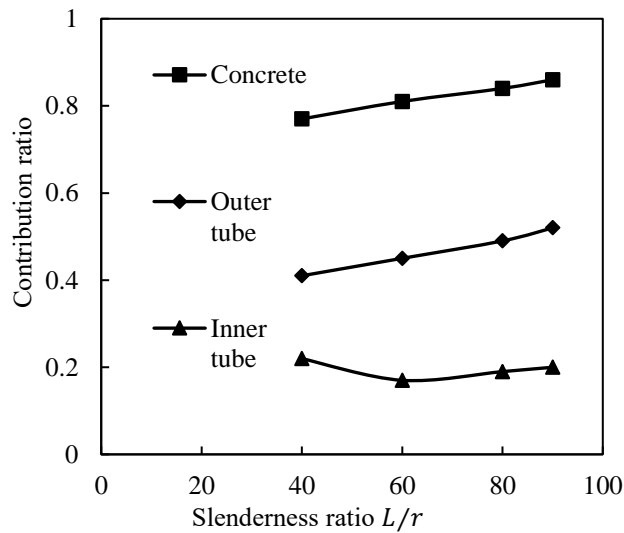
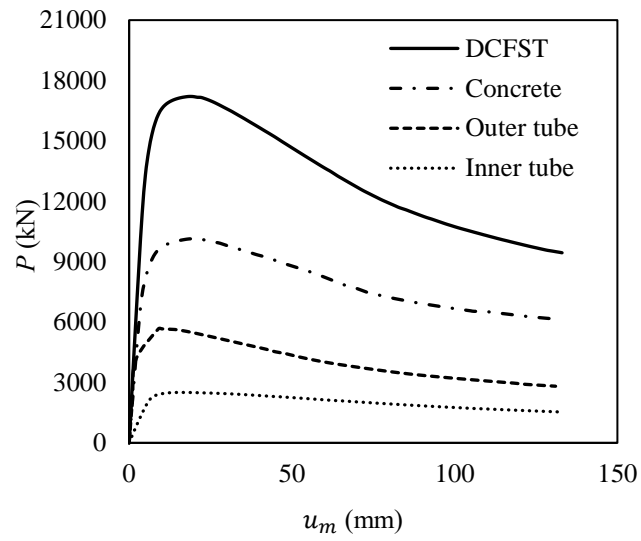
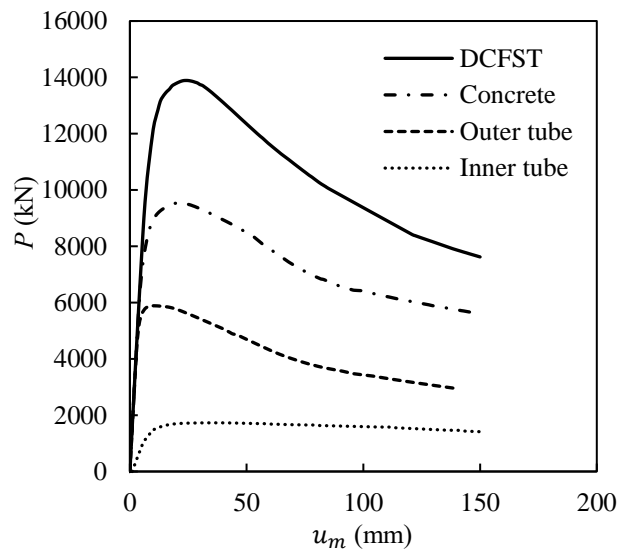


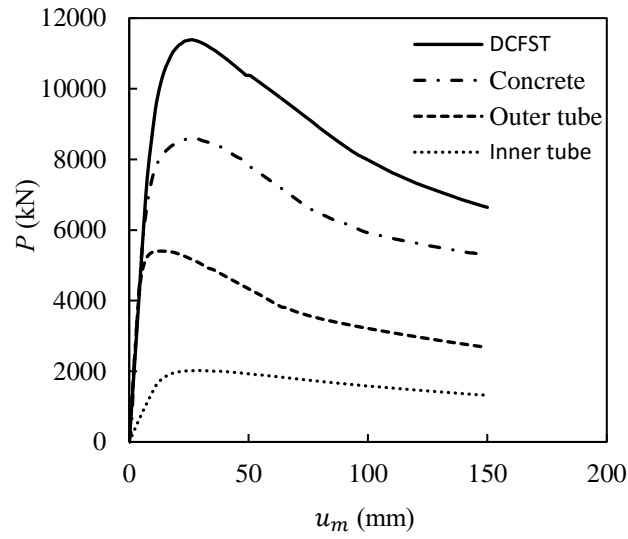
Fig. 17. Concrete and steel tubes contribution ratios as a function of L/r ratio.



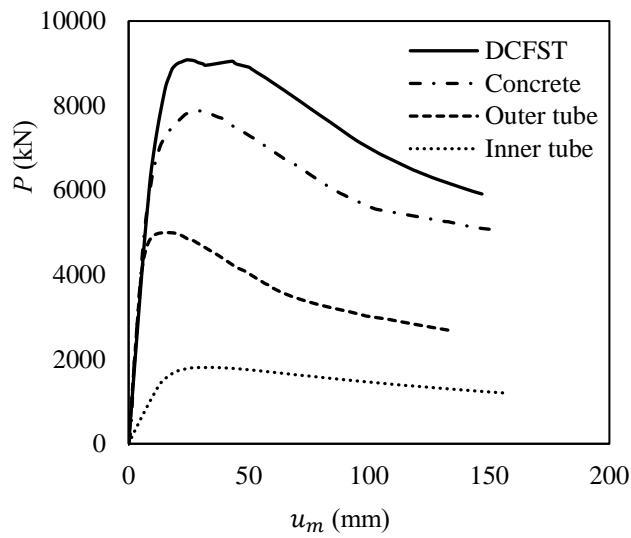
(a) $e/D_o = 0.1$



(b) $e/D_o = 0.2$



(c) $e/D_o = 0.3$



(d) $e/D_o = 0.4$

Fig. 18. Load distributions in rectangular DCFST columns with influences of e/D_o ratios.

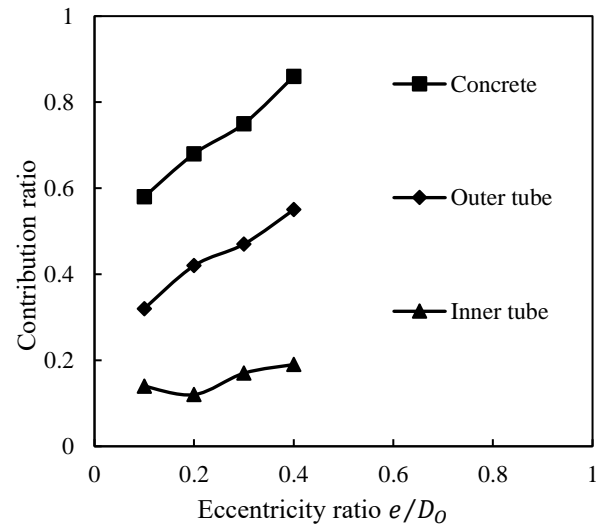


Fig. 19. Concrete and steel tubes contribution ratios as a function of e/D_0 ratio.

Table 1: Ultimate strengths of rectangular DCFST slender columns.

Specimen	Outer tube			Inner tube			Concrete	Ultimate axial load			Ref
	$B_o \times D_o \times t_o$ (mm)	L (mm)	f_{sy0} (MPa)	$B_i \times D_i \times t_i$ (mm)	e (mm)	f_{syi} (MPa)	f'_{cc} (MPa)	$P_{u,exp}$ (kN)	$P_{u,num}$ (kN)	$\frac{P_{u,num}}{P_{u,exp}}$	
DST1-1a	100×150×3.2	1214	380	45×75×3.2	0	429	50	1290	1262.8	0.97	[1]
DST1-1b	100×150×3.2	1214	380	45×75×3.2	0	429	50	1250	1262.8	1.01	
DST1-2a	100×150×3.2	1214	380	45×75×3.2	30	429	50	850	834.01	0.98	
DST1-2b	100×150×3.2	1214	380	45×75×3.2	30	429	50	855	834.01	0.97	
DST1-3a	100×150×3.2	1214	380	45×75×3.2	60	429	50	610	584.99	0.95	
DST1-3b	100×150×3.2	1214	380	45×75×3.2	60	429	50	595	584.99	0.98	
DST2-1a	100×150×3.2	2314	380	45×75×3.2	0	429	50	1214	1006.32	0.82	
DST2-1b	100×150×3.2	2314	380	45×75×3.2	0	429	50	1235	1006.32	0.81	
DST2-2a	100×150×3.2	2314	380	45×75×3.2	30	429	50	690	701.94	1.01	
DST2-2b	100×150×3.2	2314	380	45×75×3.2	30	429	50	715	701.94	0.98	
DST2-3a	100×150×3.2	2314	380	45×75×3.2	60	429	50	479	488.99	1.02	
DST2-3b	100×150×3.2	2314	380	45×75×3.2	60	429	50	496	488.99	0.98	
T0-4E0	100×100×2.0	400	235	40×40×2.0	0	235	43.24	500.6	543.60	1.08	[2]
T0-5E0	100×100×2.0	500	235	40×40×2.0	0	235	43.24	520.9	553.56	1.06	
T0-6E0	100×100×2.0	600	235	40×40×2.0	0	235	43.24	550.7	549.4	0.99	
T0-4E0.3	100×100×2.0	400	235	40×40×2.0	15	235	43.24	428.0	415.7	0.95	
T0-5E0.3	100×100×2.0	500	235	40×40×2.0	15	235	43.24	499.5	412.9	0.82	
T0-4E0.7	100×100×2.0	400	235	40×40×2.0	35	235	43.24	377.5	320.97	0.87	
T0-5E0.7	100×100×2.0	500	235	40×40×2.0	35	235	43.24	340.2	289.91	0.85	
T0-6E0.7	100×100×2.0	600	235	40×40×2.0	35	235	43.24	376.2	299.13	0.85	
DS-SS-20	180×180×5.0	4500	357.9	60×60×3.2	0	357	38.9	1618	1661	1.026	[3]
SS4	240×240×4.0	720	280	80×80×4	0	280	29	2687	2581	0.96	[18]
SS4	240×240×4.0	720	280	120×120×4	0	280	29	2505	2504	0.99	
Mean										0.959	
SD										0.080	
COV										0.081	

Table.2 Rectangular DCFST slender column's geometric and material properties for parametric study.

Group	Columns	$B_o \times D_o \times t_o$ (mm)	$\frac{D_o}{t_o}$	$B_i \times D_i \times t_i$ (mm)	$\frac{D_i}{t_i}$	$\frac{L}{r}$	$\frac{e}{D_o}$	$f_{sy0} \cdot f_{syi}$ (MPa)	f'_{cc} (MPa)	$f_{suo} \cdot f_{sui}$ (MPa)
1	C1	265×450×8.0	56.25	45×112.5×6	18.75	60	0.1	250	60	320
	C2	265×450×8.0	56.25	75×180×6	30	60	0.1	250	60	320
	C3	265×450×8.0	56.25	140×247×6	41.25	60	0.1	250	60	320
	C4	265×450×8.0	56.25	205×317×6	52.5	60	0.1	250	60	320
2	C5	310×500×10	50	150×350×10	35	55	0.15	350	65	430
	C6	340×550×10	55	150×350×10	35	55	0.15	350	65	430
	C7	375×600×10	60	150×350×10	35	55	0.15	350	65	430
	C8	405×650×10	65	150×350×10	35	55	0.15	350	65	430
3	C9	375×550×11	50	150×250×12.5	20	50	0.2	300	70	430
	C10	375×550×11	50	150×250×8.33	30	50	0.2	300	70	430
	C11	375×550×11	50	150×250×7.14	35	50	0.2	300	70	430
	C12	375×550×11	50	150×250×6.25	40	50	0.2	300	70	430
4	C13	390×600×10	60	150×300×10	30	40	0.25	250	75	320
	C14	390×600×10	60	150×300×10	30	60	0.25	250	75	320
	C15	390×600×10	60	150×300×10	30	80	0.25	250	75	320
	C16	390×600×10	60	150×300×10	30	90	0.25	250	75	320
5	C17	350×700×10	65	150×350×10	40	45	0.1	350	85	430
	C18	350×700×10	65	150×350×10	40	45	0.2	350	85	430
	C19	350×700×10	65	150×350×10	40	45	0.3	350	85	430
	C20	350×700×10	65	150×350×10	40	45	0.4	350	85	430
6	C21	451×700×10	70	225×330×10	33	40	0.3	300	40	430
	C22	451×700×10	70	225×330×10	33	40	0.3	300	60	430
	C23	451×700×10	70	225×330×10	33	40	0.3	300	80	430
	C24	451×700×10	70	225×330×10	33	40	0.3	300	100	430
7	C25	435×800×15	53.33	225×380×15	25.33	35	0.35	250	90	320
	C26	435×800×15	53.33	225×380×15	25.33	35	0.35	300	90	430
	C27	435×800×15	53.33	225×380×15	25.33	35	0.35	350	90	430
	C28	435×800×15	53.33	225×380×15	25.33	35	0.35	450	90	520

4.3 Range Analysis

Parametric studies have been conducted in the preceding section to investigate the effects of important parameters on the structural responses of RDCFST columns. To achieve economical designs, it is important to determine the relative significance of these design parameters on the load-carrying capacities of RDCFST slender columns. For this purpose, the range analysis based on the orthogonal design method has been undertaken. The orthogonal design method proposed by Le et al. (2022) has been employed to assess the impacts of major parameters. The orthogonal design factors A , B , C , D , E , and F are used to represent the outer depth-to-thickness (D_o/t_o), slenderness ratio (L/r), loading eccentricity ratio (e/D_o), outer steel tube yield stress (f_{syo}), inner steel tube yield strength (f_{syi}), and sandwiched concrete strength (f'_{cc}), respectively. Table 3 shows the four levels and the assigned parameters. The evaluation index is the ultimate axial load P_u of RDCFST slender columns under eccentric loading. The range analysis is a statistical approach to handle the results from the orthogonal design when the sensitivity between the factors themselves and the evaluation index is measured. The range value R_a is calculated as:

$$R_a = \max k_{a,b} - \min k_{a,b} \quad (20)$$

$$k_{a,b} = \frac{1}{N} \sum_{n=1}^N y_{b,n} \quad (21)$$

where a and b are the factor and design level, respectively; R_a denotes the range value of mean P_u of the columns considered for the factor, which indicates the significance of the factor; $y_{b,n}$ is the ultimate axial load P_u of the n -th column at the design level b ; N is the number of designed columns at the design level; and $k_{a,b}$ is the mean value of the ultimate axial loads of the columns at design level b .

Table 3. Factors and design levels

$D_o = 400$ mm						
Design level	D_o/t_o	L/r	e/D_o	f_{sy0}	f_{syi}	f'_{cc}
I	30	30	0.2	200	200	40
II	50	50	0.3	250	250	50
III	70	70	0.4	300	300	60
IV	90	90	0.5	350	350	70

The material and geometric properties of RDCFST slender columns in the range analysis are given in Table 4. The numerical model for the load-deflection analysis was employed to obtain the ultimate load-carrying capacity P_u of the columns. The internal steel tube depths were chosen as 30 mm and 90 mm, respectively, and the corresponding thickness was computed as $t_i = D_i/30$. The corresponding hollow-section ratios were 0.08 and 0.2, respectively. A total of 50 RDCFST slender columns were modelled. The outcomes obtained from the simulations are provided in Table 4.

Table 4. The ultimate axial loads P_u of RDCFST slender columns

No	Factors						P_u (kN)	
	A	B	C	D (Mpa)	E (Mpa)	F (Mpa)	$D_i = 30$ mm	$D_i = 90$ mm
1	90	90	0.3	200	300	70	2343.098	2295.736
2	70	70	0.2	200	350	60	3898.374	3840.83
3	30	70	0.4	350	300	40	4208.287	4167.326
4	70	30	0.5	350	200	70	3863.176	3843.303
5	30	30	0.2	200	200	40	5457.744	5394.309
6	30	70	0.3	300	200	40	4438.591	4385.572
7	30	30	0.5	200	250	40	3431.998	3423.469
8	50	70	0.2	250	250	70	4948.398	4857.836
9	90	50	0.2	350	350	40	3959.32	3941.925
10	50	30	0.2	200	300	40	4591.542	4582
11	70	90	0.4	250	200	40	1996.507	1965.896
12	90	30	0.2	250	200	40	4138.304	4088.72
13	30	50	0.2	300	200	70	7459.978	7328.32
14	30	90	0.2	350	250	50	5101.033	5011.633
15	70	50	0.3	200	250	40	3000.465	2982.165
16	50	30	0.3	350	200	60	5948.609	5856.402
17	50	90	0.2	300	350	50	2391.098	2356.908
18	70	30	0.2	300	300	50	5407.39	5389.436
19	30	30	0.3	250	350	50	5763.503	5737.912
20	90	70	0.5	200	200	50	3304.701	3248.245
21	30	30	0.4	200	350	70	5078.158	5055.722
22	30	90	0.5	200	200	40	2436.8	2407.996
23	30	50	0.5	250	300	60	4008.036	3982.965
24	90	30	0.4	300	250	60	3696.055	3682.107
25	50	50	0.4	200	200	60	3370.211	3345.612

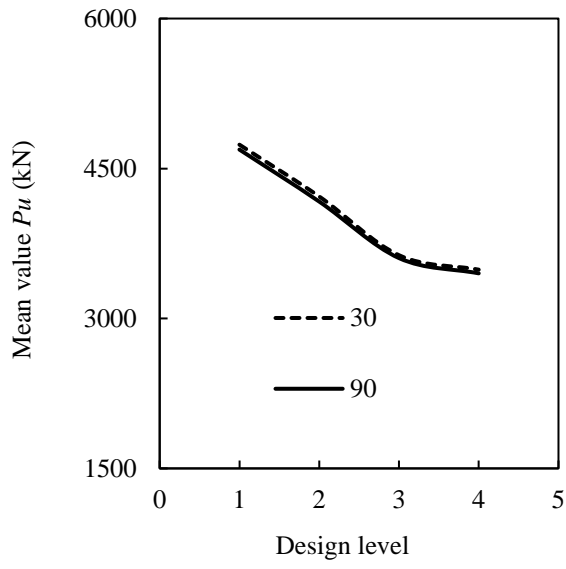
Range analysis results are shown in Table 5, which indicates that the order of substantial factors is steady irrespective of the hollow-section ratio. The slenderness ratio (L/r) is the most significant factor affecting the load-carrying capacity of RDCFST beam-columns,

followed by the loading eccentricity ratio (e/D_o), outer depth-to-thickness (D_o/t_o), outer steel tube yield strength (f_{syo}), and sandwiched concrete strength (f'_{cc}). In contrast, the inner steel tube yield strength (f_{syi}), is the least participant factor and this is attributed to the least contribution ratio.

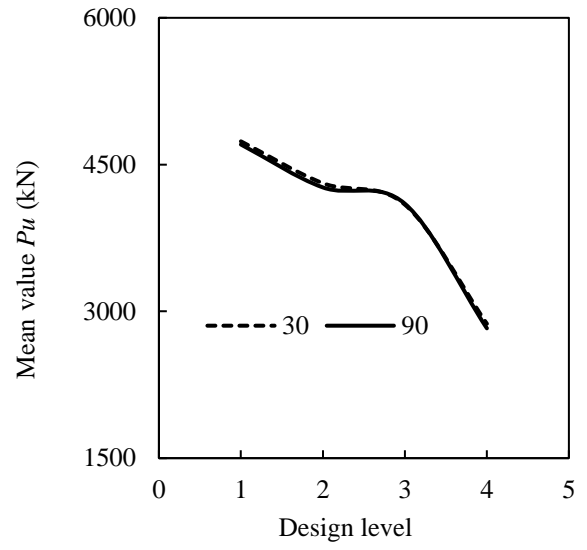
Table 5. The range values of the ultimate axial loads of RDCFST slender columns with various factors

R_u (kN)							
D_i	D_o/t_o	L/r	e/D_o	f_{syo}	f_{syi}	f'_{cc}	Order
	<i>A</i>	<i>B</i>	<i>C</i>	<i>D</i>	<i>E</i>	<i>F</i>	
30	1250	1863	1580	1032	202	972	$B > C > A > D > F > E$
90	1238	1878	1546	1014	214	942	$B > C > A > D > F > E$

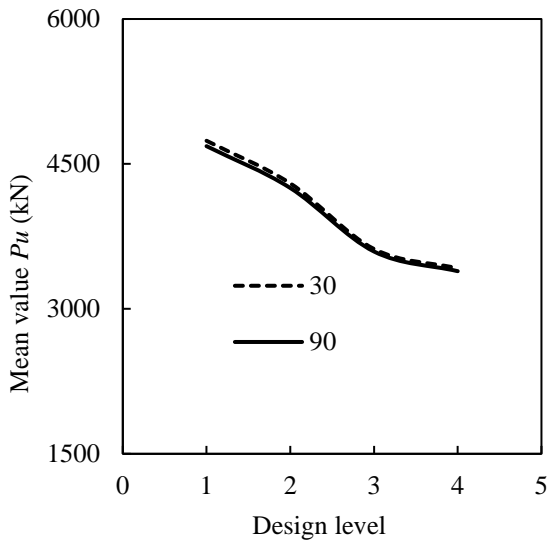
The relationship between the parameters level and the mean value P_u of the RDCFST slender beam-column is depicted in Fig. 20. The D_o/t_o ratio, the L/r ratio, and the e/D_o ratio show inversely proportionality with the ultimate strength: the bearing capacity of RDCFST slender column decreases with increasing the factor levels. In contrast, the f_{syo} , the f_{syi} , and f'_{cc} are directly proportional to the load-bearing capacity. It can be seen from Fig. 20 and Table 5 that the most effective technique to improve the ultimate axial capacity is to reduce the length of the column and loading eccentricity. However, if the column length cannot be changed, a satisfactory design can be achieved by employing thicker outer and internal steel tubes with high-strength properties.



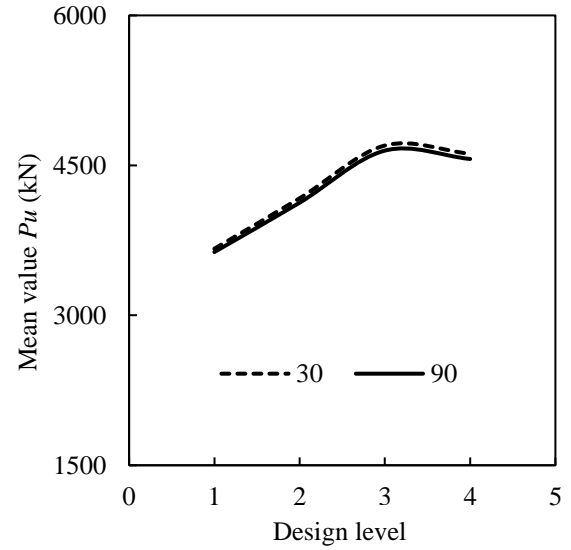
(b) Factor A



(a) Factor B



(d) Factor C



(c) Factor D

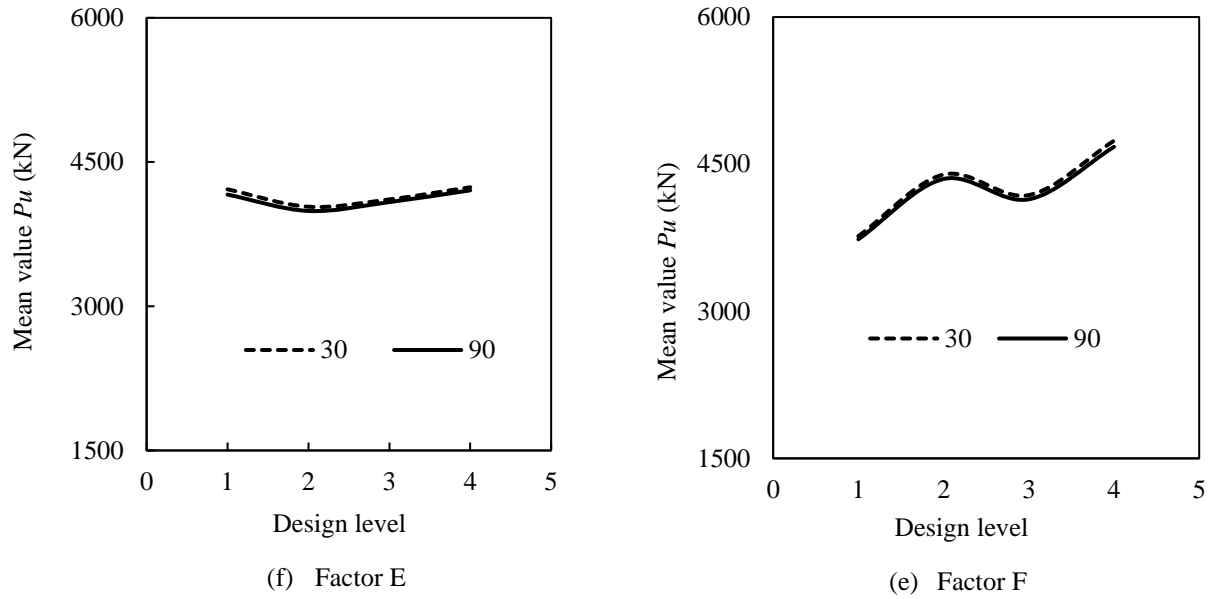


Fig.20. The mean ultimate axial load-design curves of RDCFST slender columns with $D_i = 30\text{mm}$ and $D_i = 90\text{mm}$.

4.4 CONCLUDING REMARKS

The inelastic simulation and behavior of RDCFST slender columns have been presented in this Chapter. A mathematical model employing fiber discretization has been developed that determines the load-deflection responses of thin-walled eccentrically loaded slender RDCFST columns that experience the interaction of gradual localized and global buckling. It has been shown that the computational modeling approach developed produces results that

are in good agreement with measured experimental results. The local-global interaction buckling behavior of RDCFST slender columns with an extensive range of design characteristics has been studied by employing the proposed computational model. The established computational simulation technique can be utilized in the analysis and design of RDCFST slender columns considering instability effects. The range analysis is the most effective method conclusively to determine the significant factor affecting the load-bearing capacity of RDCFST slender beam-columns.

Chapter 5

CONCLUSIONS

5.1 SUMMARY

This thesis has presented numerical investigations into the structural performance of short and slender RDCFST columns composed of concentrically deployed two rectangular steel tubes and poured with high and normal strength concrete. Computational simulation models utilizing fiber discretization have been developed to predict the structural behavior of short and slender RDCFST columns that are loaded either axially or eccentrically. The computer modeling method for short RDCFST columns has accounted for the influences of the interaction of gradual localized buckling in both thin-walled outer and inner rectangular steel sections. The interaction of localized and global instability, second order effects, material nonlinearities and geometric imperfections have explicitly been taken into account in the mathematical programming procedures for slender RDCFST columns. The incremental nonlinear equilibrium equations of slender RDCFST columns are solved by means of using robust and efficient computer algorithms developed based on Müller's method. The accuracy of the developed computer simulation techniques has been verified by experimental

measurements documented elsewhere. The computer programs have been employed to investigate the significance of important parameters on the structural responses of RDCFST columns, including the cross-sectional effect, hollow-section ratio, columns slenderness ratio, depth to thickness ratio, loading conditions, initial geometric imperfection, and material strengths. A design formula for designing short RDCFST columns has been proposed and validated by test results.

5.2 ACHIEVEMENTS

This research study has made significant contributions to the numerical modeling and simulation, structural behavior, and design of RDCFST columns covering both short and slender columns. The important achievements in the research are summarized as follows:

1. Developed an efficient computational simulation model for the performance predictions of concentrically loaded short RDCFST columns incorporating the interaction local buckling of the flanges and webs of the inner and outer thin-walled steel sections for the first time. A new fiber mesh discretization scheme was developed for RDCFST columns, which enables the progress local buckling of both inner and external steel tubes to be simulated.
2. A design model for the design of short RDCFST columns was proposed and its accuracy was validated by existing experimental data on RDCFST columns. The design model is suitable for inclusion in composite design standards.

3. A robust and computationally efficient mathematical programming model was developed to simulate the axial load-lateral deflection responses of slender RDCFST columns loaded eccentrically to failure. The model accounts for the inelastic local-global interaction buckling, distributed plasticity, steel yielding and strain-hardening, concrete cracking and crushing, second-order effects, and geometric imperfections.
4. Developed numerical solution algorithms to solve the nonlinear functions generated in the incremental-iterative nonlinear analysis of slender RDCFST columns accounting for the gradual failure mode of interaction local-global instability.
5. Conducted extensive parametric studies on the fundamental behavior of short and slender RDCFST columns that are loaded either concentrically or eccentrically to failure, incorporating the interaction buckling. The range analysis was undertaken to identify the relative significance of design parameters on the strengths of RDCFST slender columns. The benchmark numerical results provide significant insight into the interaction buckling behavior of thin-walled RDCFST columns for the first time and are valuable for the development of composite design codes.

5.3 FURTHER RESEARCH

This thesis focuses on the development of robust and efficient computational modeling technologies for capturing the structural responses of short and slender RDCFST columns under axial and eccentric loads considering the important failure mode of localized and global instability. However, further experimental and computational research works are still required to fully understand the behavior of RDCFST columns under different loading

conditions. The further research studies on the analysis, behavior, and design of RDCFST columns are recommended as follows:

1. Experimental and numerical studies on RDCFST columns under biaxial loads and cyclic loads considering interaction buckling should be carried out to capture their structural responses.
2. Tests should be undertaken on the behavior of RDCFST columns incorporating preload effects and the experimental results should be used to validate mathematical models developed for RDCFST slender columns to recognize the construction method of composite buildings.
3. Numerical investigations and experiments on the behavior of RDCFST columns filled with geopolymer concrete subjected to various loading conditions should be conducted.
4. The RDCFST columns in high-rise buildings are likely subjected to fire. Therefore, the fire and post-fire performance of RDCFST columns should be thoroughly investigated by means of experiments as well as computer models developed for such composite columns.
5. Design models should be proposed for the practical design of RDCFST slender columns under various loading conditions considering the effect of local-buckling.

REFERENCES

Ades, C. S. (1957). Bending strength of tubing in the plastic range. *Journal of the Aeronautical Sciences*, 24(8), 605-610.

Ahmed, M., Liang, Q. Q., Patel, V. I., & Hadi, M. N. S. (2018). Nonlinear analysis of rectangular concrete-filled double steel tubular short columns incorporating local buckling. *Engineering Structures*, 175, 13-26.

Ahmed, M., Liang, Q. Q., Patel, V. I., & Hadi, M. N. S. (2019a). Local-global interaction buckling of square high strength concrete-filled double steel tubular slender beam-columns. *Thin-Walled Structures*, 143, 106244.

Ahmed, M., Liang, Q. Q., Patel, V. I., & Hadi, M. N. S. (2019b). Experimental and numerical studies of square concrete-filled double steel tubular short columns under eccentric loading. *Engineering Structures*, 197, 109419.

Ahmed, M., Liang, Q. Q., Patel, V. I., & Hadi, M. N. S. (2019c). Behavior of eccentrically loaded double circular steel tubular short columns filled with concrete. *Engineering Structures*, 201, 109790.

Ahmed, M., Liang, Q. Q., Patel, V. I., & Hadi, M. N. S. (2020a). Nonlinear analysis of square concrete-filled double steel tubular slender columns incorporating preload effects. *Engineering Structures*, 207, 110272.

Ahmed, M., Liang, Q. Q., Patel, V. I., & Hadi, M. N. (2020b). Behavior of circular concrete-filled double steel tubular slender beam-columns including preload effects. *Engineering Structures*, 220, 111010.

Ahmed, M., Liang, Q. Q., Patel, V. I., & Hadi, M. N. (2020c). Experimental and numerical investigations of eccentrically loaded rectangular concrete-filled double steel tubular columns. *Journal of Constructional Steel Research*, 167, 105949.

Archer, J. S. (1965). Consistent matrix formulations for structural analysis using finite-element techniques. *AIAA journal*, 3(10), 1910-1918.

Azhari, M., & Bradford, M. A. (1993). Local buckling of I-section beams with longitudinal web stiffeners. *Thin-walled structures*, 15(1), 1-13.

Azizian, Z. G., & Dawe, D. J. (1985). Geometrically nonlinear analysis of rectangular mindlin plates using the finite strip method. *Computers & structures*, 21(3), 423-436.

Basler, K., Yen, B. T., Mueller, J. A., & Thurlimann, B. (1960). *Web buckling tests on welded plate girders*. Fritz Engineering Laboratory, Lehigh University.

Bedair, O. (2009). Analysis and limit state design of stiffened plates and shells: A world view. *Applied Mechanics Reviews*, 62(2).

Bijlaard, P. P. (1949). Theory and tests on the plastic stability of plates and shells. *Journal of the Aeronautical Sciences*, 16(9), 529-541.

Bryan, G. H. (1890). On the Stability of a Plane Plate under Thrusts in its own Plane, with Applications to the “Buckling” of the Sides of a Ship. *Proceedings of the London Mathematical Society*, 1(1), 54-67.

Bradford, M. A. (1985). Distortional buckling of monosymmetric I-beams. *Journal of Constructional Steel Research*, 5(2), 123-136.

Bradford, M. A., & Azhari, M. (1995). Buckling of plates with different end conditions using the finite strip method. *Computers & structures*, 56(1), 75-83.

Bradford, M. A., & Cuk, P. E. (1988). Elastic buckling of tapered monosymmetric I-beams. *Journal of Structural Engineering*, ASCE, 114(5), 977-996.

Bradford, M. A., & Hancock, G. J. (1984). Elastic interaction of local and lateral buckling in beams. *Thin-Walled Structures*, 2(1), 1-25.

Bulson, P. S. (1969). The strength of thin-walled tubes formed from flat elements. *International Journal of Mechanical Sciences*, 11(7), 613-620.

Cao, Y. J., Huang, M. K., Zhuang, J. Z., & Yang, J. H. (2010). Local Buckling Performance of Rectangular Concrete-Filled Steel Columns. *Chongqing Jiotong Daxue Xuebao(Ziran Kexue Ban)*, 29(1), 30-32.

Chan, S. L. (1990). Strength of cold-formed box columns with coupled local and global buckling. *The Structural Engineer*, 68(7), 125-132.

Chen, W. F., & Han, D. J. (2007). *Plasticity for Structural Engineers*. J. Ross Publishing.

Chilver, A. H. (1953). A generalised approach to the local instability of certain thin-walled struts. *The Aeronautical Quarterly*, 4(3), 245-260.

Ding, F. X., Wang, W. J., Lu, D. R., & Liu, X. M. (2020). Study on the behavior of concrete-filled square double-skin steel tubular stub columns under axial loading. *Structures*, 23, 665-676.

Elchalakani, M., Zhao, X. L., & Grzebieta, R. (2002). Tests on concrete filled double-skin (CHS outer and SHS inner) composite short columns under axial compression. *Thin-Walled Structures*, 40(5), 415-441.

Ellobody, E., & Young, B. (2006). Nonlinear analysis of concrete-filled steel SHS and RHS columns. *Thin-Walled Structures*, 44(8), 919-930.

Farahi, M., Heidarpour, A., Zhao, X. L., & Al-Mahaidi, R. (2016). Compressive behaviour of concrete-filled double-skin sections consisting of corrugated plates. *Engineering Structures*, 111, 467-477.

Gerard, G., & Becker, H. (1957). Handbook of structural stability part III: buckling of curved plates and shells. *NACA TN*, 3783, 46.

Han, L. H., Li, Y. J., & Liao, F. Y. (2011). Concrete-filled double skin steel tubular (CFDST) columns subjected to long-term sustained loading. *Thin-Walled Structures*, 49(12), 1534-1543.

Harris, J., & Speicher, M. (2018). Assessment of performance-based seismic design methods in ASCE 41 for new steel buildings: Special moment frames. *Earthquake Spectra*, 34(3), 977-999.

Hassanein, M. F., Elchalakani, M., Karrech, A., Patel, V. I., & Yang, B. (2018). Behaviour of concrete-filled double-skin short columns under compression through finite element modelling: SHS outer and SHS inner tubes. *Structures*, 14, 358-375.

Hassanein, M. F., & Kharoob, O. F. (2014). Compressive strength of circular concrete-filled double skin tubular short columns. *Thin-Walled Structures*, 77, 165-173.

Hassanein, M.F., Kharoob, O.F. and Gardner, L. (2015). Behaviour and design of square concrete-filled double skin tubular columns with inner circular tubes. *Engineering Structures*, 100, 410-424.

Hassanein, M. F., Kharoob, O. F., & Liang, Q. Q. (2013). Circular concrete-filled double skin tubular short columns with external stainless steel tubes under axial compression. *Thin-Walled Structures*, 73, 252-263.

Heidarpour, A., & Bradford, M. A. (2007). Local buckling and slenderness limits for flange outstands at elevated temperatures. *Journal of Constructional Steel Research*, 63(5), 591-598.

Heidarpour, A., & Bradford, M. A. (2008). Local buckling and slenderness limits for steel webs under combined bending, compression and shear at elevated temperatures. *Thin-walled structures*, 46(2), 128-146.

Hoff, N. J., & Mautner, S. E. (1945). The buckling of sandwich-type panels. *Journal of the Aeronautical Sciences*, 12(3), 285-297.

Hutchinson, J. W., & Budiansky, B. (1966). Dynamic buckling estimates. *AIAA Journal*, 4(3), 525-530.

Hu, H. T., Huang, C. S., Wu, M. H., & Wu, Y. M. (2003). Nonlinear analysis of axially loaded concrete-filled tube columns with confinement effect. *Journal of Structural Engineering*, ASCE, 129(10), 1322-1329.

Hu, H. T., & Su, F. C. (2011). Nonlinear analysis of short concrete-filled double skin tube columns subjected to axial compressive forces. *Marine Structures*, 24(4), 319-337.

Huang, H., Han, L. H., Tao, Z., & Zhao, X. L. (2010). Analytical behaviour of concrete-filled double skin steel tubular (CFDST) stub columns. *Journal of Constructional Steel Research*, 66(4), 542-555.

Kamil, G. M., Liang, Q. Q., & Hadi, M. N. S. (2019a). Fiber element simulation of interaction behavior of local and global buckling in axially loaded rectangular concrete-filled steel tubular slender columns under fire exposure. *Thin-Walled Structures*, 145, 106403.

Kamil, G. M., Liang, Q. Q., & Hadi, M. N. S. (2019b). Numerical analysis of axially loaded rectangular concrete-filled steel tubular short columns at elevated temperatures. *Engineering Structures*, 180, 89-102.

Kapur, K. K., & Hartz, B. J. (1966). Stability of plates using the finite element method. *Journal of the Engineering Mechanics Division*, 92(2), 177-195.

Knobloch, M., & Fontana, M. (2006). Strain-based approach to local buckling of steel sections subjected to fire. *Journal of Constructional Steel Research*, 62(1-2), 44-67.

Kromm, A. (1939). *The Limit of Stability of a Curved Plate Under Shear and Axial Stresses*. National advisory committee for aeronautics Langley field VA Langley aeronautical laboratory.

Le, T.T., Patel, V. I., Liang, Q. Q. and Huynh, P. (2022). Simulation modeling of circular concrete-filled double-skin tubular slender beam-columns with outer stainless-steel tube. *Engineering Structures*. (Submitted)

Liang, Q. Q. (2004). *Performance-based Optimization of Structures: Theory and Applications*. Spon Press, Taylor and Francis Group, London and New York.

Liang, Q. Q. (2009a). Performance-based analysis of concrete-filled steel tubular beam columns, Part I: Theory and algorithms. *Journal of Constructional Steel Research*, 65(2), 363-372.

Liang, Q. Q. (2009b). Performance-based analysis of concrete-filled steel tubular beam-columns, Part II: Verification and applications. *Journal of Constructional Steel Research*, 65(2), 351-362.

Liang, Q. Q. (2011a). High strength circular concrete-filled steel tubular slender beam–columns, Part I: Numerical analysis. *Journal of Constructional Steel Research*, 67(2), 164-171.

Liang, Q. Q. (2011b). High strength circular concrete-filled steel tubular slender beam–columns, Part II: Fundamental behavior. *Journal of Constructional Steel Research*, 67(2), 172-180.

Liang, Q. Q. (2014). *Analysis and Design of Steel and Composite Structures*. CRC Press, Taylor and Francis Group, Boca Raton and London.

Liang, Q. Q. (2018). Numerical simulation of high strength circular double-skin concrete-filled steel tubular slender columns. *Engineering Structures*, 168, 205-217.

Liang, Q. Q., & Fragomeni, S. (2009). Nonlinear analysis of circular concrete-filled steel tubular short columns under axial loading. *Journal of Constructional Steel Research*, 65(12), 2186-2196.

Liang, Q. Q., & Fragomeni, S. (2010). Nonlinear analysis of circular concrete-filled steel tubular short columns under eccentric loading. *Journal of Constructional Steel Research*, 66(2), 159-169.

Liang, Q. Q., Patel, V. I., & Hadi, M. N. S. (2012). Biaxially loaded high-strength concrete-filled steel tubular slender beam-columns, Part I: Multiscale simulation. *Journal of Constructional Steel Research*, 75, 64-71.

Liang, Q. Q., & Uy, B. (1998). Parametric study on the structural behaviour of steel plates in concrete-filled fabricated thin-walled box columns. *Advances in Structural Engineering*, 2(1), 57-71.

Liang, Q. Q., & Uy, B. (2000). Theoretical study on the post-local buckling of steel plates in concrete-filled box columns. *Computers & Structures*, 75(5), 479-490.

Liang, Q. Q., Uy, B., & Liew, J. Y. R. (2005). Strength of concrete-filled steel box columns with local buckling effects. In *Australian Structural Engineering Conference 2005* (p. 1104). Engineers Australia.

Liang, Q. Q., Uy, B., & Liew, J. Y. R. (2006). Nonlinear analysis of concrete-filled thin-walled steel box columns with local buckling effects. *Journal of Constructional Steel Research*, 62(6), 581-591.

Liang, Q. Q., Uy, B., & Liew, J. Y. R. (2007). Local buckling of steel plates in concrete-filled thin-walled steel tubular beam-columns. *Journal of Constructional Steel Research*, 63(3), 396-405.

Liang, Q. Q., Uy, B., Wright, H. D., & Bradford, M. A. (2003). Local and post-local buckling of double skin composite panels. *Proceedings of the Institution of Civil Engineers-Structures and Buildings*, 156(2), 111-119.

Liang, Q. Q., Uy, B., Wright, H. D., & Bradford, M. A. (2004). Local buckling of steel plates in double skin composite panels under biaxial compression and shear. *Journal of Structural Engineering*, ASCE, 130(3), 443-451.

Lundquist, E. E., Stowell, E. Z., & Schuette, E. H. (1943). Principles of moment distribution applied to stability of structures composed of bars or plates.

Mahendran, M., & Murray, N. W. (1986). Elastic buckling analysis of ideal thin-walled structures under combined loading using a finite strip method. *Thin-walled structures*, 4(5), 329-362.

Maquoi, R., & Massonnet, C. (1976). Interaction between Local Plate Buckling and Overall Buckling in Thin-Walled Compression Members—Theories and Experiments. In *Buckling of structures* (pp. 365-382). Springer, Berlin, Heidelberg.

McDermott, J. F. (1969). Local plastic buckling of A514 steel members. *Journal of the Structural Division*, 95(9), 1837-1850.

Melosh, R. J. (1963). Structural analysis of solids. *Journal of the Structural Division*, 89(4), 205-248.

Murray, D. W., & Wilson, E. L. (1969). Finite-element postbuckling analysis of thin elastic plates. *AIAA Journal*, 7(10), 1915-1920.

Mursi, M., & Uy, B. (2003). Strength of concrete filled steel box columns incorporating interaction buckling. *Journal of Structural Engineering*, ASCE, 129(5), 626-639.

Oehlers, D. J., & Bradford, M. A. (1999). *Elementary behaviour of composite steel and concrete structural members*. Elsevier.

Pagoulatou, M., Sheehan, T., Dai, X. H., & Lam, D. (2014). Finite element analysis on the capacity of circular concrete-filled double-skin steel tubular (CFDST) stub columns. *Engineering Structures*, 72, 102-112.

Patel, V. I. (2020). Analysis of uniaxially loaded short round-ended concrete-filled steel tubular beam-columns. *Engineering Structures*, 205, 110098.

Patel, V. I., Liang, Q. Q., & Hadi, M. N. S. (2012). High strength thin-walled rectangular concrete-filled steel tubular slender beam-columns, Part II: Behavior. *Journal of Constructional Steel Research*, 70, 368-376.

Patel, V. I., Liang, Q. Q., & Hadi, M. N. S. (2014). Behavior of biaxially-loaded rectangular concrete-filled steel tubular slender beam-columns with preload effects. *Thin-Walled Structures*, *79*, 166-177.

Patel, V. I., Liang, Q. Q., & Hadi, M. N. S. (2015a). *Nonlinear Analysis of Concrete-Filled Steel Tubular Columns*. Scholar Press, Germany.

Patel, V. I., Liang, Q. Q., & Hadi, M. N. (2015b). Biaxially loaded high-strength concrete-filled steel tubular slender beam-columns, Part II: Parametric study. *Journal of Constructional Steel Research*, *110*, 200-207.

Patel, V. I., Liang, Q. Q., & Hadi, M. N. (2017a). Nonlinear analysis of circular high strength concrete-filled stainless steel tubular slender beam-columns. *Engineering Structures*, *130*, 1-13.

Patel, V. I., Liang, Q. Q., & Hadi, M. N. S. (2017b). Nonlinear analysis of biaxially loaded rectangular concrete-filled stainless steel tubular slender beam-columns. *Engineering Structures*, *140*, 120-133.

Patel, V. I., Liang, Q. Q., & Hadi, M. N. S. (2018). *Concrete-Filled Stainless Steel Tubular Columns*. CRC Press, Taylor and Francis Group, Boca Raton and London.

Patel, V. I., Liang, Q. Q., & Hadi, M. N. S. (2019). Numerical study of circular double-skin concrete-filled aluminum tubular stub columns. *Engineering Structures*, *197*, 109418.

Patel, V. I., Liang, Q. Q., & Hadi, M. N. S. (2020). Numerical analysis of circular double-skin concrete-filled stainless steel tubular short columns under axial loading. *Structures*, 24, 754-765.

PIFKO, A., & ISAKSON, G. (1969). A finite-element method for the plastic buckling analysis of plates. *AIAA Journal*, 7(10), 1950-1957.

Przemieniecki, J. S. (1963). Matrix structural analysis of substructures. *AIAA Journal*, 1(1), 138-147.

Przemieniecki, J. S. (1968). Discrete-element methods for stability analysis of complex structures. *The Aeronautical Journal*, 72(696), 1077-1086.

Reissner, E. (1948). Finite deflections of sandwich plates. *Journal of the Aeronautical Sciences*, 15(7), 435-440.

Ritz, W. (1909). "Über eine neue Methode zur Lösung gewisser Variationsprobleme der mathematischen Physik." *Journal Für Die Reine und Angewandte Mathematik*, 1909, 135, 1-61.

Roberts, T. M., & Rockey, K. C. (1979). A mechanism solution for predicting the collapse loads of slender plate girders when subjected to in-plane patch loading. *Proceedings of the Institution of Civil Engineers*, 67(1), 155-175.

Singer, J. (1962). On the equivalence of the Galerkin and Rayleigh-Ritz methods. *The Aeronautical Journal*, 66(621), 592-592.

Stowell, E. Z., & Lundquist, E. E. (1939). Local instability of columns with I-, Z-, channel, and rectangular-tube sections.

Tao, Z., Han, L. H., & Zhao, X. L. (2004). Behaviour of concrete-filled double skin (CHS inner and CHS outer) steel tubular stub columns and beam-columns. *Journal of Constructional Steel Research*, 60(8), 1129-1158.

Tao, Z., & Han, L. H. (2006). Behaviour of concrete-filled double skin rectangular steel tubular beam-columns. *Journal of Constructional Steel Research*, 62(7), 631-646.

Uenaka, K. (2016). CFDST stub columns having outer circular and inner square sections under compression. *Journal of Constructional Steel Research*, 120, 1-7.

Usami, T. (1982). Post-buckling of plates in compression and bending. *Journal of the Structural Division, ASCE*, 108(3), 591-609.

Usami, T., & Fukumoto, Y. (1982). Local and overall buckling of welded box columns. *Journal of the Structural Division, ASCE*, 108(3), 525-542.

Usami, T., & Fukumoto, Y. (1984). Welded box compression members. *Journal of Structural Engineering, ASCE*, 110(10), 2457-2470.

Uy, B. (2000). Strength of concrete filled steel box columns incorporating local buckling. *Journal of Structural Engineering, ASCE*, 126(3), 341-352.

Uy, B. (2001). Strength of short concrete filled high strength steel box columns. *Journal of Constructional Steel Research*, 57(2), 113-134.

Uy, B., & Bradford, M. A. (1995). Local buckling of thin steel plates in composite construction: Experimental and theoretical study. *Proceedings of the Institution of Civil Engineers-Structures and Buildings*, 110(4), 426-440.

Uy, B., & Bradford, M. A. (1996). Elastic local buckling of steel plates in composite steel-concrete members. *Engineering Structures*, 18(3), 193-200.

Vrcelj, Z., & Uy, B. (2002). Strength of slender concrete-filled steel box columns incorporating local buckling. *Journal of Constructional Steel Research*, 58(2), 275-300.

Wang, F. C., Han, L. H., & Li, W. (2018). Analytical behavior of CFDST stub columns with external stainless steel tubes under axial compression. *Thin-Walled Structures*, *127*, 756-768.

Wang, F., Young, B., & Gardner, L. (2017). Experimental investigation of concrete-filled double skin tubular stub columns with ferritic stainless steel outer tubes. *ce/papers*, *1*(2-3), 2070-2079.

Wei, S., Mau, S. T., Vipulanandan, C., & Mantrala, S. K. (1995). Performance of new sandwich tube under axial loading: experiment. *Journal of Structural Engineering*, ASCE, *121*(12), 1806-1814.

Wittrick, W. H., & Curzon, P. L. V. (1968). Local buckling of long polygonal tubes in combined compression and torsion. *International Journal of Mechanical Sciences*, *10*(10), 849-857.

Williams, F. W., & Wittrick, W. H. (1969). Computational procedures for a matrix analysis of the stability and vibration of thin flat-walled structures in compression. *International Journal of Mechanical Sciences*, *11*(12), 979-998.

Williams, F. W., & Wittrick, W. H. (1972). Numerical results for the initial buckling of some stiffened panels in compression. *The Aeronautical Quarterly*, *23*(1), 24-40.

Wright, H. D. (1995). Local stability of filled and encased steel sections. *Journal of Structural Engineering*, ASCE, *121*(10), 1382-1388.

Xilin, Y. Y. L., & Satoshi, T. K. S. (1999). Experimental Study on Connection between Concrete filled Square Tube Column and Steel beams under Tensile Loading. *Structural Engineering*, 01.

Yuan, W. B., & Yang, J. J. (2013). Experimental and numerical studies of short concrete-filled double skin composite tube columns under axially compressive loads. *Journal of Constructional Steel Research*, 80, 23-31.

Zhao, X. L., & Grzebieta, R. (2002). Strength and ductility of concrete filled double skin (SHS inner and SHS outer) tubes. *Thin-Walled Structures*, 40(2), 199-213.

Zhao, X. L., Han, B., & Grzebieta, R. H. (2002). Plastic mechanism analysis of concrete-filled double-skin (SHS inner and SHS outer) stub columns. *Thin-Walled Structures*, 40(10), 815-833.